ESD-TR-88-421

(2)

Technical Report
799

Lower Bounds on Multiple-Source Direction Finding in the Presence of Direction-Dependent Antenna-Array-Calibration Errors

A.R. Kuruc

24 October 1989

Lincoln Laboratory
MASSACHUSETTS INSTITUTE OF TECHNOLOGY
LEXINGTON, MASSACHUSETTS

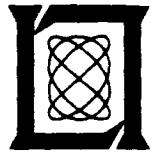

Prepared for the Department of Defense
under Air Force Contract F19628-90-C-0002.

This report is based on studies performed at Lincoln Laboratory, a center for research operated by Massachusetts Institute of Technology. This work was sponsored by the Department of Defense under Air Force Contract F19628-90-C-0002.

The ESD Public Affairs Office has reviewed this report, and it is releasable to the National Technical Information Service, where it will be available to the general public, including foreign nationals.

This technical report has been reviewed and is approved for publication.

FOR THE COMMANDER

Hugh L. Southall

Hugh L. Southall, Lt. Col., USAF
Chief, ESD Lincoln Laboratory Project Office

(2)

MASSACHUSETTS INSTITUTE OF TECHNOLOGY
LINCOLN LABORATORY

LOWER BOUNDS ON MULTIPLE-SOURCE DIRECTION FINDING IN THE PRESENCE OF DIRECTION-DEPENDENT ANTENNA-ARRAY-CALIBRATION ERRORS

A.R. KURUC
Group 44

TECHNICAL REPORT 799

24 OCTOBER 1989

LEXINGTON MASSACHUSETTS

ABSTRACT

We consider the problem of direction finding (DF) of multiple, cofrequency narrowband signals with a phased antenna array when direction-dependent array-calibration errors as well as thermal noise are present. Lower bounds on the variance of unbiased estimators for DF are derived under two different types of signal models: completely unknown (i.e., generic) signals and unknown constant-envelope signals. In both models, the complex amplitudes of the signals are modeled as unknown parameters. We derive and evaluate lower bounds on DF of these signals when complex Gaussian array errors and thermal noise are present. In our numerical examples, the bound for generic signals tended to decrease with increasing interference power and, for closely spaced signals, became more optimistic when small array errors were added. With a sufficiently large signal-of-interest (SOI) array signal-to-noise power ratio (ASNR) and number of looks, the bound numerically approached the bound on DF of multiple generic signals with array errors but no thermal noise (i.e., the multiple-generic-signal, array-errors-only bound). The latter bound depended on the signal separation and the power of the array errors. It was independent of the signal waveforms and powers and was largest at moderate signal separations (e.g., 0.3 beamwidths). The latter bound approached the single-signal array-errors-only bound as the signal separation approached zero.

The results for constant-envelope signals showed that the bound with array errors and thermal noise was more optimistic than the analogous generic-signal bound and had little dependence on signal separation and interference power. This was also the case in the absence of direction-dependent errors. The improvements in the bound were more significant at small array errors, low ASNR, small numbers of looks, and moderate signal separations. At all signal separations, with a sufficiently high SOI ASNR and number of looks, the bound numerically approached the single-signal, one-look, array-errors-only bound (the latter bound is the same for generic and constant-envelope signals).

TABLE OF CONTENTS

LIST OF ILLUSTRATIONS

LIST OF TABLES

ACKNOWLEDGEMENTS

The author would like to thank John Ramsey for extending the software to compute the constant-envelope signal bound, Claude Barsotti for his assistance in generating and plotting the numerical results, Keith Forsythe for many helpful discussions, John Jayne for his careful review of the manuscript, and Steve Krich for his interest in and encouragement of this project. A special thank you goes to Larry Horowitz for his numerous contributions to this report.

PREFACE

To perform direction finding (DF) of multiple, cofrequency narrowband signals with a phased antenna array, it is necessary to know the array-response pattern as a function of the signal direction. In practice, this function is known only approximately. It is therefore appropriate to model the array-response pattern vector as a perturbed version of a deterministic function of the signal direction (i.e., the assumed array-response vector). It is useful to decompose the perturbations into two components, a direction-independent component and a direction-dependent component. The direction-independent component is commonly modeled as multiplicative errors that are the same for all of the signals in each receiver channel (e.g., internal receiver-calibration errors). The direction-dependent component is due to errors that are different for each of the signals in each receiver channel (e.g., errors due to array-response pattern calibration residuals and near-field multipath). The direction-dependent component is modeled as adding errors to the assumed array-response vectors of the individual signals. In this report, we shall limit our consideration to the direction-dependent component of the errors.

Direction-dependent array errors can be an important limiting factor in the performance of DF algorithms. To help determine whether current algorithms are performing near the intrinsic limitations of the problem, it is useful to compute lower bounds on the variance of unbiased DF estimates in the presence of direction-dependent errors.

In Section 1 of this report, we derive lower bounds on the variance of unbiased estimators for DF of unknown generic and constant-envelope signals when independent, complex Gaussian, direction-dependent array-calibration errors as well as complex Gaussian thermal noise are present. (Note that, in a real environment, the array errors might be correlated antenna-element-to-antenna-element and/or signal-direction-to-signal-direction, which could impact the performance achievable.) Numerical results for some cases of interest are presented in Section 2. Conclusions and directions for future work are presented in Section 3 and Section 4, respectively.

1. SIGNAL MODELS AND LOWER BOUND DERIVATIONS

1.1 NOTATION AND SOME MATHEMATICAL NOTIONS

Real and complex scalars are denoted by lowercase Roman or Greek letters. Vectors are denoted by lowercase Roman or Greek letters with an arrow on top (e.g., $\vec{x}$). Matrices are denoted by uppercase Roman or Greek letters. Exceptions are the symbols used to denote the dimensions of vectors and matrices as well as the symbols used to denote the number of signals, antenna elements, observations (i.e., looks), and unknown parameters, namely S, M, N, and P, respectively. The letters s, m, n, and p are used to index over the signals, antenna elements, looks, and unknown parameters, respectively. The ith column of the matrix X will be denoted by $X_{\cdot i}$, the ith row of the matrix X (written as a column vector) will be denoted by $X_{i\cdot}$, and the ijth component of the matrix X will be denoted by $(X)_{ij}$. The ith component of the vector $\vec{x}$ will be denoted by $(\vec{x})_i$. The real and imaginary parts of a quantity X will be denoted by $\Re(X)$ and $\Im(X)$, respectively. The transpose, complex conjugate, and Hermitian (i.e., complex conjugate transpose) of a matrix X are denoted by X^T, X^*, and X^H, respectively.

We define $\vec{e}_i$ as the vector whose ith component equals 1 and whose remaining components equal 0, $\vec{1}_N$ as the N-vector whose components all equal 1, I_N as the $N \times N$ identity matrix, $0_{M,N}$ as the $M \times N$ matrix whose components all equal 0, and E_{ij} as the matrix whose ijth component equals 1 and whose remaining components equal 0. We shall need the identities

$$\mathrm{tr}(AB) = \mathrm{tr}(BA) \tag{1.1}$$

[2, Eq. 1.40], and

$$\begin{aligned} \mathrm{tr}(AE_{ij}) &= \mathrm{tr}(A_{\cdot i}\vec{e}_j^T) \quad ([2, \text{Eq. } 1.28]) \\ &= \mathrm{tr}(\vec{e}_j^T A_{\cdot i}) \quad (\text{Eq. } 1.1) \\ &= \mathrm{tr}[(A)_{ji}] \\ &= (A)_{ji}. \end{aligned} \tag{1.2}$$

1.1.1 The Kronecker Product

The Kronecker product of the $I \times J$ matrix A and the $K \times L$ matrix B is defined as the $IK \times JL$ matrix [2, Sec. 2.2]

$$A \otimes B \stackrel{\mathrm{def}}{=} \begin{bmatrix} (A)_{11}B & (A)_{12}B & \cdots & (A)_{1J}B \\ (A)_{21}B & (A)_{22}B & \cdots & (A)_{2J}B \\ \vdots & \vdots & \ddots & \vdots \\ (A)_{I1}B & (A)_{I2}B & \cdots & (A)_{IJ}B \end{bmatrix}. \tag{1.3}$$

It has the properties

$$A \otimes (\alpha B) = (\alpha A) \otimes B = \alpha(A \otimes B) \tag{1.4}$$

([2, Eq. 2.5] and a trivial extension),

$$(A \otimes B)^H = A^H \otimes B^H \tag{1.5}$$

([1, p. 9]),

$$(A \otimes B)^{-1} = A^{-1} \otimes B^{-1} \tag{1.6}$$

([2, Eq. 2.12]), if the inverses exist, and

$$(A \otimes B)(C \otimes D) = AC \otimes BD \tag{1.7}$$

([2, Eq. 2.11]), where C is a $J \times M$ matrix and D is an $L \times N$ matrix.

1.1.2 The Hadamard Product

The Hadamard product of the $I \times J$ matrices A and B is defined as the $I \times J$ matrix

$$A \square B \stackrel{\text{def}}{=} \begin{bmatrix} (A)_{11}(B)_{11} & (A)_{12}(B)_{12} & \cdots & (A)_{1J}(B)_{1J} \\ (A)_{21}(B)_{21} & (A)_{22}(B)_{22} & \cdots & (A)_{2J}(B)_{2J} \\ \vdots & \vdots & \ddots & \vdots \\ (A)_{I1}(B)_{I1} & (A)_{I2}(B)_{I2} & \cdots & (A)_{IJ}(B)_{IJ} \end{bmatrix}. \tag{1.8}$$

The Hadamard product is obviously commutative and associative, so that

$$A \square B = B \square A \tag{1.9}$$

and

$$(A \square B) \square C = A \square (B \square C). \tag{1.10}$$

We shall need the identities

$$(A \square B)^T = A^T \square B^T, \tag{1.11}$$

$$(\vec{a}\vec{b}^T) \square (\vec{c}\vec{d}^T) = (\vec{a} \square \vec{c})(\vec{b} \square \vec{d})^T, \tag{1.12}$$

and

$$\begin{aligned}(E_{qr}A)\square(BE_{st}) &= [\vec{e}_q(A_{r\cdot})^T]\square(B_{\cdot s}\vec{e}_t^T) \quad ([2, \text{Eqs. } 1.27 \text{ and } 1.28]) \\ &= (\vec{e}_q\square B_{\cdot s})(\vec{e}_t\square A_{r\cdot})^T \quad (\text{Eq. } 1.12) \\ &= [(B)_{qs}\vec{e}_q][(A)_{rt}\vec{e}_t]^T \\ &= (A)_{rt}(B)_{qs}\vec{e}_q\vec{e}_t^T \\ &= (A)_{rt}(B)_{qs}E_{qt} \quad ([2, \text{Eq. } 1.5]). \end{aligned} \tag{1.13}$$

1.1.3 The Khatri-Rao Product

The Khatri-Rao product of the $M \times N$ matrix A and the $P \times N$ matrix B is defined by the $MP \cdot N$ matrix

$$A \cdot B \stackrel{\text{def}}{=} \left[\begin{array}{cccc} A_{\cdot 1} \otimes B_{\cdot 1} & A_{\cdot 2} \otimes B_{\cdot 2} & \cdots & A_{\cdot N} \otimes B_{\cdot N} \end{array} \right]. \tag{1.14}$$

We shall need the identities

$$(A \otimes B)(C \otimes D) = (AC \otimes BD) \quad ([4, \text{Eq. } 1.5.9]) \tag{1.15}$$

and

$$(A \otimes B)^H(C \otimes D) = (A^HC)\square(B^HD). \tag{1.16}$$

The latter is proved by noting that the ijth element of the left-hand side is equal to

$$\begin{aligned}(A_{\cdot i} \otimes B_{\cdot i})^H(C_{\cdot j} \otimes D_{\cdot j}) &= (A_{\cdot i}^H \otimes B_{\cdot i}^H)(C_{\cdot j} \otimes D_{\cdot j}) \quad (\text{Eq. } 1.5) \\ &= (A_{\cdot i}^HC_{\cdot j}) \otimes (B_{\cdot i}^HD_{\cdot j}) \quad (\text{Eq. } 1.7) \\ &= (A^HC)_{ij} \otimes (B^HD)_{ij} \\ &= (A^HC)_{ij}(B^HD)_{ij}. \end{aligned} \tag{1.17}$$

We shall also need the identity

$$\begin{aligned}(A \otimes B)^H(C \otimes D)(E \otimes F) &= (A \otimes B)^H(CE \otimes DF) \quad (\text{Eq. } 1.15) \\ &= A^HCE\square B^HDF \quad (\text{Eq. } 1.16). \end{aligned} \tag{1.18}$$

1.1.4 Matrix-Inversion Identities

We shall need the matrix identity

$$[A + BC^{-1}D]^{-1} = A^{-1} - A^{-1}B[C + DA^{-1}B]^{-1}DA^{-1} \tag{1.19}$$

(assuming the necessary inverses exist) [5, Eq. A.3], and the following result on the inverse of a partitioned matrix [5, Eq. A.2]. Let A be an invertible square matrix partitioned as

$$A = \begin{bmatrix} A_{11} & A_{12} \\ A_{21} & A_{22} \end{bmatrix}, \tag{1.20}$$

with A_{22} invertible. Then the upper-left block of A^{-1}, ${A^{-1}}_{11}$, is given by

$${A^{-1}}_{11} = (A_{11} - A_{12}{A_{22}}^{-1}A_{21})^{-1} \tag{1.21}$$

(the inverse indicated on the right side of the equation can be shown to exist under the given conditions), and

$$A^{-1} = \begin{bmatrix} {A^{-1}}_{11} & -{A^{-1}}_{11}A_{12}{A_{22}}^{-1} \\ -{A_{22}}^{-1}A_{21}{A^{-1}}_{11} & {A_{22}}^{-1} + {A_{22}}^{-1}A_{21}{A^{-1}}_{11}A_{12}{A_{22}}^{-1} \end{bmatrix}. \tag{1.22}$$

Note the notational distinction between the ii^{th} block of A^{-1}, ${A^{-1}}_{ii}$, and the inverse of the ii^{th} block of A, ${A_{ii}}^{-1}$.

1.2 DATA MODEL

1.2.1 Array-Response Model

The signal environment will be modeled as S narrowband cofrequency signals. The complex amplitude of the sth signal during the nth observation (i.e., look) will be denoted by c_{ns}. The c_{ns} will represent an unknown generic or constant-envelope signal. The details of these signal models will be described in Subsections 1.2.2 and 1.2.3. We define the S-vector of complex amplitudes during the nth look, $\vec{c}_n$, by

$$\vec{c}_n \stackrel{\text{def}}{=} \begin{bmatrix} c_{n1} & c_{n2} & \cdots & c_{nS} \end{bmatrix}^T, \tag{1.23}$$

the concatenation of these vectors, $\vec{c}$, by

$$\vec{c} \stackrel{\text{def}}{=} \sum_{n=1}^{N} (\vec{c}_n \otimes \vec{c}_n), \tag{1.24}$$

and the $N \times S$ matrix of complex amplitudes, C, by

$$C \stackrel{\text{def}}{=} \begin{bmatrix} c_{11} & c_{12} & \cdots & c_{1S} \\ c_{21} & c_{22} & \cdots & c_{2S} \\ \vdots & \vdots & \ddots & \vdots \\ c_{N1} & c_{N2} & \cdots & c_{NS} \end{bmatrix}. \tag{1.25}$$

We will assume that $N \geq S$ and that C is of full rank, S.

The signals are observed using an array of M antenna elements. The ideal (i.e., error-free) array-response vector of the sth signal will be denoted by $\vec{v}_s$, and the error in this vector will be denoted by $\vec{\xi}_s$. Define the complex $M \times S$ matrices of ideal array-response vectors and their errors, V and Ξ, by

$$V \stackrel{\text{def}}{=} \begin{bmatrix} \vec{v}_1 & \vec{v}_2 & \cdots & \vec{v}_S \end{bmatrix} \tag{1.26}$$

and

$$\Xi \stackrel{\text{def}}{=} \begin{bmatrix} \vec{\xi}_1 & \vec{\xi}_2 & \cdots & \vec{\xi}_S \end{bmatrix}. \tag{1.27}$$

The response of the array during the nth look[1], $\vec{z}_n$, will be modeled as

$$\vec{z}_n \stackrel{\text{def}}{=} (V + \Xi)\vec{c}_n + \vec{\kappa}_n, \tag{1.28}$$

where $\vec{\kappa}_n$ denotes the thermal-noise vector corrupting the observation. The vectors $\{\vec{\xi}_s\}$ and $\{\vec{\kappa}_n\}$ will be modeled as sequences of independent, zero-mean complex (circular) Gaussian[2] random vectors with covariance matrices $\epsilon^2 I_M$ and $\sigma^2 I_M$, respectively. The $\{\vec{\xi}_s\}$ and $\{\vec{\kappa}_n\}$ are assumed to be statistically independent of each other.

Define the concatenated thermal-noise vector, $\vec{\kappa}$, by

$$\vec{\kappa} \stackrel{\text{def}}{=} \sum_{n=1}^{N} (\vec{\epsilon}_n \otimes \vec{\kappa}_n) \tag{1.29}$$

and the concatenated observation vector, $\vec{z}$, by

$$\vec{z} \stackrel{\text{def}}{=} \sum_{n=1}^{N} (\vec{\epsilon}_n \otimes \vec{z}_n)$$

---

[1] A look (or observation) is defined as a simultaneous vector snapshot of the baseband complex amplitudes at the outputs of the M antenna elements composing the array.

[2] In the report, we shall often use the terminology 'complex Gaussian' in place of 'complex circular Gaussian' for simplicity.

$$
\begin{aligned}
&= \sum_{n=1}^{N} \{\vec{c}_n \otimes [(V - \Xi)\vec{c}_n - \vec{\kappa}_n]\} \\
&= \sum_{n=1}^{N} \{\vec{c}_n \otimes [\sum_{s=1}^{S} c_{ns}(V - \Xi)_s]\} + \sum_{n=1}^{N} (\vec{c}_n \otimes \vec{\kappa}_n) \\
&= \sum_{s=1}^{S}\sum_{n=1}^{N} [c_{ns}\vec{c}_n \otimes (V - \Xi)_s] - \vec{\kappa} \quad \text{(Eq. 1.4)} \\
&= \sum_{s=1}^{S} [C_s \otimes (V - \Xi)_s] - \vec{\kappa} \\
&= [C \cdot (V - \Xi)]\vec{1}_S - \vec{\kappa} \quad \text{(Eq. 1.14).}
\end{aligned} \tag{1.30}
$$

Thus the vector $\vec{z}$ is a complex Gaussian random MN-vector with mean

$$
\vec{\mu} = (C \cdot V)\vec{1}_S \tag{1.31}
$$

and covariance

$$
\begin{aligned}
\Lambda &= E\{[(C \cdot \Xi)\vec{1}_S - \vec{\kappa}][\vec{1}_S^H(C \cdot \Xi)^H + \vec{\kappa}^H]\} \\
&= E\{\sum_{s=1}^{S}(C_s \otimes \vec{\xi}_s)\sum_{s'=1}^{S}[(C_{s'})^H \otimes \vec{\xi}_{s'}^H]\} + E(\vec{\kappa}\vec{\kappa}^H) \\
&= E\{\sum_{s=1}^{S}\sum_{s'=1}^{S}[C_s(C_{s'})^H \otimes \vec{\xi}_s\vec{\xi}_{s'}^H]\} + E(\vec{\kappa}\vec{\kappa}^H) \quad \text{(Eq. 1.7)} \\
&= \sum_{s=1}^{S}\sum_{s'=1}^{S}[C_s(C_{s'})^H \otimes \delta_{s,s'}\epsilon^2 I_M] + \sigma^2 I_{MN} \\
&= \sum_{s=1}^{S}[C_s(C_s)^H \otimes \epsilon^2 I_M] + \sigma^2(I_N \otimes I_M) \\
&= (\sigma^2 I_N + \epsilon^2 CC^H) \otimes I_M \quad \text{([2, p. 16]).}
\end{aligned} \tag{1.32}
$$

Define Λ_N by

$$
\Lambda_N \stackrel{\text{def}}{=} \sigma^2 I_N + \epsilon^2 CC^H; \tag{1.33}
$$

then

$$
\Lambda = \Lambda_N \otimes I_M. \tag{1.34}
$$

We will assume that either $\sigma^2 > 0$ or that both $N = S$ and $\epsilon^2 > 0$ so that Λ_N is of full rank, N. Then, using Equation (1.6),

$$
\Lambda^{-1} = \Lambda_N^{-1} \otimes I_M. \tag{1.35}
$$

with Λ_N^{-1} being given by

$$\begin{aligned}
\Lambda_N^{-1} &= (\sigma^2 I_N + \epsilon^2 C C^H)^{-1} \\
&= [\sigma^2 (I_N + \frac{\epsilon^2}{\sigma^2} C C^H)]^{-1} \\
&= \frac{1}{\sigma^2} (I_N + \frac{\epsilon^2}{\sigma^2} C C^H)^{-1} \\
&= \frac{1}{\sigma^2} [I_N - \frac{\epsilon^2}{\sigma^2} C (I_S + \frac{\epsilon^2}{\sigma^2} C^H C)^{-1} C^H] \quad \text{(Eq. 1.19)}
\end{aligned} \tag{1.36}$$

when $\sigma^2 > 0$, and by

$$\Lambda_N^{-1} = \frac{1}{\epsilon^2} C^{-H} C^{-1} \tag{1.37}$$

when $\sigma^2 = 0$, $N = S$, and $\epsilon^2 > 0$.

The ideal array-response vector of the sth signal, $\vec{v}_s$, is assumed to be a differentiable function of the one-dimensional direction of the sth signal, which we denote by u_s. (The assumption of a one-dimensional space of signal directions is made only for simplicity; the method of analysis could be extended to a multidimensional space of signal directions.) The real S-vector of signal directions, $\vec{u}$, is defined by

$$\vec{u} \stackrel{\text{def}}{=} \begin{bmatrix} u_1 & u_2 & \cdots & u_S \end{bmatrix}^T. \tag{1.38}$$

We denote the derivative of $\vec{v}_s$ with respect to u_s (evaluated at the true value of u_s) by $\dot{\vec{v}}_s$ and define the matrix $\dot{V}$ by

$$\dot{V} \stackrel{\text{def}}{=} \begin{bmatrix} \dot{\vec{v}}_1 & \dot{\vec{v}}_2 & \cdots & \dot{\vec{v}}_S \end{bmatrix}. \tag{1.39}$$

1.2.2 Generic-Signal Model

In the generic-signal model, the complex amplitudes of the signals are modeled as being unknown. More specifically, c_{ns} will be modeled as

$$c_{ns} = a_{ns} e^{j\phi_{ns}}, \tag{1.40}$$

where a_{ns} and ϕ_{ns} are the unknown magnitude and phase, respectively, of the sth signal during the nth look.

We define the real S-vector of signal magnitudes during the nth look, $\vec{a}_n$, by

$$\vec{a}_n \stackrel{\text{def}}{=} \begin{bmatrix} a_{n1} & a_{n2} & \cdots & a_{nS} \end{bmatrix}^T, \tag{1.41}$$

the concatenation of these vectors, $\vec{a}$, by

$$\vec{a} \stackrel{\text{def}}{=} \sum_{n=1}^{N} \vec{e}_n \otimes \vec{a}_n. \tag{1.42}$$

the real S-vector of phases during the nth look, $\vec{\phi}_n$, by

$$\vec{\phi}_n \stackrel{\text{def}}{=} \begin{bmatrix} \phi_{n1} & \phi_{n2} & \cdots & \phi_{nS} \end{bmatrix}^T. \tag{1.43}$$

and the concatenation of these vectors, $\vec{\phi}$, by

$$\vec{\phi} \stackrel{\text{def}}{=} \sum_{n=1}^{N} \vec{e}_n \otimes \vec{\phi}_n. \tag{1.44}$$

We also define the complex S-vector, $\vec{\psi}_n$, of phases (in exponential notation) during the nth look by

$$\vec{\psi}_n \stackrel{\text{def}}{=} \begin{bmatrix} e^{j\phi_{n1}} & e^{j\phi_{n2}} & \cdots & e^{j\phi_{nS}} \end{bmatrix}^T, \tag{1.45}$$

and the concatenation of these vectors, $\vec{\psi}$, by

$$\vec{\psi} \stackrel{\text{def}}{=} \sum_{n=1}^{N} \vec{e}_n \otimes \vec{\psi}_n. \tag{1.46}$$

The vector of unknowns, $\vec{r}$, is defined by

$$\vec{r} \stackrel{\text{def}}{=} \begin{bmatrix} \vec{u}^T & \vec{a}^T & \vec{\phi}^T \end{bmatrix}^T. \tag{1.47}$$

1.2.3 Unknown Constant-Envelope Signal Model

In the unknown constant-envelope signal model, the complex amplitudes of the signals are *modeled as being of unknown, but constant,* magnitude and of unknown phase. More specifically, c_{ns} will be modeled as

$$c_{ns} = \alpha_s e^{j\phi_{ns}}, \tag{1.48}$$

where α_s is the unknown magnitude of the sth signal and ϕ_{ns} is the unknown phase of the sth signal during the nth look.

We define the real S-vector of signal magnitudes, $\vec{\alpha}$, by

$$\vec{\alpha} \stackrel{\text{def}}{=} \begin{bmatrix} \alpha_1 & \alpha_2 & \cdots & \alpha_S \end{bmatrix}^T, \tag{1.49}$$

and $\vec{\alpha}_u$ and $\vec{\phi}$ as in Section 1.2.2. The vector of unknowns, $\vec{r}$, is defined by

$$\vec{r} \stackrel{\text{def}}{=} \begin{bmatrix} \vec{u}^T & \vec{\alpha}^T & \vec{\phi}^T \end{bmatrix}^T. \tag{1.50}$$

1.3 The Cramér-Rao Bound on DF

1.3.1 The Cramér-Rao Bound

Define $\frac{\partial f}{\partial \vec{r}}$ as the row vector whose ith component is equal to $\frac{\partial f}{\partial (\vec{r})_i}$. Let $\vec{z}$ be a random vector whose probability density function, $p(\vec{z};\vec{r})$, depends upon an unknown L-dimensional real parameter vector $\vec{r}$ with true value $\vec{r}_t$. Let $\hat{\vec{r}}$ denote an estimator of $\vec{r}$ ($\hat{\vec{r}}$ is a function of $\vec{z}$) and define

$$\vec{m}(\vec{r}_t) \stackrel{\text{def}}{=} E_{\vec{r}_t}(\hat{\vec{r}}), \tag{1.51}$$

where $E_{\vec{r}_t}$ denotes expectation with respect to the probability density function $p(\vec{z};\vec{r}_t)$. The covariance of the estimator $\hat{\vec{r}}$ when $\vec{r} = \vec{r}_t$ is defined by

$$R \stackrel{\text{def}}{=} E_{\vec{r}_t}\{[\hat{\vec{r}} - \vec{m}(\vec{r}_t)][\hat{\vec{r}} - \vec{m}(\vec{r}_t)]^H\}. \tag{1.52}$$

We say that $\hat{\vec{r}}$ is differentially unbiased for $(\vec{r})_l$ at $\vec{r}_t$ if

$$\left(\frac{\partial \vec{m}(\vec{r})}{\partial \vec{r}} \Big|_{\vec{r}=\vec{r}_t} \right)_l = \vec{e}_l \tag{1.53}$$

and that $\hat{\vec{r}}$ is differentially unbiased at $\vec{r}_t$ if

$$\frac{\partial \vec{m}(\vec{r})}{\partial \vec{r}} \Big|_{\vec{r}=\vec{r}_t} = I_L. \tag{1.54}$$

Define the Fisher information matrix by

$$F \stackrel{\text{def}}{=} E_{\vec{r}_t}\left\{ \left[\left(\frac{\partial \ln p(\vec{z};\vec{r})}{\partial \vec{r}} \Big|_{\vec{r}=\vec{r}_t} \right)^T \left(\frac{\partial \ln p(\vec{z};\vec{r})}{\partial \vec{r}} \Big|_{\vec{r}=\vec{r}_t} \right) \right] \right\}. \tag{1.55}$$

The Cramér-Rao bound states that

$$R \geq \left(\frac{\partial \vec{m}}{\partial \vec{r}} \Big|_{\vec{r}=\vec{r}_t} \right) F^{-1} \left(\frac{\partial \vec{m}}{\partial \vec{r}} \Big|_{\vec{r}=\vec{r}_t} \right)^T. \tag{1.56}$$

where $\geq$ means that the difference between the matrices is positive semidefinite [3, Th. 2.7.3].

If $\hat{\vec{r}}$ is differentially unbiased for $(\vec{r})_l$ at $\vec{r}_t$, then

$$\begin{aligned}
\mathrm{var}\,(\hat{\vec{r}})_l &= (R)_{ll} \\
&= \vec{\epsilon}_l^T R \vec{\epsilon}_l \quad \text{([2, Eq. 1.19])} \\
&\geq \vec{\epsilon}_l^T \left(\frac{\partial \vec{m}}{\partial \vec{r}}_{|\vec{r}=\vec{r}_t} \right) F^{-1} \left(\frac{\partial \vec{m}}{\partial \vec{r}}_{|\vec{r}=\vec{r}_t} \right)^T \vec{\epsilon}_l \\
&= \left[\left(\frac{\partial \vec{m}}{\partial \vec{r}}_{|\vec{r}=\vec{r}_t} \right)_l \right]^T F^{-1} \left(\frac{\partial \vec{m}}{\partial \vec{r}}_{|\vec{r}=\vec{r}_t} \right)_l \quad \text{([2, Eqs. 1.16 and 1.17])} \\
&= \vec{\epsilon}_l^T F^{-1} \vec{\epsilon}_l \quad \text{(Eq. 1.53)} \\
&= (F^{-1})_{ll} \quad \text{([2, Eq. 1.19])}.
\end{aligned} \tag{1.57}$$

In this case, the bound on the variance of the lth unknown parameter is given simply by the lth diagonal element of F^{-1}. In the sequel, for any parameter of interest, $(\vec{r})_l$, we shall only consider estimators which are differentially unbiased for $(\vec{r})_l$ at $\vec{r}_t$. For an estimator which is differentially unbiased at $\vec{r}_t$, Equation (1.56) reduces to

$$R \geq F^{-1}. \tag{1.58}$$

Lastly, we note that locally unbiased estimators of $(\vec{r})_l$ at $\vec{r}_t$ (i.e., estimators for which $(\vec{m}(\vec{r}))_l = (\vec{r})_l$ for all $\vec{r}$ in some neighborhood of $\vec{r}_t$) are always also differentially unbiased estimators of $(\vec{r})_l$ at $\vec{r}_t$. This is shown by noting that

$$\begin{aligned}
\left(\frac{\partial \vec{m}(\vec{r})}{\partial \vec{r}}_{|\vec{r}=\vec{r}_t} \right)_l &= \left(\frac{\partial \vec{r}}{\partial \vec{r}}_{|\vec{r}=\vec{r}_t} \right)_l \\
&= (I_L)_l \\
&= \vec{\epsilon}_l.
\end{aligned} \tag{1.59}$$

1.3.2 Generic-Signal Case

Using Equation (1.47), the symmetric matrix F may be partitioned as

$$F = \begin{bmatrix} F_{\vec{u}\vec{u}} & F_{\vec{u}\vec{a}} & F_{\vec{u}\vec{\phi}} \\ F_{\vec{a}\vec{u}} & F_{\vec{a}\vec{a}} & F_{\vec{a}\vec{\phi}} \\ F_{\vec{\phi}\vec{u}} & F_{\vec{\phi}\vec{a}} & F_{\vec{\phi}\vec{\phi}} \end{bmatrix}$$

$$= \begin{bmatrix} F_{\vec{u}\vec{u}} & F_{\vec{u}\vec{a}_1} & \cdots & F_{\vec{u}\vec{a}_N} & F_{\vec{u}\vec{\phi}_1} & \cdots & F_{\vec{u}\vec{\phi}_N} \\ F_{\vec{a}_1\vec{u}} & F_{\vec{a}_1\vec{a}_1} & \cdots & F_{\vec{a}_1\vec{a}_N} & F_{\vec{a}_1\vec{\phi}_1} & \cdots & F_{\vec{a}_1\vec{\phi}_N} \\ \vdots & \vdots & \ddots & \vdots & \vdots & \ddots & \vdots \\ F_{\vec{a}_N\vec{u}} & F_{\vec{a}_N\vec{a}_1} & \cdots & F_{\vec{a}_N\vec{a}_N} & F_{\vec{a}_N\vec{\phi}_1} & \cdots & F_{\vec{a}_N\vec{\phi}_N} \\ F_{\vec{\phi}_1\vec{u}} & F_{\vec{\phi}_1\vec{a}_1} & \cdots & F_{\vec{\phi}_1\vec{a}_N} & F_{\vec{\phi}_1\vec{\phi}_1} & \cdots & F_{\vec{\phi}_1\vec{\phi}_N} \\ \vdots & \vdots & \ddots & \vdots & \vdots & \ddots & \vdots \\ F_{\vec{\phi}_N\vec{u}} & F_{\vec{\phi}_N\vec{a}_1} & \cdots & F_{\vec{\phi}_N\vec{a}_N} & F_{\vec{\phi}_N\vec{\phi}_1} & \cdots & F_{\vec{\phi}_N\vec{\phi}_N} \end{bmatrix}, \tag{1.60}$$

where $F_{\vec{\jmath}\vec{\kappa}}$ is defined by

$$F_{\vec{\jmath}\vec{\kappa}} \stackrel{\text{def}}{=} E_{\vec{r}_t}\left\{ \left[\left(\frac{\partial \ln p(\vec{z};\vec{r})}{\partial \vec{\jmath}} \right)^T \frac{\partial \ln p(\vec{z};\vec{r})}{\partial \vec{\kappa}} \right]_{\vec{r}=\vec{r}_t} \right\}. \tag{1.61}$$

Since F is symmetric, we need only explicitly compute the diagonal and lower-left subblocks of F.

The observation is a complex Gaussian random vector with mean $\vec{\mu}$ and covariance Λ. For this case, it follows from [1, Eqs 2.6 and 2.23] that the ijth element of F is given by

$$F_{ij} = 2\Re\left[\left(\frac{\partial \vec{\mu}}{\partial r_i} \right)^H \Lambda^{-1} \frac{\partial \vec{\mu}}{\partial r_j} \right] + \mathrm{tr}\left(\Lambda^{-1} \frac{\partial \Lambda}{\partial r_i} \Lambda^{-1} \frac{\partial \Lambda}{\partial r_j} \right), \tag{1.62}$$

where Λ and the derivatives are evaluated at the true value of the unknown parameter vector. Explicit expressions for the submatrices of F are given in Appendix A.

1.3.3 Constant-Envelope Signal Case

Using Equation (1.50), the symmetric Fisher information matrix F may be partitioned as

$$F = \begin{bmatrix} F_{\vec{u}\vec{u}} & F_{\vec{u}\vec{\alpha}} & F_{\vec{u}\vec{\phi}} \\ F_{\vec{\alpha}\vec{u}} & F_{\vec{\alpha}\vec{\alpha}} & F_{\vec{\alpha}\vec{\phi}} \\ F_{\vec{\phi}\vec{u}} & F_{\vec{\phi}\vec{\alpha}} & F_{\vec{\phi}\vec{\phi}} \end{bmatrix}$$

$$= \begin{bmatrix} F_{\vec{u}\vec{u}} & F_{\vec{u}\vec{\alpha}} & F_{\vec{u}\vec{\phi}_1} & \cdots & F_{\vec{u}\vec{\phi}_N} \\ F_{\vec{\alpha}\vec{u}} & F_{\vec{\alpha}\vec{\alpha}} & F_{\vec{\alpha}\vec{\phi}_1} & \cdots & F_{\vec{\alpha}\vec{\phi}_N} \\ F_{\vec{\phi}_1\vec{u}} & F_{\vec{\phi}_1\vec{\alpha}} & F_{\vec{\phi}_1\vec{\phi}_1} & \cdots & F_{\vec{\phi}_1\vec{\phi}_N} \\ \vdots & \vdots & \vdots & \ddots & \vdots \\ F_{\vec{\phi}_N\vec{u}} & F_{\vec{\phi}_N\vec{\alpha}} & F_{\vec{\phi}_N\vec{\phi}_1} & \cdots & F_{\vec{\phi}_N\vec{\phi}_N} \end{bmatrix}. \tag{1.63}$$

As in the generic-signal case, the observation is a complex circular Gaussian random vector with mean $\vec{\mu}$ and covariance Λ, so that the ijth element of F is again given by Equation (1.62). It is shown in Appendix B that the information matrix for the unknown constant-envelope signal case is easily constructed from the information matrix for the generic-signal case.

1.4 A BOUND ON DF OF STOCHASTIC SIGNALS

The bounds on estimation of u_1 derived in Section 1.3.2 and Section 1.3.3 depend, in general, on the specific complex amplitudes of the signals (as well as their directions) and apply to estimators which are differentially unbiased for u_1 (see Section 1.3.1). In this section, we will use this bound to obtain a lower bound on the variance of a more restricted class of estimators for the case where the complex amplitudes of the signals have a probabilistic distribution. This bound has the desirable property of not depending on the specific complex amplitudes of the signals.

Partition the parameter vector $\vec{r}$ into

$$\vec{r} = \begin{bmatrix} \vec{r}' \\ \vec{r}'' \end{bmatrix}. \tag{1.64}$$

We say that $\hat{\vec{r}}$ is globally differentially unbiased for $(\vec{r})_1$ with respect to $\vec{r}''$ and differentially unbiased with respect to $\vec{r}'$ at $\vec{r}_t'$ if

$$\left(\frac{\partial \vec{m}(\vec{r})}{\partial \vec{r}} \Big|_{\vec{r} = \begin{bmatrix} \vec{r}_t' \\ \vec{r}'' \end{bmatrix}} \right)_1 = \vec{0}_1 \tag{1.65}$$

holds for all possible $(\vec{r}'')$. Note that this implies that $(\vec{m}(\vec{r}_t', \vec{r}''))_1$ is constant with respect to $\vec{r}''$. For the remainder of this section, we will refer to this quantity as $m_1(\vec{r}_t')$.

In this section, we consider estimators of u_1 which are globally differentially unbiased with respect to the signal complex amplitudes as well as differentially unbiased with respect to the signal directions at $\vec{u}_t$. Note that the requirement of global differential unbiasedness with respect to the complex amplitudes essentially means that the estimator still treats the complex amplitudes as being unknown parameters rather than as having some known probability distribution.[3]

Let $\vec{r}''$ denote the parameters associated with the complex amplitudes. These parameters are now assumed to have some fixed probability distribution. Let $\vec{\zeta}$ denote the remainder of the random variables in the problem. Let $p(\vec{\zeta}, \vec{r}'')$ denote the joint probability density function of $\vec{\zeta}$ and $\vec{r}''$.

[3] An estimator which 'knows' the probability distribution of the complex amplitudes is said to be differentially unbiased for u_1 at $\vec{r}_t$ if it satisfies Equation (1.53) with $l = 1$ and $\vec{r}_t = \vec{u}_t$ (i.e., the unknown parameter vector does not include the complex amplitudes), where the expectation in the definition of $\vec{m}$ (Equation (1.51)) is taken with respect to the distribution of the complex amplitudes as well as the other random quantities in the problem. It can be shown that any estimator of u_1 which is globally differentially unbiased with respect to the signal complex amplitudes as well as differentially unbiased with respect to the signal directions also satisfies this condition. However, the converse statement is not true.

Let y be an unbiased (in the sense given above) estimator of the direction u_1. The mean of y with respect to the joint distribution of $\vec{\zeta}$ and $\vec{r}''$ is given by

$$\begin{aligned}\int y p(\vec{\zeta}, \vec{r}'')\, d\vec{\zeta}\, d\vec{r}'' &= \int_{\Omega} \left[\int_{Z} y p(\vec{\zeta}, \vec{r}'')\, d\vec{\zeta} \right] p(\vec{r}'')\, d\vec{r}'' \\ &= \int_{\Omega} m_1(\vec{r}_t') p(\vec{r}'')\, d\vec{r}'' \\ &= m_1(\vec{r}_t'). \end{aligned} \tag{1.66}$$

where Z denotes the domain of $\vec{\zeta}$, Ω denotes the domain of $\vec{r}''$, and the second equality follows by the comment after Equation (1.65). Let η^2 denote the variance of y with respect to $p(\vec{\zeta}, \vec{r}'')$. Let $s^2_{\vec{r}}$ denote the Cramér-Rao bound (obtained in Section 1.3.2 or Section 1.3.3) on the estimation of u_1 for the parameter vector $\vec{r}$. We have

$$\begin{aligned}\eta^2 &= \int y - m_1(\vec{r}_t')^2 p(\vec{\zeta}, \vec{r}'')\, d\vec{\zeta}\, d\vec{r}'' \\ &= \int_{\Omega} \left[\int_{Z} y - m_1(\vec{r}_t')^2 p(\vec{\zeta}, \vec{r}'')\, d\vec{\zeta} \right] p(\vec{r}'')\, d\vec{r}'' \\ &\geq \int_{\Omega} s^2_{\begin{bmatrix} \vec{r}' \\ \vec{r}'' \end{bmatrix}} p(\vec{r}'')\, d\vec{r}''. \end{aligned} \tag{1.67}$$

This is the desired lower bound on the variance of estimators of u_1 which are globally differentially unbiased with respect to the signal complex amplitudes and differentially unbiased with respect to the signal directions. In the sequel, we will evaluate this bound, which we term the 'integrated' bound. We will make a few exceptions to this, because, in some cases, the Cramér-Rao bounds derived in Section 1.3.2 and Section 1.3.3 turn out to be numerically independent of the specific complex amplitudes of the signals. In such cases, the integrated bound in Equation (1.67) is numerically identical to the Cramér-Rao bound which is obtained for any allowable set of complex amplitudes. In such cases, we find it useful to continue to refer to the relevant Cramér-Rao bound rather than the integrated bound. In what follows, the term Cramér-Rao bound will be used when and only when the integrated bound given by Equation (1.67) is not intended.

2. NUMERICAL EVALUATION OF THE BOUNDS

2.1 METHODS

2.1.1 Array Signal-to-Noise Power Ratio (ASNR)

In what follows, it is useful to define the ASNR of a given source. In our bound evaluations, we will consider only stationary stochastic signal sources. We define

$$\rho_s \stackrel{\text{def}}{=} E(|c_{ns}|^2);\ (n = 1, \ldots, N), (s = 1, \ldots, S), \tag{2.1}$$

where E denotes mathematical expectation.

Using Equation (1.28) in the absence of array errors and interferers, if one were to apply a complex M-vector of weights, $\vec{w}$, to the antenna element outputs at the nth look, one would obtain an array output of

$$\begin{aligned} y_n &= \vec{w}^H \vec{z}_n \\ &= \vec{w}^H \vec{v}_s c_{ns} + \vec{w}^H \vec{\kappa}_n. \end{aligned} \tag{2.2}$$

The first term in Equation (2.2) can be identified as the signal component of the array output and the second as the noise component. The signal-to-noise power ratio (SNR) at the array output can thus be defined as

$$\begin{aligned} \mathrm{SNR}_{\mathrm{out}} &\stackrel{\text{def}}{=} \frac{E(|\vec{w}^H \vec{v}_s c_{ns}|^2)}{E(|\vec{w}^H \vec{\kappa}_n|^2)} \\ &= \frac{|\vec{w}^H \vec{v}_s|^2 E(|c_{ns}|^2)}{\sigma^2 \|\vec{w}\|^2} \\ &= \frac{\rho_s}{\sigma^2} \frac{|\vec{w}^H \vec{v}_s|^2}{\|\vec{w}\|^2}. \end{aligned} \tag{2.3}$$

By the Schwarz inequality, the weights which maximize the output SNR are of the form $\beta \vec{v}_s$, where β is an arbitrary nonzero complex scalar. The resulting maximized output SNR is termed the ASNR:

$$\begin{aligned} \mathrm{ASNR} &\stackrel{\text{def}}{=} \max_{\vec{w}} \mathrm{SNR}_{\mathrm{out}} \\ &= \frac{\rho_s}{\sigma^2}, \end{aligned} \tag{2.4}$$

where, for convenience, we will assume in the sequel that the ideal array-response vectors, the $\{\vec{v}_s\}$, are of unit norm. Thus the ASNR of a given signal is defined as the maximum SNR obtainable for that signal at the output of the array in the absence of array errors and interferers.

2.1.2 Array-Response Vector Model

The ideal array response was modeled as that of a uniform linear array of $M = 10$ isotropic antenna elements. For this array, the mth component of $\vec{v}_s$ is equal to

$$\frac{1}{\sqrt{M}} e^{j2\pi d \sin\theta_s (m - m_0)/\lambda}, \quad (m = 1, \ldots, M), \tag{2.5}$$

[6, p. 72] where

$$m_0 \stackrel{\text{def}}{=} \frac{M+1}{2} \tag{2.6}$$

is the phase center of the array, λ is the wavelength of the carrier, d is the interelement spacing of the array (here 0.2λ), and θ_s is the angle of arrival of the sth signal relative to the broadside plane (defined as the plane that passes through the phase center of the array and is perpendicular to the array axis (see Figure 2-1)). Each $\vec{v}_s$ is of unit norm, as desired.

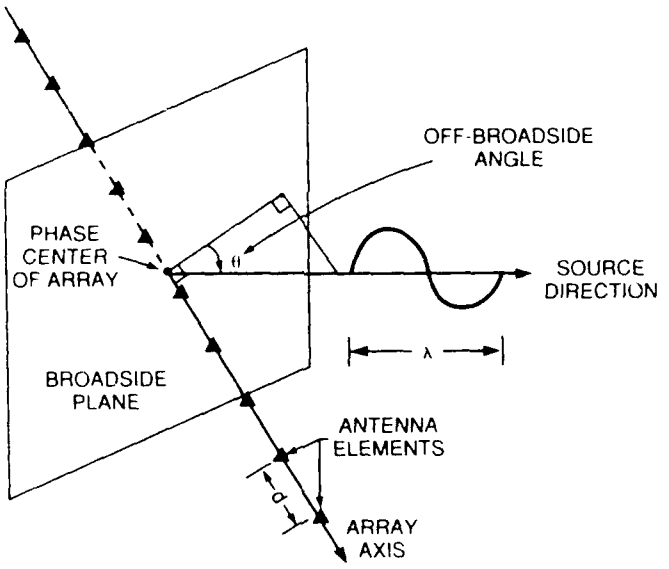

116880-58

Figure 2-1. Uniform linear array geometry.

We will use beamwidth (BW) units for angle of arrival, where the angle of arrival of the sth signal in BW is defined by

$$a_s \stackrel{\text{def}}{=} \frac{Md \sin\theta_s}{\lambda}. \tag{2.7}$$

The use of BW units is motivated as follows. In Section 2.1.1, we determined that, in the absence of array errors and interferers, the SNR at the output of the array could be maximized by selecting a weighting vector for the array element outputs which is a scalar multiple of the array-response vector of the source, i.e.,

$$\vec{w} = \beta \vec{v}_s \tag{2.8}$$

for some nonzero complex scalar β. Use of this array weighting vector is commonly termed conventional beamforming. If these weights were held constant while the source were moved away from direction u_s to direction u, then the output SNR of the array would change from the ASNR, ρ_s/σ^2, to (see Equation (2.3))

$$\begin{aligned} \mathrm{SNR}_{\mathrm{out}}(u) &= \frac{\rho_s}{\sigma^2} \frac{|\vec{w}^H \vec{v}(u)|^2}{\|\vec{w}\|^2} \\ &= \frac{\rho_s}{\sigma^2} |\vec{v}^H(u_s)\vec{v}(u)|^2. \end{aligned} \tag{2.9}$$

We thus obtain a 'gain pattern' for the array, as a function of the source direction, u. For the linear array which we have defined, this pattern is given by

$$\mathrm{SNR}_{\mathrm{out}}(u) = \frac{\rho_s}{\sigma^2} \left(\frac{\sin[\pi(u-u_s)]}{M \sin[\pi(u-u_s)/M]} \right)^2 \tag{2.10}$$

([6, p. 98], which, as expected, has its peak value of ρ_s/σ^2 at $u = u_s$, and also has its first nulls (i.e., directions of zero gain) for signals which are one BW away from u_s (i.e., for which $|u - u_s| = 1$). Use of BW units facilitates performance comparisons for arrays having different interelement spacings (e.g., note that Equation (2.10) is a function of u, but not of (d/λ)).

Array-error powers are given in dB relative to the elements of the ideal array-response vectors. Since the magnitude of each element of the $\vec{v}_s$ is $1/\sqrt{M}$, this means array errors of x dB correspond to an ϵ^2 of $\frac{1}{M} 10^{x/10}$. Approximate gain and phase error equivalents of various array-error powers are given in Table 2-1.[1]

2.1.3 Numerical Implementation of the Bound Calculations

We computed the integrated bounds given by Equation (1.67) with the s_r^2 derived in Sections 1.3.2 and 1.3.3. For evaluating the generic-signal bound, two classes of distribution functions on the signals were considered; we shall term these the random constant-envelope signal model and the Gaussian-signal model. In the random constant-envelope signal model, the signal waveforms were modeled as having phases that were independent (*look-to-look* and *signal-to-signal*) *random* variables uniformly distributed over the interval $[0, 2\pi)$ with a constant magnitude for each signal.

[1] The values in this table were obtained from a Monte Carlo simulation using 10^5 trials for each error power.

TABLE 2-1.

Approximate Standard Deviations of Gain and Phase Errors Induced in Each Antenna Element by Complex Gaussian Errors of Various Powers

Array-Error Power (dB)	Std. Dev. of Gain Error (dB)	Std. Dev. of Phase Error (°)
-30	1.9×10^{-1}	1.3
-25	3.5×10^{-1}	2.3
-20	6.2×10^{-1}	4.1
-15	1.1×10^{0}	7.3

In the Gaussian-signal model, the signal waveforms were modeled as being independent (look-to-look and signal-to-signal) complex Gaussian random variables with, possibly different, fixed powers for each signal. For evaluating the constant-envelope signal bound, we considered only the random constant-envelope signal model.

The Fisher information matrix for the generic-signal case was computed using Equations (A.22), (A.30), (A.31), (A.38), (A.39), and (A.40). The matrix Λ_N^{-1} was evaluated using Equation (1.36) or Equation (1.37), as appropriate. Note that evaluation of Λ_N^{-1} using Equation (1.36) requires the inversion of only an $S \times S$ matrix, not an $N \times N$ matrix. The information matrix for the constant-envelope signal case was computed from the information matrix for the generic-signal case using Equations (B.5), (B.7), and (B.9).

The Cramér-Rao bounds on DF for use in Equation (1.67) are given by the diagonal elements of the upper-left $S \times S$ submatrix of F^{-1} (see Section 1.3.1). This submatrix was computed according to the procedure outlined in Appendix C.

The expectation integral in the expression for the integrated bound [Equation (1.67)] was approximated by a Monte Carlo method using 3, 100, 1000, and 1000 Monte Carlo trials for experiments with 100, 10, 2, and 1 look(s), respectively. For each Monte Carlo trial, a sample value of the appropriate random signal was obtained using a pseudorandom number generator, and the Cramér-Rao bound for that sample value was computed using the procedure described above. The integrated bound was approximated by the mean of the Cramér-Rao bounds for the signals generated. (The number of Monte Carlo trials was varied as a function of looks since the bound took longer to compute when the number of looks became large and it was found that as the number of looks became large, the bound became relatively independent of the particular signal waveforms.) We also computed the standard error of the estimate (SEE) of this mean (i.e., the ratio

of the standard deviation of the Cramér-Rao bounds for the signals generated to the square root of the number of Monte Carlo trials) as an index of the error in the approximation. We expressed the SEE as a percentage of the mean.

2.2 RESULTS

For scenarios including thermal noise, we evaluated bounds for the following scenario parameters: two signals, 10 and 100 looks, signal-of-interest (SOI) ASNR's of 10, 30, and 50 dB relative to thermal noise, interferer ASNR's of 10, 30, and 50 dB, direction-dependent array error powers of $-\infty$, -30, -25, -20, and -15 dB and signal separations of 0.01, 0.0316, 0.1, 0.316, and 1.0 BW.

We also computed bounds on DF with direction-dependent errors in the absence of thermal noise. We shall refer to these bounds as array-errors-only bounds. Since, in the absence of thermal noise, the probability distribution function of the observation is singular for $N > S$ (where N is the number of looks and S is the number of signals), we restricted ourselves to scenarios where $N = S$ when thermal noise was absent. (Cramér-Rao bounds can be generalized to handle singular distributions, such as those that occur in the $N > S$ case here. Moreover, when this is done for generic signals, the array-errors-only bound in the $N > S$ case can be shown to be equal to the analogous bound in the $N = S$ case. However, the necessary analysis would take us too far afield, and so is not included here.)

Monte Carlo estimation of the expectation of the Cramér-Rao bound (see Section 2.1.3) was found to be quite satisfactory, with an SEE of the mean of the bound on variance of less than 9% in all cases. This corresponds approximately to an SEE of the mean of the bound on standard deviation of less than 5%. (To see this, note that a small fractional change a in x results in approximately a fractional change of $2a$ in x^2, since

$$\begin{aligned}(x \pm ax)^2 &= x^2 \pm 2ax^2 + a^2x^2 \\ &\approx x^2 \pm 2ax^2.)\end{aligned} \tag{2.11}$$

When the ASNR and/or number of looks was high, the SEE of the mean of the bound was much smaller.

2.2.1 Array-Errors-Only Bounds

In the one-signal, one-look case, it is easily shown from Equations (1.40) and (1.48) that the models, and hence the Cramér-Rao bounds for the unknown generic and constant-envelope signals, are identical. This also holds in the absence of thermal noise, when the only DF perturbations are caused by the array errors. In this case, the observation simply consists of an unknown scalar multiple of the perturbed array-response vector. It is shown in Appendix D that this bound is

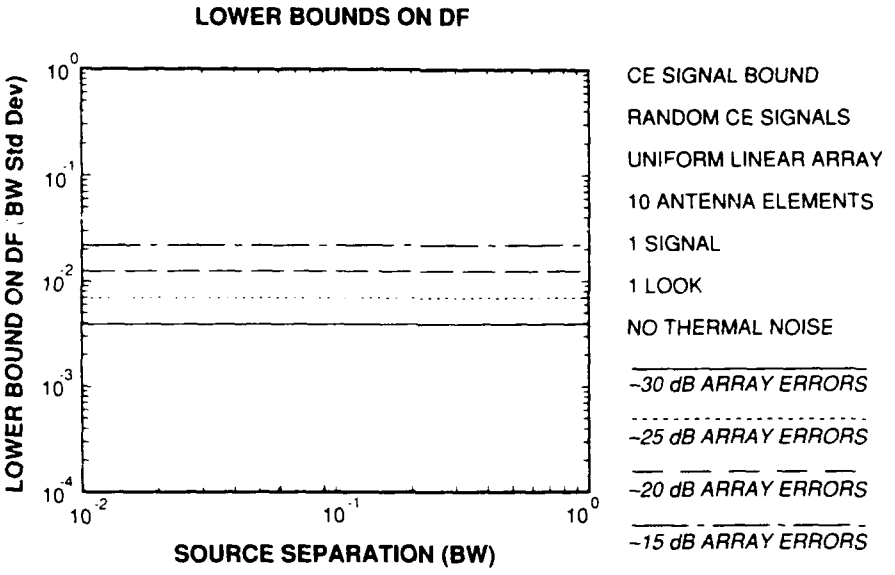

Figure 2-2. Generic or constant-envelope signal Cramér-Rao bounds - 1 signal, 1 look, no thermal noise.

independent of the signal waveform sample. The results of numerically evaluating this Cramér-Rao bound are presented in Figure 2-2.

In the two-signal, two-look case, the Cramér-Rao bound on DF of generic signals with array errors only was found numerically to be independent of the sample values of the signal waveforms, depending only on the power of the array errors and the signal separation. This bound is plotted in Figure 2-3. The bound increased with the power of the array errors, was largest at the 0.316 BW signal separation, and approached the one-signal, array-errors-only bound as the signal separation approached 0 (c.f., Figure 2-2). In contrast, the array-errors-only Cramér-Rao bound for constant-envelope signals was found to depend on the signal waveforms. The results of numerically evaluating the integrated version of this bound with random constant-envelope signals are presented in Figure 2-4. The bound attained a maximum at moderate signal separations (0.1 and 0.316 BW) and approached the one-signal, array-errors-only Cramér-Rao bound as the signal separation approached 0.

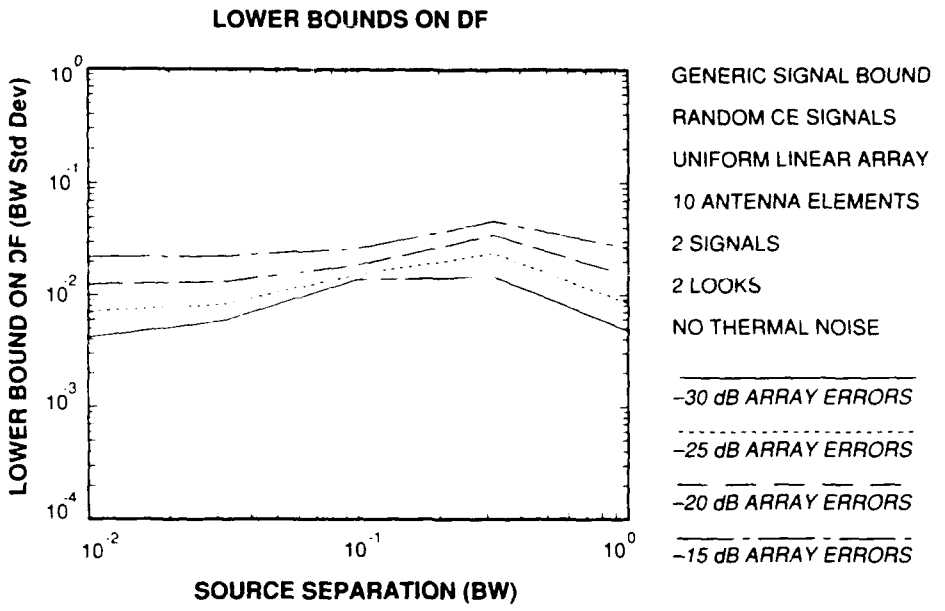

116880-2

Figure 2-3. Generic signal Cramér-Rao bounds - 2 signals, 2 looks, no thermal noise.

2.2.2 Integrated Generic-Signal Bound with Thermal Noise

2.2.2.1 Evaluation Using Random Constant-Envelope Signals

The results for this case are presented in Figures E-1 to E-18. They may be summarized as follows:

Effect of signal separation In the absence of array errors, the bound increased monotonically and unboundedly as the signal separation decreased. When array errors were included, the bound for signals at large separations generally increased, particularly for high SOI ASNR and a large number of looks. However, the bound for signals at small separations generally decreased. In addition, for a fixed power of array error, the bound became well behaved as the signal separation decreased. With all of the array-error powers tested, the bound generally was largest at moderate signal separations and smallest at the extreme separations of 0.01 and 1.0 BW.

Effect of array-error power With high SOI ASNR and numbers of looks, the bound decreased as the (nonzero) power of the array errors decreased. However, when the SOI ASNR and the number of looks were sufficiently small, the opposite occurred.

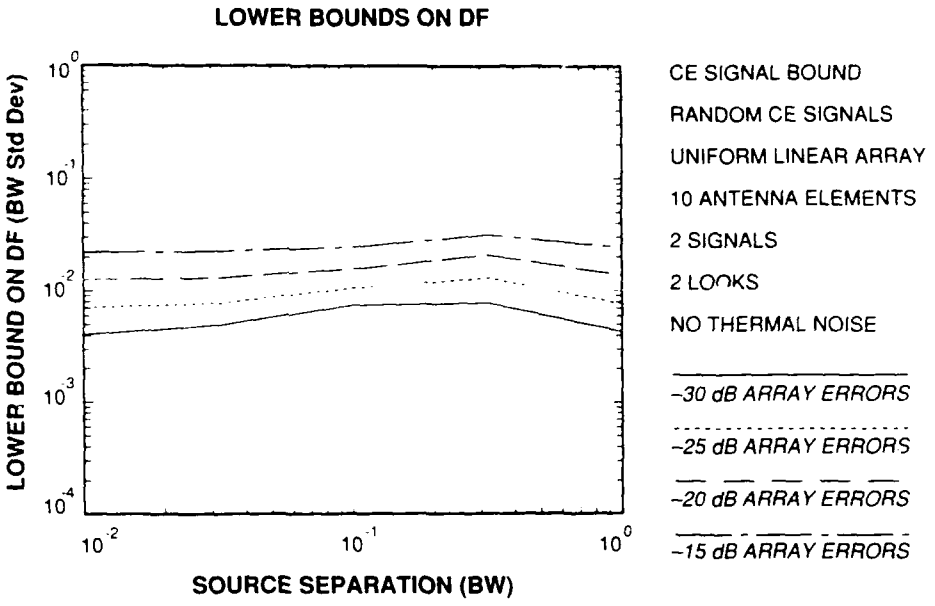

Figure 2-4. Constant-envelope signal bounds - 2 random constant-envelope signals, 2 looks, no thermal noise.

Effects of signal power and number of looks In the absence of array errors, the bound decreased as the power of the SOI or the number of looks increased. It was independent of the power of the interferer. In the presence of array errors, the bound continued to decrease as the power of the SOI or the number of looks increased when the SOI ASNR and number of looks were small. However, given a sufficient SOI ASNR and number of looks, the bound became almost independent of number of looks and signal powers, numerically approaching the two-signal, array-errors-only Cramér-Rao bound. The bound for a signal at a given power tended to decrease to a limiting value when the power of the other signal was increased. The tendency to decrease was most noticeable when the signal separations, the ASNR of both signals, the number of looks, and the array-error powers were small.

2.2.2.2 Evaluation Using Gaussian Signals

The results obtained by evaluating the generic-signal bound with Gaussian rather than random constant-envelope signals are presented in Figures E-19 to E-36. These results, though slighter higher in the 10-look cases, are qualitatively similar to the results for random constant-envelope signals.

2.2.3 Integrated Unknown Constant-Envelope Signal Bound with Thermal Noise

The results for this case are presented in Figures E-37 to E-54. They may be summarized as follows.

2.2.3.1 Effect of Signal Separation

In the absence of array errors, the bound had a very weak dependence on signal separation with a maximum at moderate signal separations. This pattern persisted in the presence of array errors, with the bound becoming numerically independent of signal separation, given sufficient SOI ASNR and number of looks. Both with and without array errors, the constant-envelope signal bounds were close to the analogous generic-signal bounds at a signal separation of one BW.

2.2.3.2 Effect of Array-Error Power

Unlike the generic-signal bound, the constant-envelope signal bound generally increased with increasing array-error power at all SOI ASNR's and numbers of looks.

2.2.3.3 Effects of Signal Power and Number of Looks

In the absence of array errors, the bound decreased with increasing power of the SOI or number of looks. In the presence of array errors, a similar pattern occurred when the SOI ASNR and number of looks were small. However, given sufficient SOI ASNR and number of looks, the bound numerically approached the one-signal, array-errors-only Cramér-Rao bound. Thus, in contrast to the limiting bound for the generic-signal case, the limiting bound for the constant-envelope case was independent of signal separation. The bounds (with and without array errors) showed little variation with the power of the interferer. The constant-envelope signal bounds tended to be more optimistic than the generic-signal bounds. When array errors were present, this difference was most noticeable at moderate signal separations, when the SOI ASNR and number of looks were low and the array errors were small. When array errors were absent, this difference was largest at small signal separations and quite significant at all ASNRs and numbers of looks examined.

2.3 DISCUSSION

Several aspects of the results bear some discussion. One significant aspect is the tendency of the bound on DF of a generic signal to decrease as the power of the generic interferer increases. This may be due to the fact that the subspace spanned by the array-response vectors (i.e., the signal subspace) becomes easier to estimate as the power of the interferer increases. While the bound is not necessarily achievable, it suggests that the presence of direction-dependent errors does not preclude accurate DF of signals at low signal-to-interference power ratios.

Another significant aspect is that the presence of small array errors improved the bound on DF of generic signals at small signal separations. This finding may be due, in part, to the fact that array errors increase the mean distance (in complex M-space) between the actual array-response vectors of the signals and thus result in an apparent increase in signal separation. However, the increase in mean distance between the array-response vectors does not entirely explain this phenomenon, since the bound with array errors actually decreased significantly as the signal separation went from moderate to small. While the bound is again not necessarily achievable, it is consistent with the possibility of performing DF with direction-dependent errors and small signal separations.

In the generic-signal case, the integrated bound on DF of 2 signals with array errors and thermal noise approached the 2-signal, array-errors-only Cramér-Rao bound as the SOI ASNR and the number of looks became sufficiently high. The array-errors-only Cramér-Rao bound was found to be independent of the signal waveforms, depending only on the power of the array errors and the signal separation. This finding is consistent with the notion that, given a sufficient SOI ASNR and number of looks, the array errors are the dominant factor limiting DF. The array-errors-only Cramér-Rao bound was found to be markedly different from the integrated bound on DF with thermal noise, but no array errors, with respect to its dependence on signal separation. The latter bound increased sharply as the signal separation decreased, while the former did not. In fact, the array-errors-only Cramér-Rao bound for two signals approached the array-errors-only Cramér-Rao bound for a single signal as the signal separation approached zero. This latter bound is independent of the signal waveforms, depending only on the power of the array errors, and is identical for generic and constant-envelope signals (see Section 2.2.1).

With respect to the integrated bound for constant-envelope signals, the results are significant in that, in many cases, in spite of the presence of array errors, the bound remained more optimistic than the analogous bound for generic signals, particularly in scenarios with moderate signal separations, small array errors, and a low SOI ASNR and number of looks. This suggests some potential improvement in DF still exists through use of the constant-envelope signal assumption in the presence of small direction-dependent errors, though not to the extent that is true in the absence of errors.

In the constant-envelope signal case, the integrated bound on DF of 2 signals with array errors and thermal noise approached the single-signal, array-errors-only Cramér-Rao bound as the SOI ASNR and number of looks became sufficiently high. The latter bound is simply the bound on DF of a signal given an observation consisting of an unknown scalar multiple of the perturbed array-response vector of that signal (see Section 2.2.1). This finding is consistent with the notion that, given a sufficient SOI ASNR and number of looks, the array-response vector of the SOI becomes determinable to within a complex scalar. Since the dependence of the observation on the direction occurs only through this vector and the array errors on this vector were modeled as independent of all the other random quantities in the problem, we may conclude that the interfering signal has little degrading impact on DF.

3. CONCLUSIONS

Cramér-Rao lower bounds, on the variance of unbiased DF algorithms, were derived for unknown generic and constant-envelope signals received with complex Gaussian direction-dependent array errors and thermal noise. These bounds were, in general, functions of the specific complex amplitudes of the signals. The Cramér-Rao bounds were used to obtain other lower bounds, which we term integrated bounds, on the variance of DF algorithms for the case where the complex amplitudes of the signals have a probabilistic distribution which is unknown to the algorithm. The integrated bounds have the desirable property of not depending on the specific complex amplitudes of the signals. In some cases, the Cramér-Rao bounds on DF turn out to be functionally independent of the specific complex amplitudes of the signals. In such cases, the integrated bound is numerically identical to the Cramér-Rao bound which is obtained for any allowable set of complex amplitudes. We evaluated the bounds under various conditions, for up to two generic or constant-envelope signals. Those Cramér-Rao bounds which were independent of the specific complex amplitudes of the signals were evaluated exactly, while the integrated bounds were evaluated using a Monte Carlo simulation to approximate expectation integrals with respect to the probability distributions of the complex amplitudes [see Equation (1.67)]. The behavior of the bounds is briefly summarized below; nonzero array-error powers are assumed unless otherwise noted.

1. Unknown generic-signal bound:

   (a) The integrated bound tends to decrease with increasing interferer power, approaching a limiting value as the power of the interferer gets large.

   (b) At small signal separations, the integrated bound without array errors increases unboundedly as the signal separation decreases. The addition of small array errors results in a marked decrease in the integrated bound at small signal separations, with the bound becoming well behaved as the signal separation decreases. These results suggest that the presence of array errors may actually improve DF of closely spaced signals.

   (c) With a sufficiently large SOI ASNR and number of looks, the integrated bound for two signals approaches the Cramér-Rao bound for DF of two signals (given two looks) with array errors only. The latter bound was numerically independent of the complex amplitudes of the signals.

   (d) The array-errors-only bound on DF of two signals (given two looks) depends only on the power of the array errors and the signal separation. The bound increases with the power of the array errors, is largest at moderate signal separations, and approaches the single-signal (one-look)

bound as the signal separation approaches 0. The latter bound is also independent of the signal waveform.

2. Unknown constant-envelope signal bound:

   (a) The integrated bounds, both with and without array errors, are only weakly dependent on the power of the interferer and signal separation, and are close to the analogous bounds for generic signals at a signal separation of one BW.

   (b) With no array errors, the integrated bound for constant-envelope signals is far more optimistic at small signal separations than the integrated bound for generic signals, as can be concluded from observations (1b) and (2a) above. With array errors, the integrated bound for constant-envelope signals is still somewhat more optimistic than the analogous bound for generic signals, particularly at small array errors, low SOI ASNR and numbers of looks, and moderate signal separations.

   (c) With a sufficiently large SOI ASNR and number of looks, the integrated bound for two signals approaches the Cramér-Rao bound for DF of one signal with array errors only. The latter bound is identical to that for a single generic signal, discussed in (1d) above.

4. FUTURE WORK

For practical applications, it would be useful to have bounds with more realistic models for the direction-dependent errors. For example, one should allow for errors of unknown, possibly different variances for each signal with possible element-to-element and/or signal-to-signal error correlations. One should also incorporate other error sources into the model, such as multiplicative direction-independent errors and deviations of the signals from perfect constant-envelopeness. Finally, arrays designed to have different response vectors for, say, vertically vs. horizontally polarized sources could have different sensitivities to the various error sources, in terms of their DF capabilities.

APPENDIX A
THE INFORMATION MATRIX FOR GENERIC SIGNALS

In the derivation that follows, we shall use a number of defined terms. For the convenience of the reader, we list a number of these here.

We define the $S \times S$ matrices W, $\dot{W}$, and $\ddot{W}$ by

$$W \stackrel{\text{def}}{=} V^H V, \tag{A.1}$$

$$\dot{W} \stackrel{\text{def}}{=} V^H \dot{V}, \tag{A.2}$$

and

$$\ddot{W} \stackrel{\text{def}}{=} \dot{V}^H \dot{V} \tag{A.3}$$

(the notations $\dot{W}$ and $\ddot{W}$ are mnemonic only: they do not indicate derivatives of W), the $S \times S$ Hermitian matrix P by

$$P \stackrel{\text{def}}{=} C^H \Lambda_N^{-1} C, \tag{A.4}$$

the $S \times N$ matrix Q by

$$Q \stackrel{\text{def}}{=} C^H \Lambda_N^{-1}, \tag{A.5}$$

the S-vector $\vec{q}_n$ by

$$\vec{q}_n \stackrel{\text{def}}{=} Q_{\cdot n}, \tag{A.6}$$

the $S \times S$ matrices D_n by

$$D_n \stackrel{\text{def}}{=} 2(\vec{v}_n \vec{q}_n^T) \square \dot{W}^*, \tag{A.7}$$

the $S \times S$ Hermitian matrix B by

$$B \stackrel{\text{def}}{=} W + M\epsilon^4 P^*, \tag{A.8}$$

the $S \times S$ matrices $G_{nn'}$ by

$$G_{nn'} \stackrel{\text{def}}{=} 2(\Lambda_N^{-1})_{nn'} (\vec{v}_n^* \vec{v}_{n'}^T) \square B, \tag{A.9}$$

and the $S \times S$ matrices $H_{nn'}$ by

$$H_{nn'} \stackrel{\text{def}}{=} 2M\epsilon^4 (\vec{v}_n \vec{v}_{n'}^T) \square (\vec{q}_{n'} \vec{q}_n^T). \tag{A.10}$$

When $\sigma^2 > 0$, P is given explicitly by

$$\begin{aligned} P &= \frac{1}{\sigma^2} C^H [I_N - \frac{\epsilon^2}{\sigma^2} C (I_S + \frac{\epsilon^2}{\sigma^2} C^H C)^{-1} C^H] C \quad \text{(Eq. 1.36)} \\ &= \frac{1}{\sigma^2} C^H C - \frac{\epsilon^2}{\sigma^4} C^H C (I_S + \frac{\epsilon^2}{\sigma^2} C^H C)^{-1} C^H C. \end{aligned} \tag{A.11}$$

When $\sigma^2 = 0$, $N = S$, and $\epsilon^2 > 0$, P is given explicitly by

$$\begin{aligned} P &= \frac{1}{\epsilon^2} C^H C^{-H} C^{-1} C \quad \text{(Eq. 1.37)} \\ &= \frac{1}{\epsilon^2} I_S. \end{aligned} \tag{A.12}$$

We will now derive an explicit expression for the Fisher information matrix in the generic-signal case. The derivatives in Equation (1.62) are given by

$$\frac{\partial \vec{\mu}}{\partial r_i} = (\frac{\partial C}{\partial r_i} \otimes V + C \otimes \frac{\partial V}{\partial r_i}) \vec{1}_S \tag{A.13}$$

and

$$\begin{aligned} \frac{\partial \Lambda}{\partial r_i} &= \epsilon^2 (\frac{\partial C}{\partial r_i} C^H + C \frac{\partial C^H}{\partial r_i}) \otimes I_M \\ &= \epsilon^2 \left[\frac{\partial C}{\partial r_i} C^H + C \left(\frac{\partial C}{\partial r_i} \right)^H \right] \otimes I_M. \end{aligned} \tag{A.14}$$

Evaluating these equations for the various components of $\vec{r}$, one obtains

$$\frac{\partial \vec{\mu}}{\partial u_s} = (C \otimes V E_{ss}) \vec{1}_S \quad \text{([2, Eq. 1.29])}. \tag{A.15}$$

$$\begin{aligned} \frac{\partial \vec{\mu}}{\partial a_{ns}} &= (\frac{\partial C}{\partial a_{ns}} \otimes V) \vec{1}_S \\ &= \frac{\partial c_{ns}}{\partial a_{ns}} (E_{ns} \otimes V) \vec{1}_S, \end{aligned} \tag{A.16}$$

$$\begin{aligned} \frac{\partial \vec{\mu}}{\partial \omega_{ns}} &= (\frac{\partial C}{\partial \omega_{ns}} \otimes V) \vec{1}_S \\ &= \frac{\partial c_{ns}}{\partial \omega_{ns}} (E_{ns} \otimes V) \vec{1}_S, \end{aligned} \tag{A.17}$$

$$\frac{\partial \Lambda}{\partial u_s} = 0_{NM}. \tag{A.18}$$

$$\begin{aligned}\frac{\partial \Lambda}{\partial a_{ns}} &= \epsilon^2 \left[\frac{\partial C}{\partial a_{ns}} C^H + C \left(\frac{\partial C}{\partial a_{ns}} \right)^H \right] \otimes I_M \\ &= \epsilon^2 \left[\frac{\partial c_{ns}}{\partial a_{ns}} E_{ns} C^H - \left(\frac{\partial c_{ns}}{\partial a_{ns}} \right)^* C E_{sn} \right] \otimes I_M. \end{aligned} \tag{A.19}$$

and

$$\begin{aligned}\frac{\partial \Lambda}{\partial c_{ns}} &= \epsilon^2 \left[\frac{\partial C}{\partial c_{ns}} C^H + C \left(\frac{\partial C}{\partial c_{ns}} \right)^H \right] \otimes I_M \\ &= \epsilon^2 \left[\frac{\partial c_{ns}}{\partial c_{ns}} E_{ns} C^H - \left(\frac{\partial c_{ns}}{\partial c_{ns}} \right)^* C E_{sn} \right] \otimes I_M. \end{aligned} \tag{A.20}$$

We shall now evaluate the $F_{\vec{\beta}\vec{\beta}'}$ starting with $F_{\vec{u}\vec{u}}$. Substituting into Equation (1.62) gives

$$\begin{aligned}(F_{\vec{u}\vec{u}})_{ss'} &= 2\Re \left[\left(\frac{\partial \vec{\mu}}{\partial u_s} \right)^H \Lambda^{-1} \frac{\partial \vec{\mu}}{\partial u_{s'}} \right] \\ &= 2\Re \left[\vec{1}_S^H (C \dot{+} \dot{V} E_{ss})^H (\Lambda_N^{-1} \otimes I_M)(C \dot{+} \dot{V} E_{s's'}) \vec{1}_S \right] \\ &= 2\Re \left[\vec{1}_S^H (C^H \Lambda_N^{-1} C) \dot{\square} (E_{ss}^H \dot{V}^H \dot{V} E_{s's'}) \vec{1}_S \right] \quad \text{(Eq. 1.18)} \\ &= 2\Re \left[\vec{1}_S^H P \dot{\square} (E_{ss}^H \ddot{W} E_{s's'}) \vec{1}_S \right] \quad \text{(Eqs. A.4 and A.3)} \\ &= 2\Re \left[\vec{1}_S^H P \dot{\square} (\ddot{W})_{ss'} E_{ss'} \right] \vec{1}_S \quad \text{(2. Eq. 1.32)} \\ &= 2\Re \left[\vec{1}_S^H (P)_{ss'} (\ddot{W})_{ss'} E_{ss'} \vec{1}_S \right] \\ &= 2\Re \left[(P)_{ss'} (\ddot{W})_{ss'} \right]. \end{aligned} \tag{A.21}$$

so that

$$F_{\vec{u}\vec{u}} = 2\Re(P \dot{\square} \ddot{W}). \tag{A.22}$$

Next we address the $F_{\vec{\beta}_n \vec{u}}$, where $\vec{\beta}_n$ equals $\vec{a}_n$ or $\vec{c}_n$. Define b_{ns} and $\vec{b}_n$ by

$$b_{ns} \stackrel{\text{def}}{=} \frac{\partial c_{ns}}{\partial \beta_{ns}} \tag{A.23}$$

and

$$\vec{b}_n \stackrel{\text{def}}{=} \begin{bmatrix} b_{n1} & b_{n2} & \cdots & b_{nS} \end{bmatrix}^T. \tag{A.24}$$

Thus for $\vec{\beta}_n = \vec{a}_n$,

$$\vec{b}_n = \vec{c}_n \quad \text{(Eqs. 1.40 and 1.45).} \tag{A.25}$$

while for $\vec{\beta}_n = \vec{\phi}_n$,

$$\vec{b}_n = j\vec{a}_n \boxdot \vec{c}_n \quad \text{(Eqs. 1.40 and 1.45).} \tag{A.26}$$

Substituting into Equation (1.62) gives

$$\begin{aligned}
(F_{\vec{\beta}_n \vec{u}})_{ss'} &= 2\Re\left[\left(\frac{\partial \vec{\mu}}{\partial \beta_{ns}}\right)^H \Lambda^{-1} \frac{\partial \vec{\mu}}{\partial u_{s'}}\right] && \text{(A.27)} \\
&= 2\Re\left[b_{ns}^* \vec{1}_S^H (E_{ns} \otimes V)^H (\Lambda_N^{-1} \otimes I_M)\right. \\
&\quad \left. \times (C \otimes V E_{s's'}) \vec{1}_S\right] \quad \text{(Eqs. A.15, A.17 and A.16)} \\
&= 2\Re\left[b_{ns}^* \vec{1}_S^H [(E_{sn} \Lambda_N^{-1} C) \boxdot (V^H V E_{s's'})] \vec{1}_S\right] \quad \text{(Eq. 1.18)} \\
&= 2\Re\left[b_{ns}^* \vec{1}_S^H [(E_{sn} Q^H) \boxdot (\dot{W} E_{s's'})] \vec{1}_S\right] \quad \text{(Eqs. A.2 and A.5)} \\
&= 2\Re\left[b_{ns}^* \vec{1}_S^H (Q^H)_{ns'} (\dot{W})_{ss'} E_{ss'} \vec{1}_S\right] \quad \text{(Eq. 1.13)} \\
&= 2\Re\left[b_{ns}^* (Q^H)_{ns'} (\dot{W})_{ss'}\right] \\
&= 2\Re\left[b_{ns}^* (Q)_{s'n}^* (\dot{W})_{ss'}\right] \\
&= 2\Re\left\{[b_{ns}(Q)_{s'n}]^* (\dot{W})_{ss'}\right\} \\
&= 2\Re\left\{[b_{ns}(\vec{q}_n)_{s'}]^* (\dot{W})_{ss'}\right\} \quad \text{(Eq. A.6)} \\
&= 2\Re\left\{(\vec{b}_n^* \vec{q}_n^H)_{ss'} (\dot{W})_{ss'}\right\} \\
&= 2\Re\left\{(\vec{b}_n \vec{q}_n^T)_{ss'} (\dot{W}^*)_{ss'}\right\}. && \text{(A.28)}
\end{aligned}$$

Thus

$$F_{\vec{\beta}_n \vec{u}} = 2\Re[(\vec{b}_n \vec{q}_n^T) \boxdot \dot{W}^*]. \tag{A.29}$$

Substituting for the $\vec{\beta}_n$, one obtains

$$\begin{aligned}
F_{\vec{a}_n \vec{u}} &= 2\Re[(\vec{c}_n \vec{q}_n^T) \boxdot \dot{W}^*] \quad \text{(Eq. A.25)} \\
&= \Re(D_n) \quad \text{(Eq. A.7)} && \text{(A.30)}
\end{aligned}$$

and

$$\begin{aligned}
F_{\vec{\sigma}_n \vec{u}} &= 2\Re\{[(j\vec{a}_n \Box \vec{\iota}_n)\vec{q}_n^T] \Box \dot{W}^*\} \quad \text{(Eq. A.26)} \\
&= 2\Re\{[(\vec{a}_n \Box \vec{\iota}_n)\vec{q}_n^T] \Box \dot{W}^*\} \\
&= -2\Im\{[(\vec{a}_n \Box \vec{\iota}_n)\vec{q}_n^T] \Box \dot{W}^*\} \\
&= -2\Im\{[(\vec{a}_n \Box \vec{\iota}_n)(\vec{1}_S^T \Box \vec{q}_n^T)] \Box \dot{W}^*\} \\
&= -2\Im\{[(\vec{a}_n \Box \vec{\iota}_n)(\vec{1}_S \Box \vec{q}_n)^T] \Box \dot{W}^*\} \quad \text{(Eq. 1.11)} \\
&= -2\Im\{(\vec{a}_n \vec{1}_S^T) \Box (\vec{\iota}_n \vec{q}_n^T) \Box \dot{W}^*\} \quad \text{(Eq. 1.12)} \\
&= -(\vec{a}_n \vec{1}_S^T) \Box 2\Im[(\vec{\iota}_n \vec{q}_n^T) \Box \dot{W}^*] \quad \text{(Eq. 1.10)} \\
&= -(\vec{a}_n \vec{1}_S^T) \Box \Im(D_n) \quad \text{(Eq. A.7).}
\end{aligned} \tag{A.31}$$

Lastly we address the $F_{\vec{\beta}_n \vec{\gamma}_{n'}}$, where $\vec{\beta}_n$ is equal to $\vec{a}_n$ or $\vec{o}_n$ and $\vec{\gamma}_{n'}$ is equal to $\vec{a}_{n'}$ or $\vec{o}_{n'}$. Define g_{ns} and $\vec{g}_n$ by

$$g_{ns} \stackrel{\text{def}}{=} \frac{\partial c_{ns}}{\partial \gamma_{ns}} \tag{A.32}$$

and

$$\vec{g}_n \stackrel{\text{def}}{=} \begin{bmatrix} g_{n1} & g_{n2} & \cdots & g_{nS} \end{bmatrix}^T. \tag{A.33}$$

Substituting into Equation (1.62) gives

$$(F_{\vec{\beta}_n \vec{\gamma}_{n'}})_{ss'} = 2\Re\left[\left(\frac{\partial \vec{\mu}}{\partial \beta_{ns}}\right)^H \Lambda^{-1} \frac{\partial \vec{\mu}}{\partial \gamma_{n's'}}\right] + \operatorname{tr}\left(\Lambda^{-1} \frac{\partial \Lambda}{\partial \beta_{ns}} \Lambda^{-1} \frac{\partial \Lambda}{\partial \gamma_{n's'}}\right). \tag{A.34}$$

The left-hand term evaluates to

$$\begin{aligned}
&2\Re\left[\left(\frac{\partial \vec{\mu}}{\partial \beta_{ns}}\right)^H \Lambda^{-1} \frac{\partial \vec{\mu}}{\partial \gamma_{n's'}}\right] \\
&= 2\Re\left[b_{ns}^* g_{n's'} \vec{1}_S^H (E_{ns} \otimes V)^H (\Lambda_N^{-1} \otimes I_M)(E_{n's'} \otimes V) \vec{1}_S\right] \\
&= 2\Re\left[b_{ns}^* g_{n's'} \vec{1}_S^H [(E_{sn} \Lambda_N^{-1} E_{n's'}) \Box (V^H V)] \vec{1}_S\right] \quad \text{(Eq. 1.18)} \\
&= 2\Re\left[b_{ns}^* g_{n's'} \vec{1}_S^H [(\Lambda_N^{-1})_{nn'} (E_{ss'}) \Box W] \vec{1}_S\right] \quad \text{([2, Eq. 1.31] and Eq. A.1)} \\
&= 2\Re\left[(\vec{b}_n^* \vec{g}_{n'}^T)_{ss'} (\Lambda_N^{-1})_{nn'} (W)_{ss'}\right] \\
&= \left(2\Re\left\{(\Lambda_N^{-1})_{nn'} [(\vec{b}_n^* \vec{g}_{n'}^T) \Box W]\right\}\right)_{ss'}.
\end{aligned} \tag{A.35}$$

The right-hand term evaluates to

$$
\begin{aligned}
&\mathrm{tr}\left(\Lambda^{-1}\frac{\partial\Lambda}{\partial\beta_{ns}}\Lambda^{-1}\frac{\partial\Lambda}{\partial\gamma_{n's'}}\right)\\
&= \mathrm{tr}\left\{(\Lambda_N^{-1}\otimes I_M)\epsilon^2\left[\frac{\partial c_{ns}}{\partial\beta_{ns}}E_{ns}C^H+\left(\frac{\partial c_{ns}}{\partial\beta_{ns}}\right)^* CE_{sn}\right]\otimes I_M\right](\Lambda_N^{-1}\otimes I_M)\\
&\quad\times\left[\epsilon^2\left[\frac{\partial c_{n's'}}{\partial\gamma_{n's'}}E_{n's'}C^H+\left(\frac{\partial c_{n's'}}{\partial\gamma_{n's'}}\right)^* CE_{s'n'}\right]\otimes I_M\right]\}\quad\text{(Eq. A.15 and A.20)}\\
&= \epsilon^4\,\mathrm{tr}\left\{\left[\Lambda_N^{-1}(b_{ns}E_{ns}C^H+b_{ns}^*CE_{sn})\right.\right.\\
&\quad\left.\left.\times\Lambda_N^{-1}(g_{n's'}E_{n's'}C^H+g_{n's'}^*CE_{s'n'})\right]\otimes I_M\right\}\quad\text{(Eq. 1.7)}\\
&= \epsilon^4\,\mathrm{tr}\left[(b_{ns}g_{n's'}\Lambda_N^{-1}E_{ns}C^H\Lambda_N^{-1}E_{n's'}C^H+b_{ns}g_{n's'}^*\Lambda_N^{-1}E_{ns}C^H\Lambda_N^{-1}CE_{s'n'}\right.\\
&\quad\left.-b_{ns}^*g_{n's'}\Lambda_N^{-1}CE_{sn}\Lambda_N^{-1}E_{n's'}C^H+b_{ns}^*g_{n's'}^*\Lambda_N^{-1}CE_{sn}\Lambda_N^{-1}CE_{s'n'})\otimes I_M\right]\\
&= M\epsilon^4\,\mathrm{tr}\,(b_{ns}g_{n's'}\Lambda_N^{-1}E_{ns}C^H\Lambda_N^{-1}E_{n's'}C^H+b_{ns}g_{n's'}^*\Lambda_N^{-1}E_{ns}C^H\Lambda_N^{-1}CE_{s'n'}\\
&\quad-b_{ns}^*g_{n's'}\Lambda_N^{-1}CE_{sn}\Lambda_N^{-1}E_{n's'}C^H+b_{ns}^*g_{n's'}^*\Lambda_N^{-1}CE_{sn}\Lambda_N^{-1}CE_{s'n'})\quad\text{([2. p.30])}\\
&= M\epsilon^4\,\mathrm{tr}\,(b_{ns}g_{n's'}\Lambda_N^{-1}E_{ns}C^H\Lambda_N^{-1}E_{n's'}C^H+b_{ns}g_{n's'}^*\Lambda_N^{-1}E_{ns}C^H\Lambda_N^{-1}CE_{s'n'}\\
&\quad-b_{ns}^*g_{n's'}E_{n's'}C^H\Lambda_N^{-1}CE_{sn}\Lambda_N^{-1}+b_{ns}^*g_{n's'}^*CE_{s'n'}\Lambda_N^{-1}CE_{sn}\Lambda_N^{-1})\quad\text{(Eq. 1.1)}\\
&= 2M\epsilon^4\Re\left[\mathrm{tr}\left(b_{ns}g_{n's'}\Lambda_N^{-1}E_{ns}C^H\Lambda_N^{-1}E_{n's'}C^H\right.\right.\\
&\quad\left.\left.-b_{ns}^*g_{n's'}E_{n's'}C^H\Lambda_N^{-1}CE_{sn}\Lambda_N^{-1}\right)\right]\\
&= 2M\epsilon^4\Re\left[\mathrm{tr}\left(b_{ns}g_{n's'}E_{ns}C^H\Lambda_N^{-1}E_{n's'}C^H\Lambda_N^{-1}\right.\right.\\
&\quad\left.\left.-b_{ns}^*g_{n's'}E_{n's'}C^H\Lambda_N^{-1}CE_{sn}\Lambda_N^{-1}\right)\right]\quad\text{(Eq. 1.1)}\\
&= 2M\epsilon^4\Re\left[\mathrm{tr}\,(b_{ns}g_{n's'}E_{ns}QE_{n's'}Q\right.\\
&\quad\left.-b_{ns}^*g_{n's'}E_{n's'}PE_{sn}\Lambda_N^{-1})\right]\quad\text{(Eqs. A.4 and A.5)}\\
&= 2M\epsilon^4\Re\left[\mathrm{tr}\,(b_{ns}g_{n's'}(Q)_{sn'}E_{ns'}Q\right.\\
&\quad\left.-b_{ns}^*g_{n's'}(P)_{s's}E_{n'n}\Lambda_N^{-1})\right]\quad\text{([2. Eq. 1.31])}\\
&= 2M\epsilon^4\Re\left[b_{ns}g_{n's'}(Q)_{sn'}(Q)_{s'n}+b_{ns}^*g_{n's'}(P)_{s's}(\Lambda_N^{-1})_{nn'}\right]\quad\text{(Eqs. 1.2 and 1.1)}\\
&= 2M\epsilon^4\Re\left[(\vec{b}_n\vec{g}_{n'}^T)_{ss'}(\vec{q}_{n'}\vec{q}_n^T)_{ss'}+(\vec{b}_n^*\vec{g}_{n'}^T)_{ss'}(P^*)_{ss'}(\Lambda_N^{-1})_{nn'}\right]\\
&= \left(2M\epsilon^4\Re\left\{\left[(\vec{b}_n\vec{g}_{n'}^T)\Box(\vec{q}_{n'}\vec{q}_n^T)\right]+(\Lambda_N^{-1})_{nn'}(\vec{b}_n^*\vec{g}_{n'}^T)\Box(P^*)\right\}\right)_{ss'}.\qquad\text{(A.36)}
\end{aligned}
$$

Thus the $F_{\vec{\beta}_n\vec{\gamma}_{n'}}$ are given by

$$\begin{aligned}
F_{\vec{\beta}_n\vec{\gamma}_{n'}} &= 2\Re\{(\Lambda_N^{-1})_{nn'}(\vec{b}_n^*\vec{g}_{n'}^T)\Box W \\
&\quad + M\epsilon^4[(\vec{b}_n\vec{g}_{n'}^T)\Box(\vec{q}_{n'}\vec{q}_n^T) + (\Lambda_N^{-1})_{nn'}(\vec{b}_n^*\vec{g}_{n'}^T)\Box P^*]\} \\
&= 2\Re\{(\Lambda_N^{-1})_{nn'}(\vec{b}_n^*\vec{g}_{n'}^T)\Box(W + M\epsilon^4 P^*) \\
&\quad + M\epsilon^4(\vec{b}_n\vec{g}_{n'}^T)\Box(\vec{q}_{n'}\vec{q}_n^T)\} \\
&= 2\Re\{(\Lambda_N^{-1})_{nn'}(\vec{b}_n^*\vec{g}_{n'}^T)\Box B + M\epsilon^4(\vec{b}_n\vec{g}_{n'}^T)\Box(\vec{q}_{n'}\vec{q}_n^T)\} \quad \text{(Eq. A.8)}.
\end{aligned} \tag{A.37}$$

Substituting for the $\vec{\beta}_n$ and $\vec{\gamma}_{n'}$, one obtains

$$\begin{aligned}
F_{\vec{\alpha}_n\vec{a}_{n'}} &= 2\Re\{(\Lambda_N^{-1})_{nn'}(\vec{\psi}_n^*\vec{\psi}_{n'}^T)\Box B + M\epsilon^4(\vec{\psi}_n\vec{\psi}_{n'}^T)\Box(\vec{q}_{n'}\vec{q}_n^T)\} \\
&= \Re(G_{nn'} + H_{nn'}) \quad \text{(Eqs. A.9 and A.10)}.
\end{aligned} \tag{A.38}$$

$$\begin{aligned}
F_{\vec{\phi}_n\vec{a}_{n'}} &= 2\Re\{(\Lambda_N^{-1})_{nn'}[(j\vec{a}_n\Box\vec{\psi}_n)^*\vec{\psi}_{n'}^T]\Box B \\
&\quad + M\epsilon^4[(j\vec{a}_n\Box\vec{\psi}_n)\vec{\psi}_{n'}^T]\Box(\vec{q}_{n'}\vec{q}_n^T)\} \\
&= 2\Re\{-j\{(\Lambda_N^{-1})_{nn'}[(\vec{a}_n\Box\vec{\psi}_n)^*\vec{\psi}_{n'}^T]\Box B \\
&\quad - M\epsilon^4[(\vec{a}_n\Box\vec{\psi}_n)\vec{\psi}_{n'}^T]\Box(\vec{q}_{n'}\vec{q}_n^T)\}\} \\
&= 2\Im\{(\Lambda_N^{-1})_{nn'}[(\vec{a}_n\Box\vec{\psi}_n)^*\vec{\psi}_{n'}^T]\Box B \\
&\quad - M\epsilon^4[(\vec{a}_n\Box\vec{\psi}_n)\vec{\psi}_{n'}^T]\Box(\vec{q}_{n'}\vec{q}_n^T)\} \\
&= 2\Im\{(\Lambda_N^{-1})_{nn'}(\vec{a}_n\vec{1}_S^T)\Box(\vec{\psi}_n^*\vec{\psi}_{n'}^T)\Box B \\
&\quad - M\epsilon^4(\vec{a}_n\vec{1}_S^T)\Box(\vec{\psi}_n\vec{\psi}_{n'}^T)\Box(\vec{q}_{n'}\vec{q}_n^T)\} \quad \text{(Eq. 1.12)} \\
&= 2(\vec{a}_n\vec{1}_S^T)\Box\Im\{(\Lambda_N^{-1})_{nn'}(\vec{\psi}_n^*\vec{\psi}_{n'}^T)\Box B \\
&\quad - M\epsilon^4(\vec{\psi}_n\vec{\psi}_{n'}^T)\Box(\vec{q}_{n'}\vec{q}_n^T)\} \\
&= (\vec{a}_n\vec{1}_S^T)\Box\Im(G_{nn'} - H_{nn'}) \quad \text{(Eqs. A.9 and A.10)},
\end{aligned} \tag{A.39}$$

and

$$\begin{aligned}
F_{\vec{\phi}_n\vec{\phi}_{n'}} &= 2\Re\{(\Lambda_N^{-1})_{nn'}[(j\vec{a}_n\Box\vec{\psi}_n)^*(j\vec{a}_{n'}\Box\vec{\psi}_{n'})^T]\Box B \\
&\quad + M\epsilon^4[(j\vec{a}_n\Box\vec{\psi}_n)(j\vec{a}_{n'}\Box\vec{\psi}_{n'})^T]\Box(\vec{q}_{n'}\vec{q}_n^T)\} \\
&= 2\Re\{(\Lambda_N^{-1})_{nn'}[(\vec{a}_n\Box\vec{\psi}_n)^*(\vec{a}_{n'}\Box\vec{\psi}_{n'})^T]\Box B \\
&\quad - M\epsilon^4[(\vec{a}_n\Box\vec{\psi}_n)(\vec{a}_{n'}\Box\vec{\psi}_{n'})^T]\Box(\vec{q}_{n'}\vec{q}_n^T)\}
\end{aligned}$$

$$
\begin{aligned}
&= 2\Re\{(\Lambda_N^{-1})_{nn'}(\vec{a}_n\vec{a}_{n'}^T)\Box(\vec{\psi}_n^*\vec{\psi}_{n'}^T)\Box B \\
&\quad -M\epsilon^4(\vec{a}_n\vec{a}_{n'}^T)\Box(\vec{\psi}_n\vec{\psi}_{n'}^T)\Box(\vec{q}_{n'}\vec{q}_n^T)\} \\
&= 2(\vec{a}_n\vec{a}_{n'}^T)\Box\Re\{(\Lambda_N^{-1})_{nn'}(\vec{\psi}_n^*\vec{\psi}_{n'}^T)\Box B \\
&\quad -M\epsilon^4(\vec{\psi}_n\vec{\psi}_{n'}^T)\Box(\vec{q}_{n'}\vec{q}_n^T)\} \\
&= (\vec{a}_n\vec{a}_{n'}^T)\Box\Re(G_{nn'} - H_{nn'}) \quad \text{(Eqs. A.9 and A.10).} \qquad \text{(A.40)}
\end{aligned}
$$

APPENDIX B
THE INFORMATION MATRIX FOR CONSTANT-ENVELOPE SIGNALS

If one makes the identification

$$\vec{a}_n = \vec{\alpha}, \tag{B.1}$$

the expressions for $\partial\vec{\mu}/\partial u_s$, $\partial\vec{\mu}/\partial o_{ns}$, $\partial\Lambda/\partial u_s$, and $\partial\Lambda/\partial o_{ns}$ given by Equations (A.15), (A.17), (A.18), and (A.20), respectively, remain valid, since the observation and its functional dependence on u and the $\vec{o}_n$ remain unchanged. We then only need to evaluate

$$\begin{aligned}
\frac{\partial\vec{\mu}}{\partial\alpha_s} &= \left(\frac{\partial C}{\partial\alpha_s} \cdot V\right)\vec{1}_S \quad \text{(Eq. A.13)} \\
&= \sum_{n=1}^{N} \frac{\partial c_{ns}}{\partial\alpha_s}(E_{ns} \cdot V)\vec{1}_S \\
&= \sum_{n=1}^{N} \frac{\partial c_{ns}}{\partial a_{ns}}(E_{ns} \cdot V)\vec{1}_S \\
&= \sum_{n=1}^{N} \frac{\partial\vec{\mu}}{\partial a_{ns}} \quad \text{(Eq. A.16)}
\end{aligned} \tag{B.2}$$

and

$$\begin{aligned}
\frac{\partial\Lambda}{\partial\alpha_s} &= \epsilon^2\left[\frac{\partial C}{\partial\alpha_s}C^H + C\left(\frac{\partial C}{\partial\alpha_s}\right)^H\right] \otimes I_M \quad \text{(Eq. A.14)} \\
&= \sum_{n=1}^{N} \epsilon^2\left[\left(\frac{\partial c_{ns}}{\partial\alpha_s}\right)E_{ns}C^H + \left(\frac{\partial c_{ns}}{\partial\alpha_s}\right)^* CE_{sn}\right] \otimes I_M \\
&= \sum_{n=1}^{N} \epsilon^2\left[\frac{\partial c_{ns}}{\partial a_{ns}}E_{ns}C^H + \left(\frac{\partial c_{ns}}{\partial a_{ns}}\right)^* CE_{sn}\right] \otimes I_M \\
&= \sum_{n=1}^{N} \frac{\partial\Lambda}{\partial a_{ns}} \quad \text{(Eq. A.19).}
\end{aligned} \tag{B.3}$$

where the partial derivatives with respect to a_{ns} in Equations (B.2) and (B.3) are understood to be defined as in the generic-signal case, to obtain expressions for all the $\partial\vec{\mu}/\partial r_i$ and $\partial\Lambda/\partial r_i$.

Since the partial derivatives of $\vec{\mu}$ and Λ with respect to $\vec{u}$ and the $\vec{o}_n$ are the same as in the generic-signal case, it follows that the $F_{\vec{\beta}\vec{\gamma}}$ with $\vec{\beta} \neq \vec{\alpha}$ and $\vec{\gamma} \neq \vec{\alpha}$ are given by the corresponding expressions in Appendix A. It remains to evaluate

$$(F_{\vec{\alpha}\vec{u}})_{ss'} = 2\Re\left[\left(\frac{\partial\vec{\mu}}{\partial\alpha_s}\right)^H \Lambda^{-1}\frac{\partial\vec{\mu}}{\partial u_{s'}}\right] \quad \text{(Eq. 1.62)}$$

$$= \sum_{n=1}^{N} 2\Re\left[\left(\frac{\partial\vec{\mu}}{\partial a_{ns}}\right)^H \Lambda^{-1}\frac{\partial\vec{\mu}}{\partial u_{s'}}\right] \quad \text{(Eq. B.2)}$$

$$= \sum_{n=1}^{N} (F_{\vec{a}_n\vec{u}})_{ss'} \quad \text{(Eq. A.27)}. \tag{B.4}$$

which gives

$$F_{\vec{\alpha}\vec{u}} = \sum_{n=1}^{N} F_{\vec{a}_n\vec{u}}; \tag{B.5}$$

$$(F_{\vec{\alpha}\vec{\alpha}})_{ss'} = 2\Re\left[\left(\frac{\partial\vec{\mu}}{\partial\alpha_s}\right)^H \Lambda^{-1}\frac{\partial\vec{\mu}}{\partial\alpha_{s'}}\right] + \mathrm{tr}\left(\Lambda^{-1}\frac{\partial\Lambda}{\partial\alpha_s}\Lambda^{-1}\frac{\partial\Lambda}{\partial\alpha_{s'}}\right) \quad \text{(Eq. 1.62)}$$

$$= \sum_{n=1}^{N}\sum_{n'=1}^{N} 2\Re\left[\left(\frac{\partial\vec{\mu}}{\partial a_{ns}}\right)^H \Lambda^{-1}\frac{\partial\vec{\mu}}{\partial a_{n's'}}\right]$$

$$+\sum_{n=1}^{N}\sum_{n'=1}^{N} \mathrm{tr}\left(\Lambda^{-1}\frac{\partial\Lambda}{\partial a_{ns}}\Lambda^{-1}\frac{\partial\Lambda}{\partial a_{n's'}}\right)$$

$$= \sum_{n=1}^{N}\sum_{n'=1}^{N} (F_{\vec{a}_n\vec{a}_{n'}})_{ss'}. \tag{B.6}$$

which gives

$$F_{\vec{\alpha}\vec{\alpha}} = \sum_{n=1}^{N}\sum_{n'=1}^{N} F_{\vec{a}_n\vec{a}_{n'}}; \tag{B.7}$$

and

$$(F_{\vec{\varphi}_n\vec{\alpha}})_{ss'} = 2\Re\left[\left(\frac{\partial\vec{\mu}}{\partial\varphi_{ns}}\right)^H \Lambda^{-1}\frac{\partial\vec{\mu}}{\partial\alpha_{s'}}\right] + \mathrm{tr}\left(\Lambda^{-1}\frac{\partial\Lambda}{\partial\varphi_{ns}}\Lambda^{-1}\frac{\partial\Lambda}{\partial\alpha_{s'}}\right) \quad \text{(Eq. 1.62)}$$

$$= \sum_{n'=1}^{N} 2\Re\left[\left(\frac{\partial\vec{\mu}}{\partial\varphi_{ns}}\right)^H \Lambda^{-1}\frac{\partial\vec{\mu}}{\partial a_{n's'}}\right] + \sum_{n'=1}^{N} \mathrm{tr}\left(\Lambda^{-1}\frac{\partial\Lambda}{\partial\varphi_{ns}}\Lambda^{-1}\frac{\partial\Lambda}{\partial a_{n's'}}\right)$$

$$= \sum_{n'=1}^{N} (F_{\vec{\varphi}_n\vec{a}_{n'}})_{ss'}. \tag{B.8}$$

which gives

$$F_{\vec{\varphi}_n\vec{\alpha}} = \sum_{n'=1}^{N} F_{\vec{\varphi}_n\vec{a}_{n'}}. \tag{B.9}$$

Thus the information matrix for the unknown constant-envelope signal case is easily constructed from the information matrix for the generic-signal case.

APPENDIX C
NUMERICAL REDUCTION OF THE INFORMATION MATRIX

For notational convenience in this section, let $Y_{[m]}$ denote the upper-left $m \times m$ submatrix of a positive-definite symmetric $N \times N$ matrix Y. Suppose F is the $L \times L$ Fisher information matrix for the L-dimensional vector of unknown parameters, $\vec{r}$. As derived in Section 1.3.1, the Cramér-Rao bounds on DF for the individual signals are given by the diagonal elements of the upper-left $S \times S$ submatrix of F^{-1}, $(F^{-1})_{[S]}$. We shall now describe a procedure for obtaining $(F^{-1})_{[S]}$.

Partition Y as

$$Y = \begin{bmatrix} Y_{[N-1]} & \vec{y}_N \\ \vec{y}_N^T & (Y)_{NN} \end{bmatrix}. \tag{C.1}$$

Define the function R_N mapping the set of $N \times N$ positive-definite symmetric matrices to the set of $(N-1) \times (N-1)$ positive-definite symmetric matrices by

$$R_N(Y) = Y_{[N-1]} - \frac{1}{(Y)_{NN}} \vec{y}_N \vec{y}_N^T. \tag{C.2}$$

Thus we have that,

$$(Y^{-1})_{[N-1]} = [R_N(Y)]^{-1}, \tag{C.3}$$

(Eq. 1.21). We shall show that $(F^{-1})_{[q]}$ can be obtained by applying, $L - q$ times, the operator R (appropriately dimensioned) to F, i.e., that

$$(F^{-1})_{[q]} = [R_{q+1} R_{q+2} \cdots R_L(F)]^{-1}. \tag{C.4}$$

The result is true for $q = L - 1$ by Equation (C.3). Assume (the induction hypothesis) that it is true for $q + 1$. Then

$$\begin{aligned} (F^{-1})_{[q]} &= [(F^{-1})_{[q+1]}]_{[q]} \\ &= \{[R_{q+2} R_{q+3} \cdots R_L(F)]^{-1}\}_{[q]} \\ &= \{R_{q+1}[R_{q+2} R_{q+3} \cdots R_L(F)]\}^{-1} \quad \text{(Eq. C.3)} \\ &= [R_{q+1} R_{q+2} \cdots R_L(F)]^{-1} \end{aligned} \tag{C.5}$$

(the first line merely identifies the upper-left $q \times q$ submatrix of F^{-1} with the upper-left $q \times q$ submatrix of the upper-left $(q+1) \times (q+1)$ submatrix of F^{-1}). The result is thus true for q, and the theorem follows by mathematical induction.

We used the technique described above to obtain $(F^{-1})_{[S]}$.

APPENDIX D
THE ARRAY-ERRORS-ONLY CRAMÉR-RAO BOUND FOR $S = N = 1$

In this appendix, we shall evaluate the array-errors-only Cramér-Rao bound for the case where $S = N = 1$. As noted in Section 2.2.1, the models for generic and constant-envelope signals are identical for this case. Thus, with no loss of generality, we shall compute this bound using the notation of the generic-signal case. For simplicity, we shall assume that the ideal array-response vectors are obtained from an array of omnidirectional elements with pairwise symmetry about some phase-reference point in space. For such an array, the ideal array-response vectors are of unit length and have real inner products with each other. Letting u_t denote the true value of u, we have

$$\begin{aligned} W &= \vec{v}^H(u_t)\vec{v}(u_t) \quad \text{(Eq. A.1)} \\ &= \|\vec{v}(u_t)\|^2 \\ &= 1. \end{aligned} \tag{D.1}$$

$$\begin{aligned} \dot{W} &= \vec{v}^H(u_t)\dot{\vec{v}}(u_t) \quad \text{(Eq. A.2)} \\ &= \frac{d}{du}[\vec{v}^H(u_t)\vec{v}(u)]|_{u=u_t} \\ &= \Re\{\frac{d}{du}[\vec{v}^H(u_t)\vec{v}(u)]|_{u=u_t}\} \\ &= \Re\{\vec{v}^H(u_t)\dot{\vec{v}}(u_t)\} \\ &= \frac{1}{2}[\vec{v}^H(u_t)\dot{\vec{v}}(u_t) + \dot{\vec{v}}^H(u_t)\vec{v}(u_t)] \\ &= \frac{1}{2}\left\{\frac{d}{du}[\vec{v}^H(u)\vec{v}(u)]|_{u=u_t}\right\} \\ &= \frac{1}{2}\left\{\frac{d}{du}[\|\vec{v}(u)\|^2]|_{u=u_t}\right\} \\ &= 0. \end{aligned} \tag{D.2}$$

$$\begin{aligned} \ddot{W} &= \dot{\vec{v}}^H(u_t)\dot{\vec{v}}(u_t) \quad \text{(Eq. A.3)} \\ &= \|\dot{\vec{v}}(u_t)\|^2, \end{aligned} \tag{D.3}$$

$$\Lambda_N = \epsilon^2 a_{11}^2 \tag{D.4}$$

(Eq. 1.33),

$$\Lambda_N^{-1} = \frac{1}{\epsilon^2 a_{11}^2} \tag{D.5}$$

(Eq. D.4),

$$P = \frac{1}{\epsilon^2} \tag{D.6}$$

(Eq. A.4),

$$\begin{aligned} Q &= \frac{1}{\epsilon^2 c_{11}} \\ &= \frac{1}{\epsilon^2 a_{11} e^{j\phi_{11}}} \end{aligned} \tag{D.7}$$

(Eq. A.5),

$$D = 0 \tag{D.8}$$

(Eq. A.7),

$$B = 1 + M\epsilon^2 \tag{D.9}$$

(Eq. A.8),

$$G = \frac{2 + 2M\epsilon^2}{\epsilon^2 a_{11}^2} \tag{D.10}$$

(Eq. A.9),

$$\begin{aligned} H &= \frac{2M\epsilon^4 e^{j2\phi_{11}}}{\epsilon^4 a_{11}^2 e^{j2\phi_{11}}} \quad \text{(Eq. A.10)} \\ &= \frac{2M}{a_{11}^2}, \end{aligned} \tag{D.11}$$

$$F_{uu} = \frac{2\|\dot{\vec{v}}(u_t)\|^2}{\epsilon^2} \tag{D.12}$$

(Eq. A.22),

$$F_{au} = 0 \tag{D.13}$$

(Eq. A.30),

$$F_{\phi u} = 0 \tag{D.14}$$

(Eq. A.31),

$$F_{aa} = \frac{2+2M\epsilon^2}{\epsilon^2 a_{11}^2} + \frac{2M}{a_{11}^2} \quad \text{(Eq. A.38)}$$

$$= \frac{2+2M\epsilon^2+2M\epsilon^2}{\epsilon^2 a_{11}^2}$$

$$= \frac{2+4M\epsilon^2}{\epsilon^2 a_{11}^2}. \tag{D.15}$$

$$F_{\phi a} = 0 \tag{D.16}$$

(Eq. A.39),

$$F_{\phi\phi} = a_{11}^2 \left(\frac{2+2M\epsilon^2}{\epsilon^2 a_{11}^2} - \frac{2M}{a_{11}^2} \right) \quad \text{(Eq. A.40)}$$

$$= \frac{2+2M\epsilon^2-2M\epsilon^2}{\epsilon^2}$$

$$= \frac{2}{\epsilon^2}. \tag{D.17}$$

and

$$F = \begin{bmatrix} \frac{2\|\dot{\vec{v}}(u_t)\|^2}{\epsilon^2} & 0 & 0 \\ 0 & \frac{2+4M\epsilon^2}{\epsilon^2 a_{11}^2} & 0 \\ 0 & 0 & \frac{2}{\epsilon^2} \end{bmatrix} \tag{D.18}$$

(Eq. 1.60). Thus the Cramér-Rao bound on DF is given by

$$\text{var}\,(\hat{u}) \geq \frac{\epsilon^2}{2\|\dot{\vec{v}}(u_t)\|^2}, \tag{D.19}$$

which is independent of the complex amplitudes of the signals. This is equal to the thermal-noise-only Cramér-Rao bound on DF of a generic signal with an ASNR of $\frac{1}{\epsilon^2}$ in the $S = N = 1$ case [1, Eq. 2.17], where the value of $\|\dot{\vec{v}}(u_t)\|^2$ here is equal to the quantity $(2\pi\ell)^2$ in [1], where ℓ^2 is the mean-squared distance of the (linear) array elements from the phase center of the array in units of wavelengths-squared.

APPENDIX E
GRAPHICAL RESULTS

This appendix gives a graphical presentation of the results discussed in Sections 2.2.2 and 2.2.3.

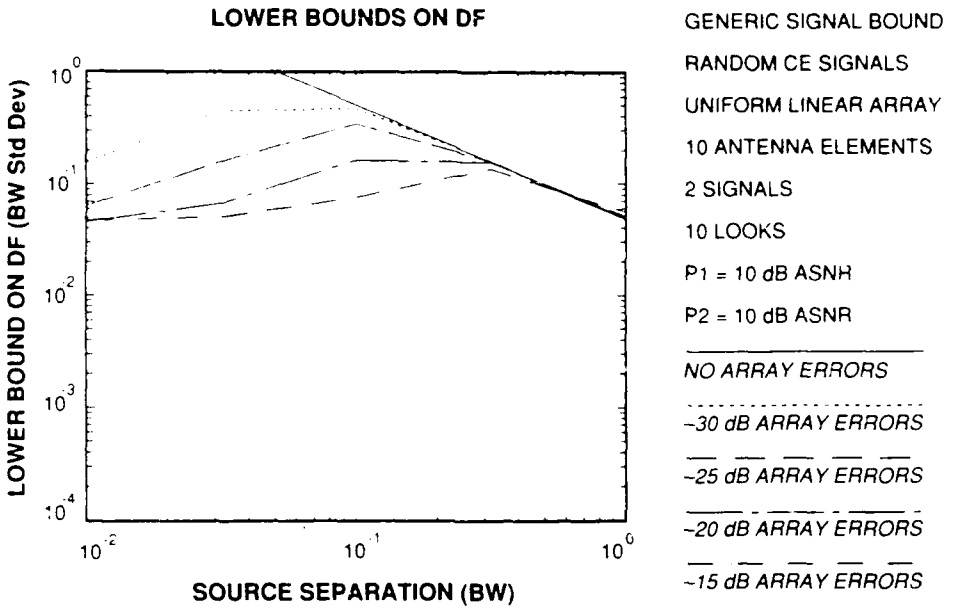

Figure E-1. Generic signal bounds - 2 random constant-envelope signals, 10 looks, SOI ASNR = 10 dB, interferer ASNR = 10 dB.

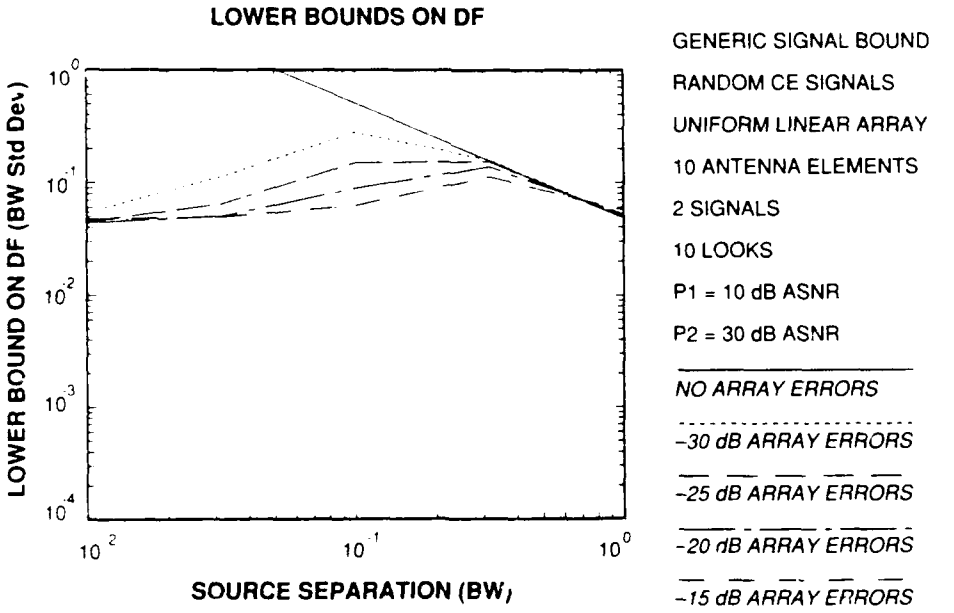

Figure E-2. Generic signal bounds - 2 random constant-envelope signals, 10 looks, SOI ASNR = 10 dB, interferer ASNR = 30 dB

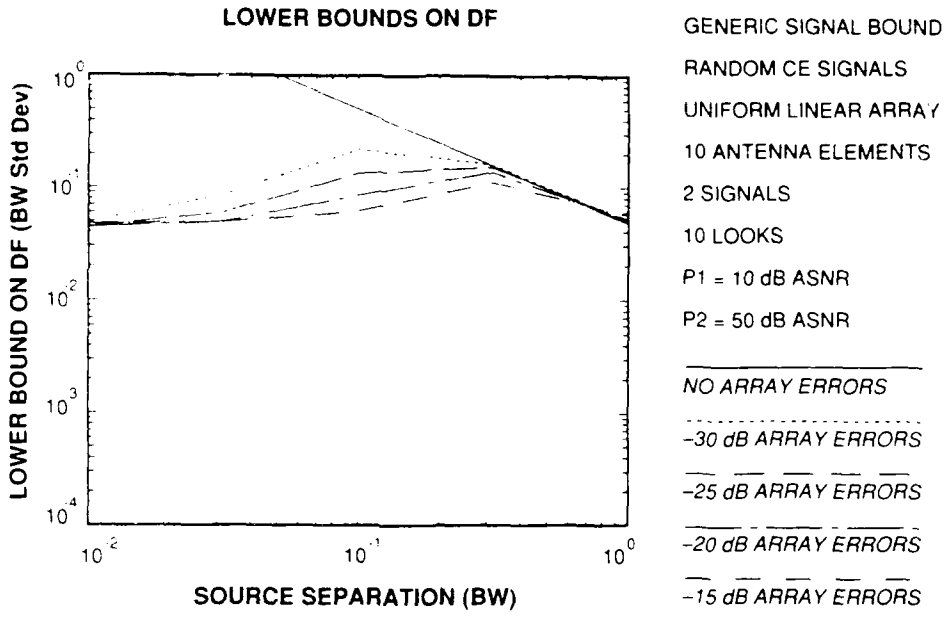

116880-6

Figure E-3. Generic signal bounds - 2 random constant-envelope signals, 10 looks, SOI ASNR = 10 dB, interferer ASNR = 50 dB.

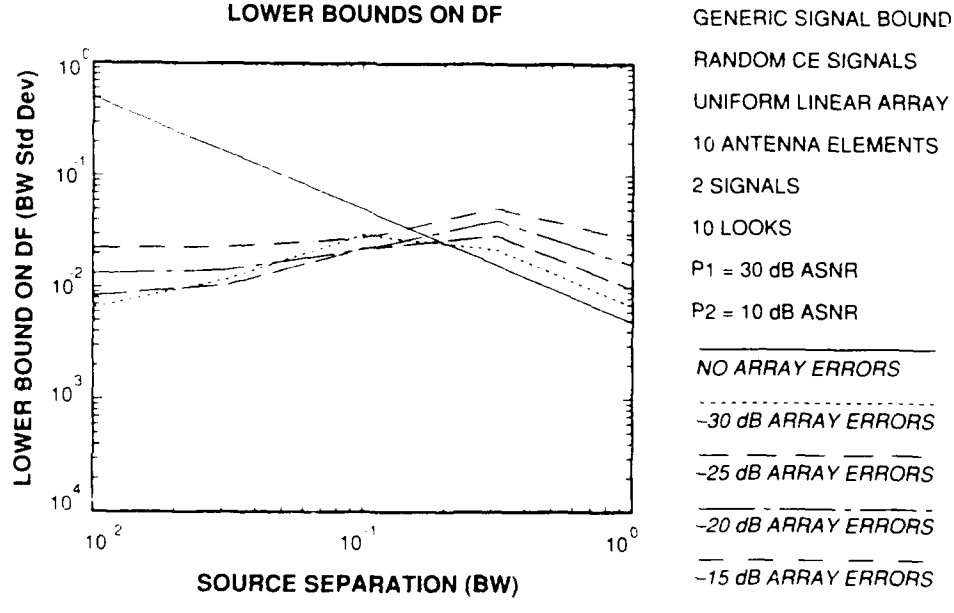

116880-7

Figure E-4. Generic signal bounds - 2 random constant-envelope signals, 10 looks, SOI ASNR = 30 dB, interferer ASNR = 10 dB.

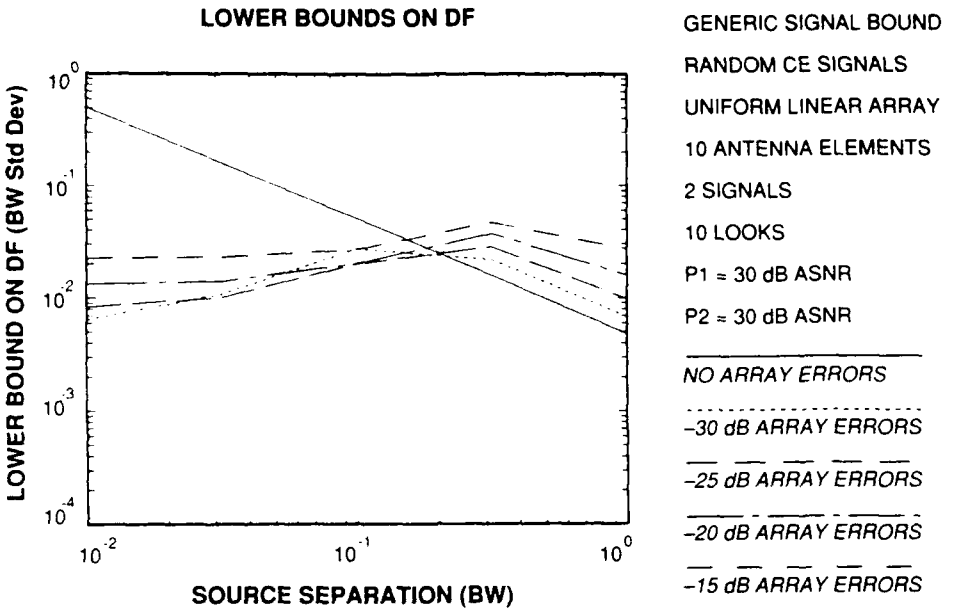

Figure E-5. Generic signal bounds - 2 random constant-envelope signals, 10 looks, SOI ASNR = 30 dB, interferer ASNR = 30 dB.

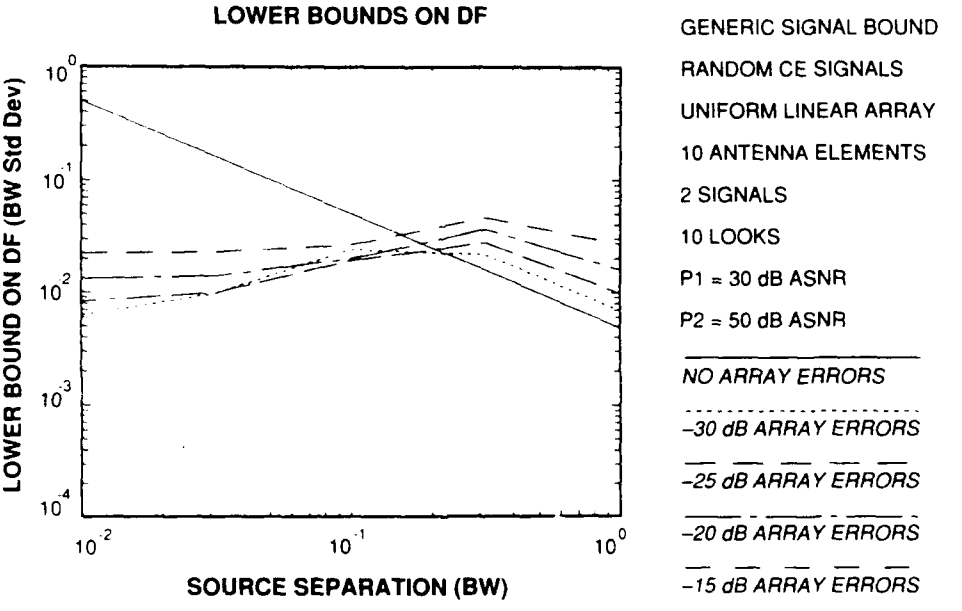

Figure E-6. Generic signal bounds - 2 random constant-envelope signals, 10 looks, SOI ASNR = 30 dB, interferer ASNR = 50 dB.

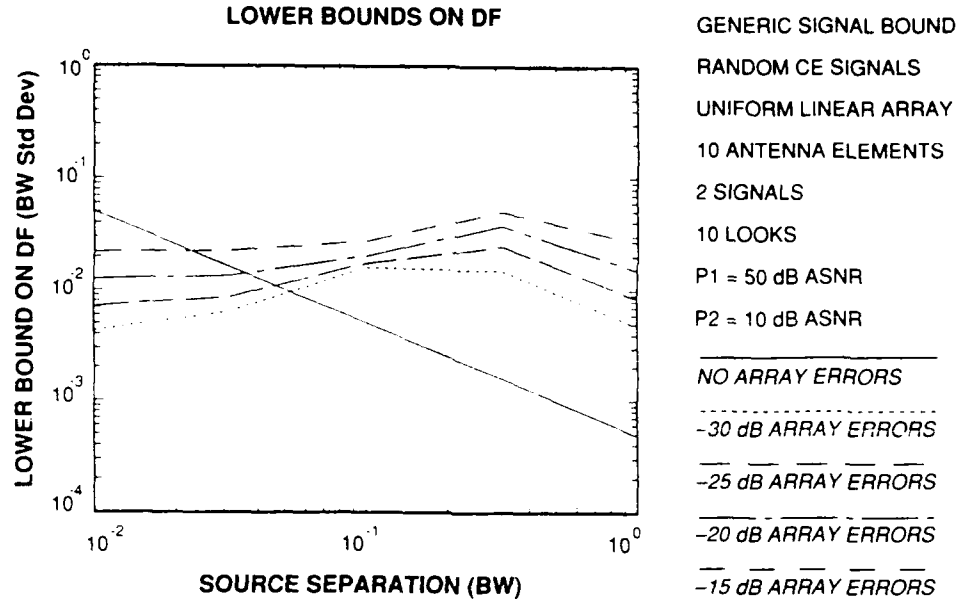

116880-10

Figure E-7. Generic signal bounds - 2 random constant-envelope signals, 10 looks, SOI ASNR = 50 dB, interferer ASNR = 10 dB.

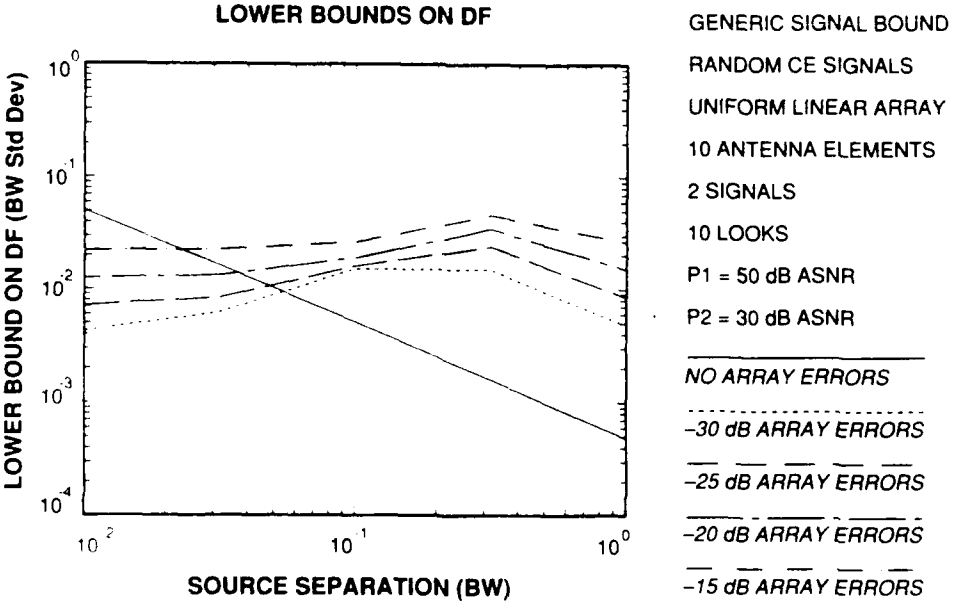

116880-11

Figure E-8. Generic signal bounds - 2 random constant-envelope signals, 10 looks, SOI ASNR = 50 dB, interferer ASNR = 30 dB.

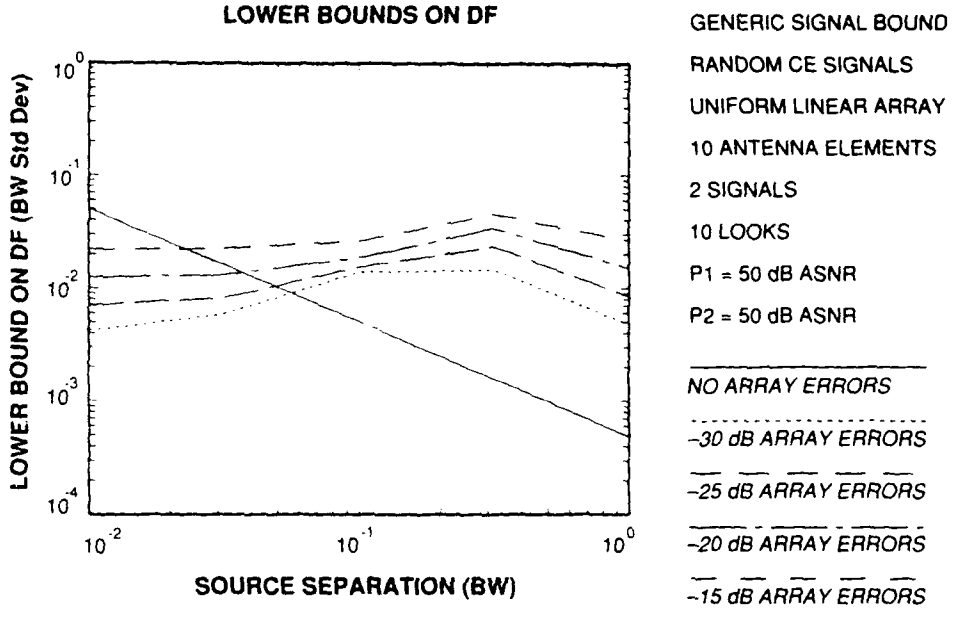

Figure E-9. Generic signal bounds - 2 random constant-envelope signals, 10 looks, SOI ASNR = 50 dB, interferer ASNR = 50 dB.

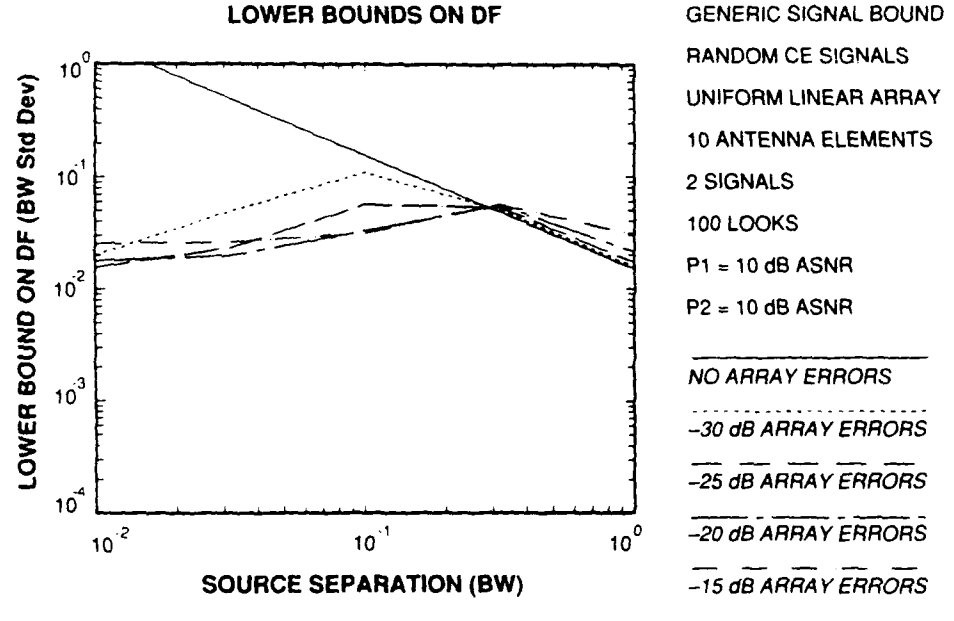

Figure E-10. Generic signal bounds - 2 random constant-envelope signals, 100 looks, SOI ASNR = 10 dB, interferer ASNR = 10 dB.

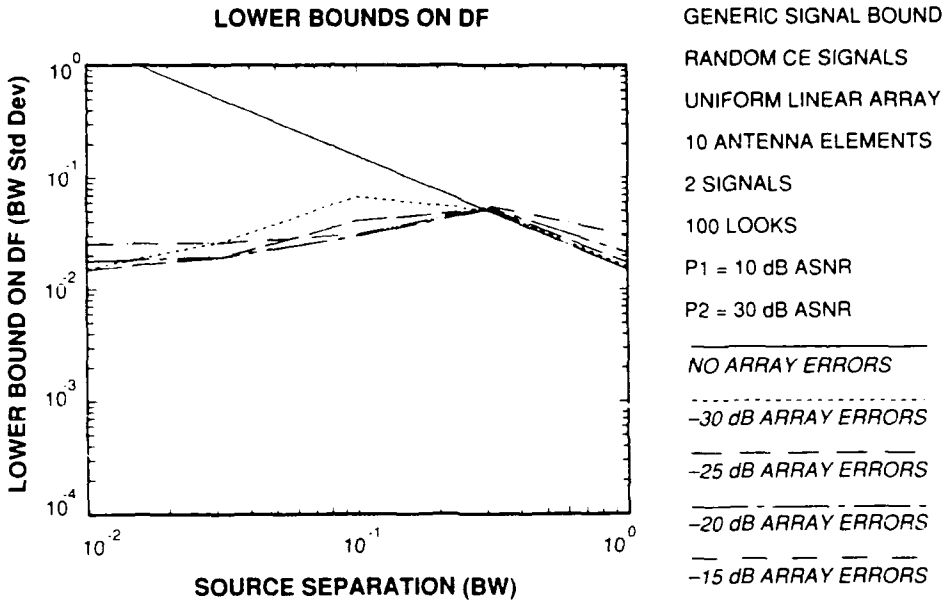

116880-14

Figure E-11. Generic signal bounds - 2 random constant-envelope signals, 100 looks, SOI ASNR = 10 dB, interferer ASNR = 30 dB.

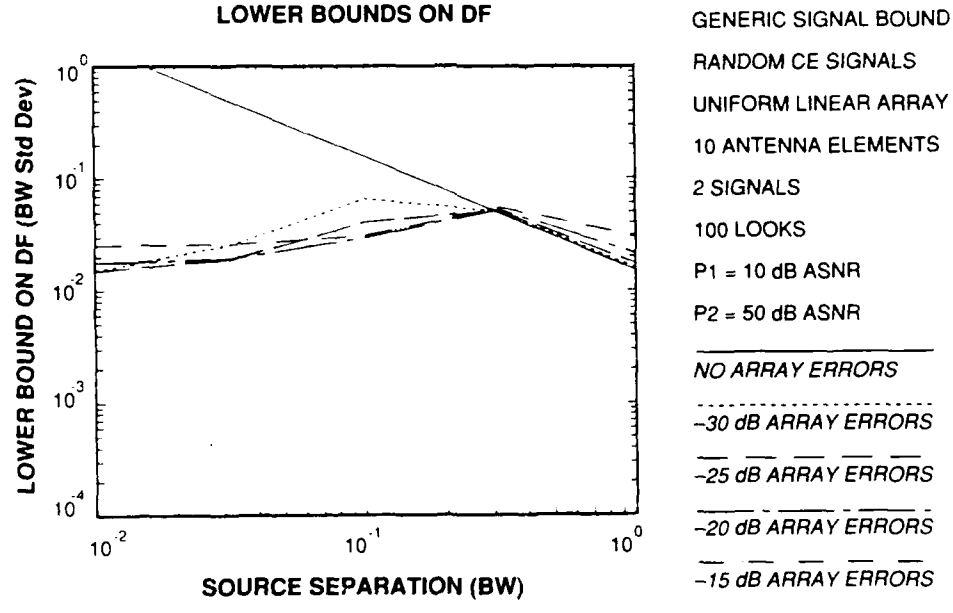

116880-15

Figure E-12. Generic signal bounds - 2 random constant-envelope signals, 100 looks, SOI ASNR = 10 dB, interferer ASNR = 50 dB.

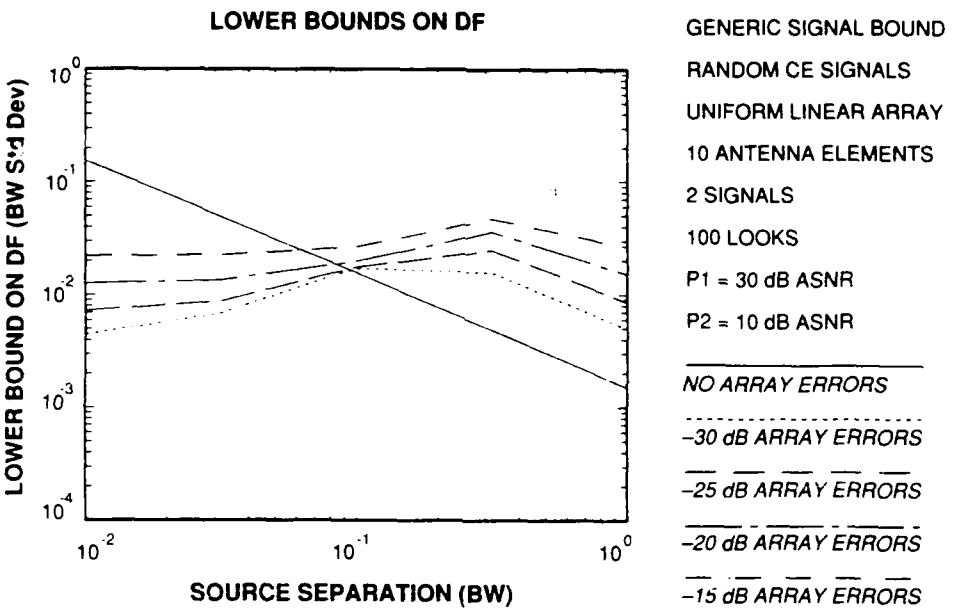

Figure E-13. Generic signal bounds - 2 random constant-envelope signals, 100 looks, SOI ASNR = 30 dB, interferer ASNR = 10 dB.

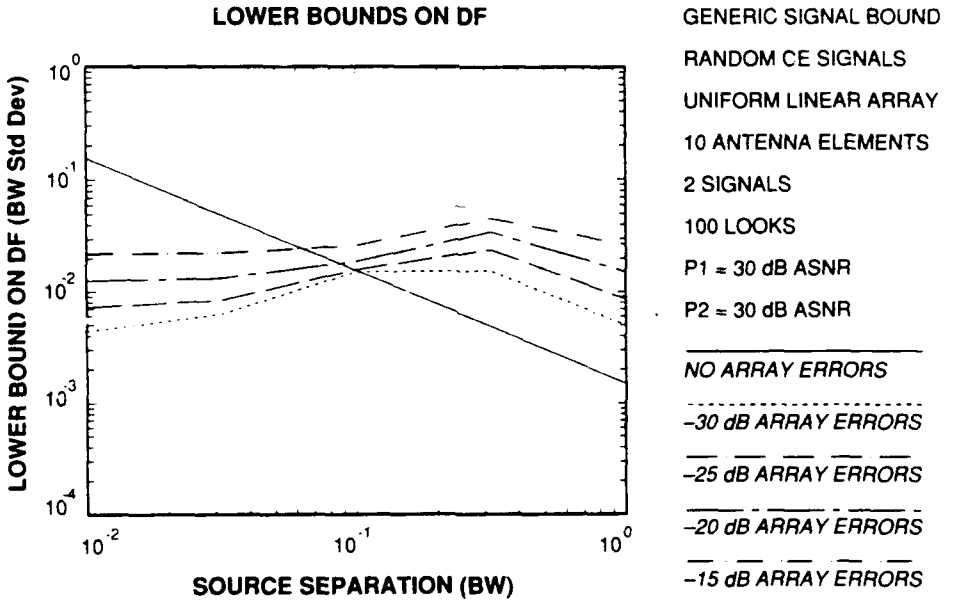

Figure E-14. Generic signal bounds - 2 random constant-envelope signals, 100 looks, SOI ASNR = 30 dB, interferer ASNR = 30 dB.

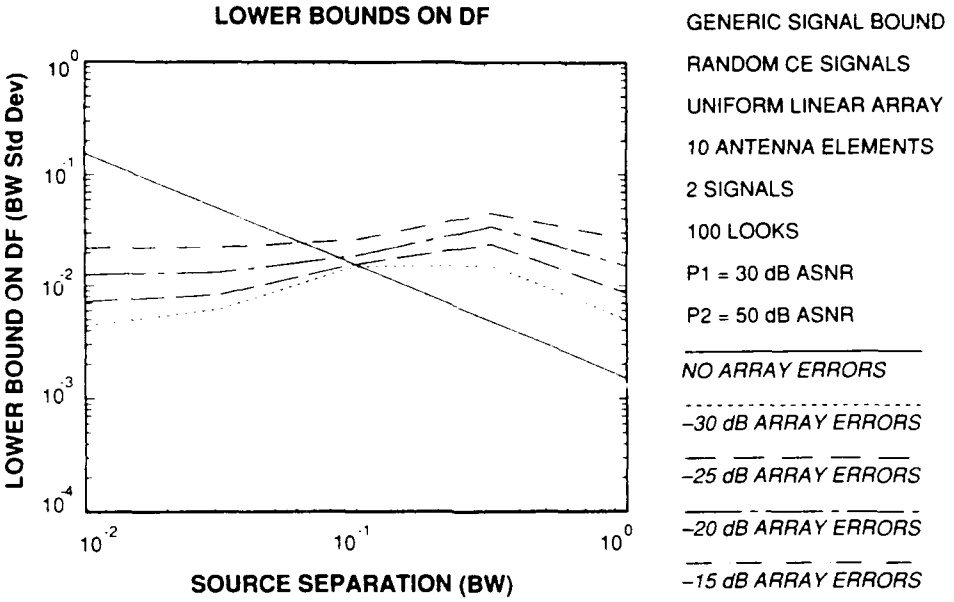

116880-18

Figure E-15. Generic signal bounds - 2 random constant-envelope signals, 100 looks, SOI ASNR = 30 dB, interferer ASNR = 50 dB.

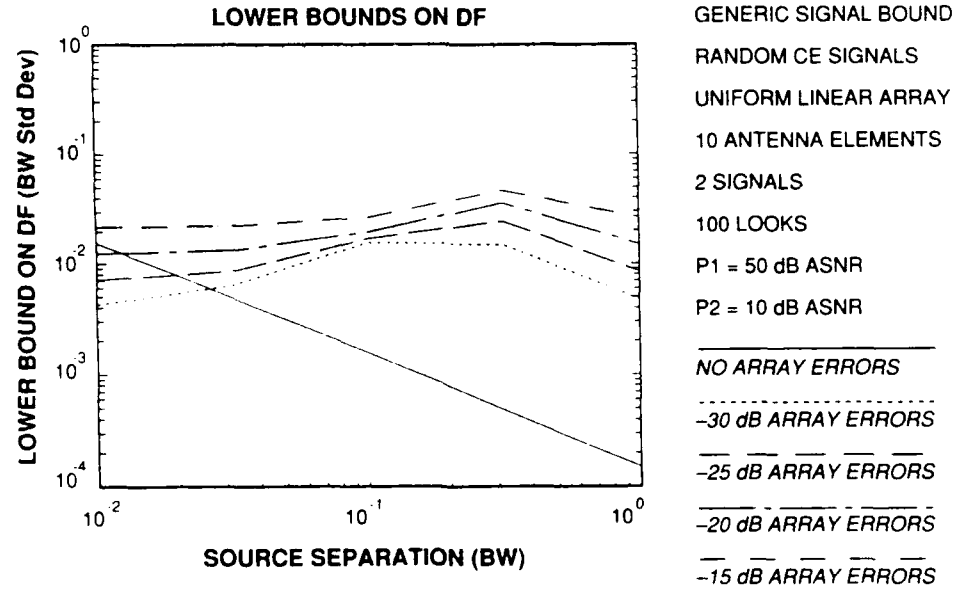

116880-19

Figure E-16. Generic signal bounds - 2 random constant-envelope signals, 100 looks, SOI ASNR = 50 dB, interferer ASNR = 10 dB.

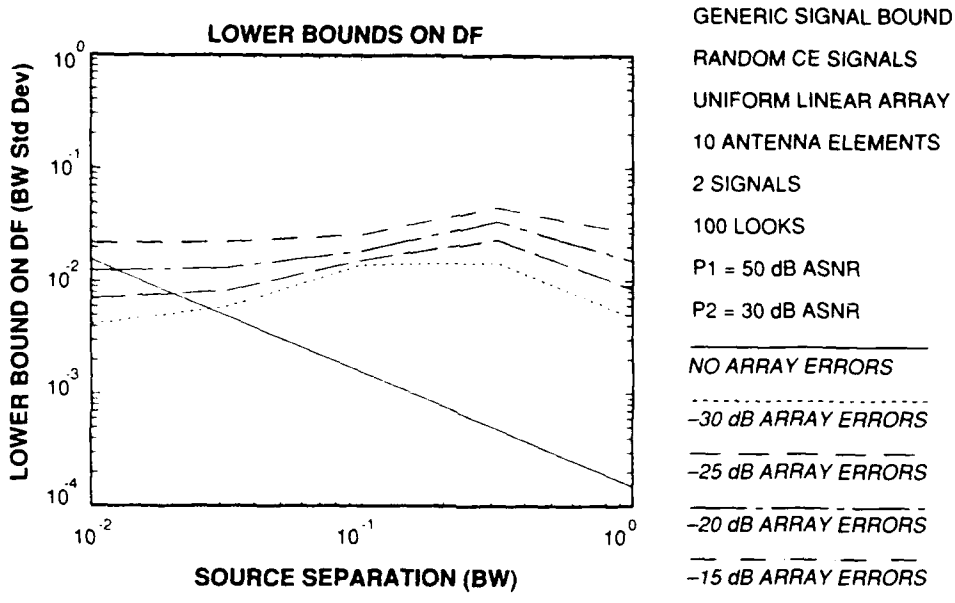

Figure E-17. Generic signal bounds - 2 random constant-envelope signals, 100 looks, SOI ASNR = 50 dB, interferer ASNR = 30 dB.

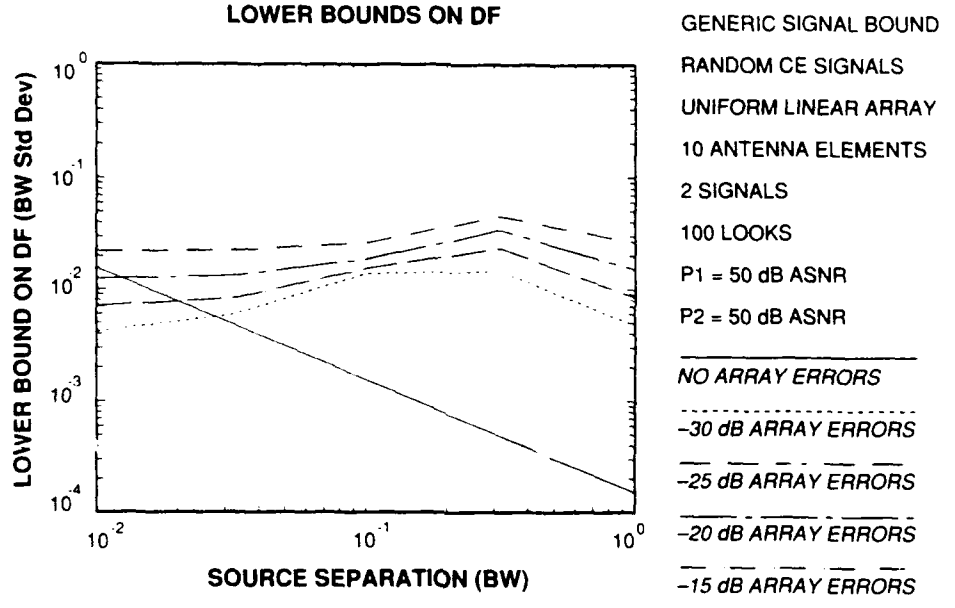

Figure E-18. Generic signal bounds - 2 random constant-envelope signals, 100 looks, SOI ASNR = 50 dB, interferer ASNR = 50 dB.

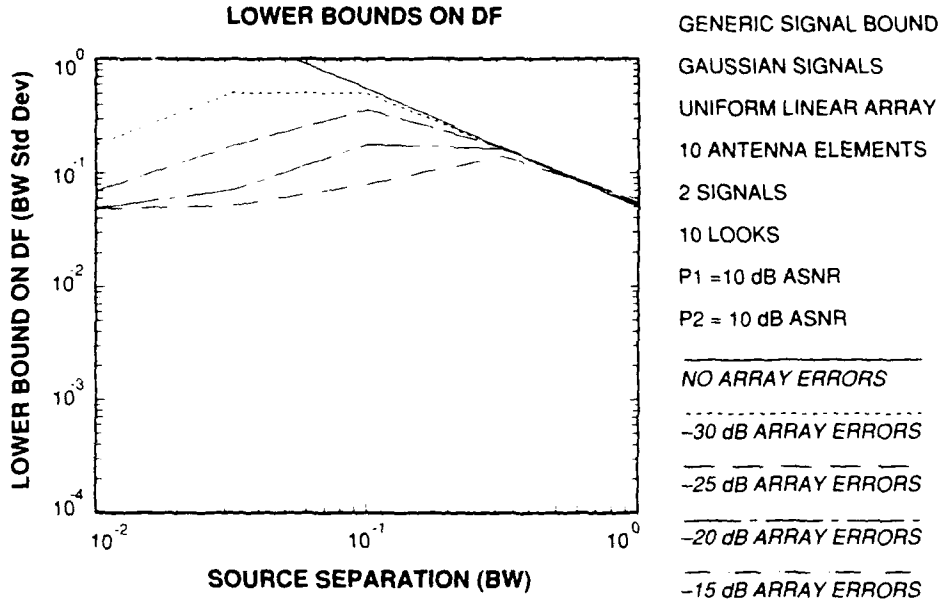

116880-22

Figure E-19. Generic signal bounds - 2 complex Gaussian signals, 10 looks, SOI ASNR = 10 dB, interferer ASNR = 10 dB.

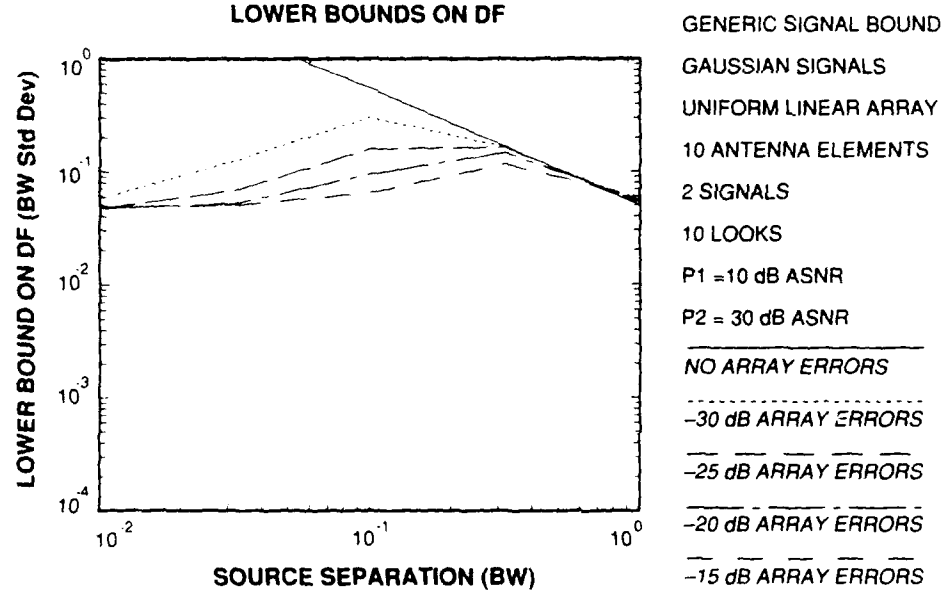

116880-23

Figure E-20. Generic signal bounds - 2 complex Gaussian signals, 10 looks, SOI ASNR = 10 dB, interferer ASNR = 30 dB.

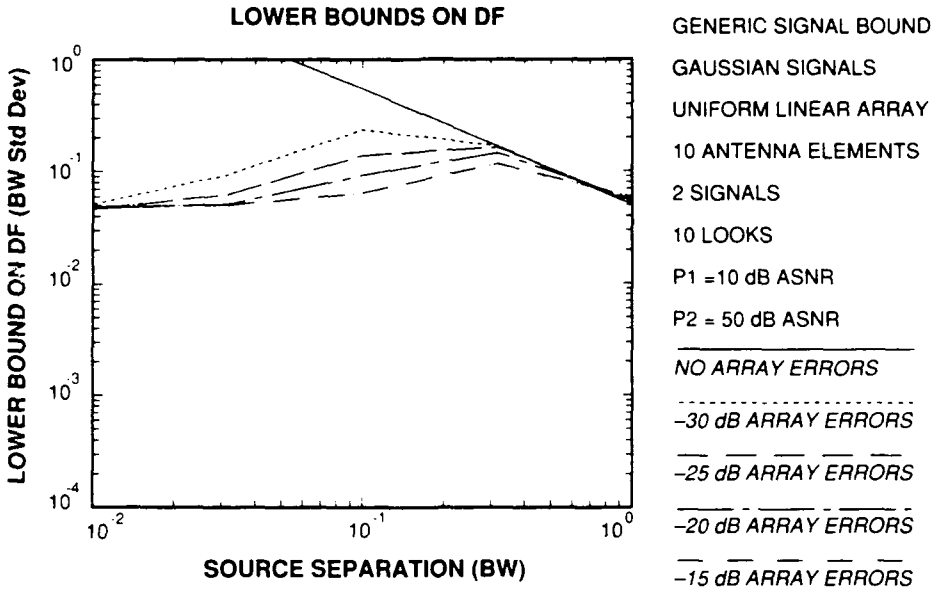

Figure E-21. Generic signal bounds - 2 complex Gaussian signals, 10 looks, SOI ASNR = 10 dB, interferer ASNR = 50 dB.

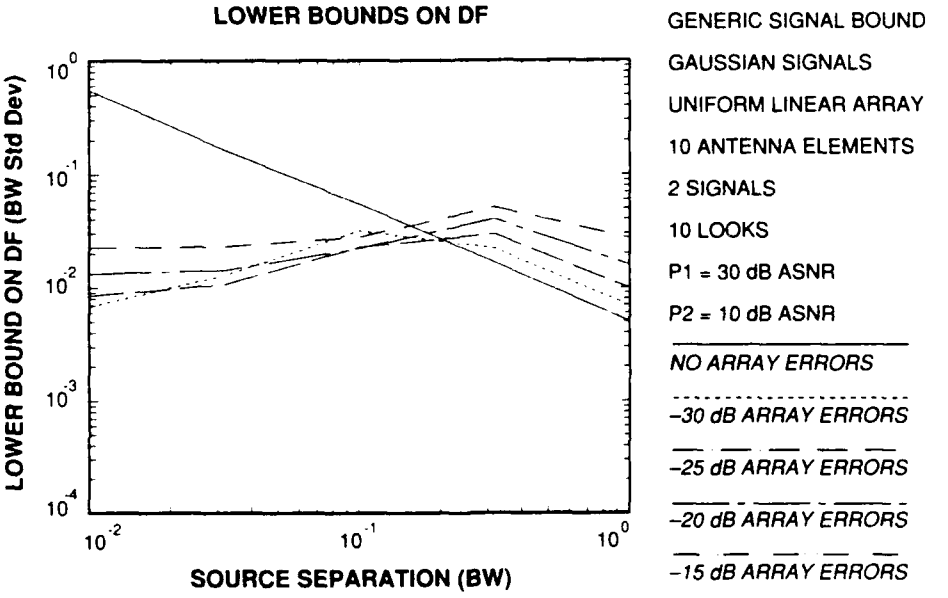

Figure E-22. Generic signal bounds - 2 complex Gaussian signals, 10 looks, SOI ASNR = 30 dB, interferer ASNR = 10 dB.

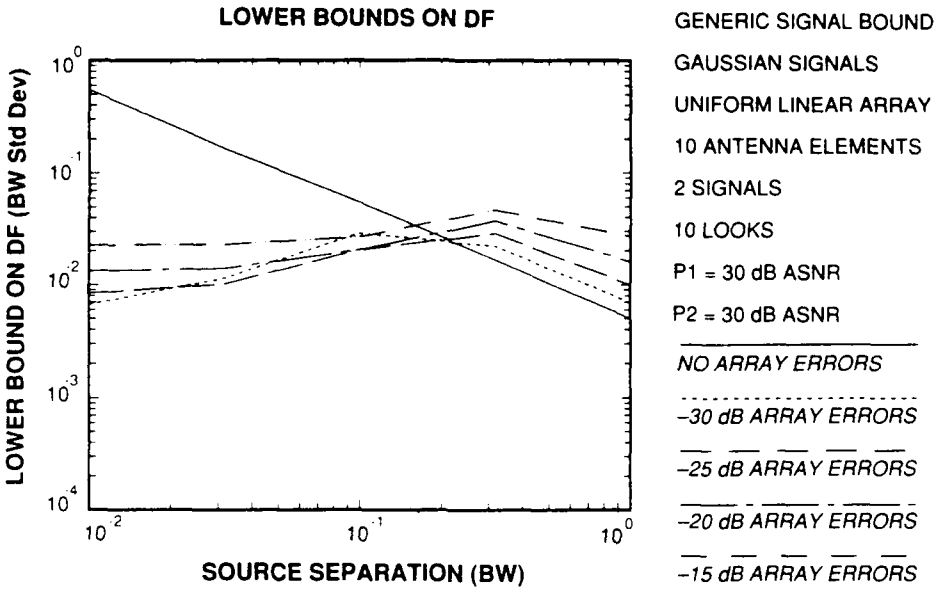

116880-26

Figure E-23. Generic signal bounds - 2 complex Gaussian signals, 10 looks, SOI ASNR = 30 dB, interferer ASNR = 30 dB.

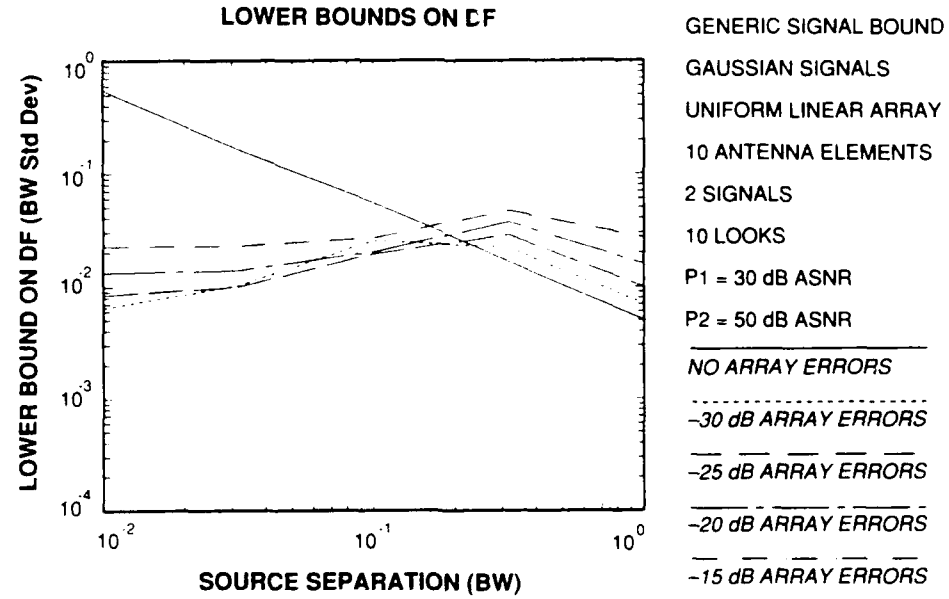

116880-27

Figure E-24. Generic signal bounds - 2 complex Gaussian signals, 10 looks, SOI ASNR = 30 dB, interferer ASNR = 50 dB.

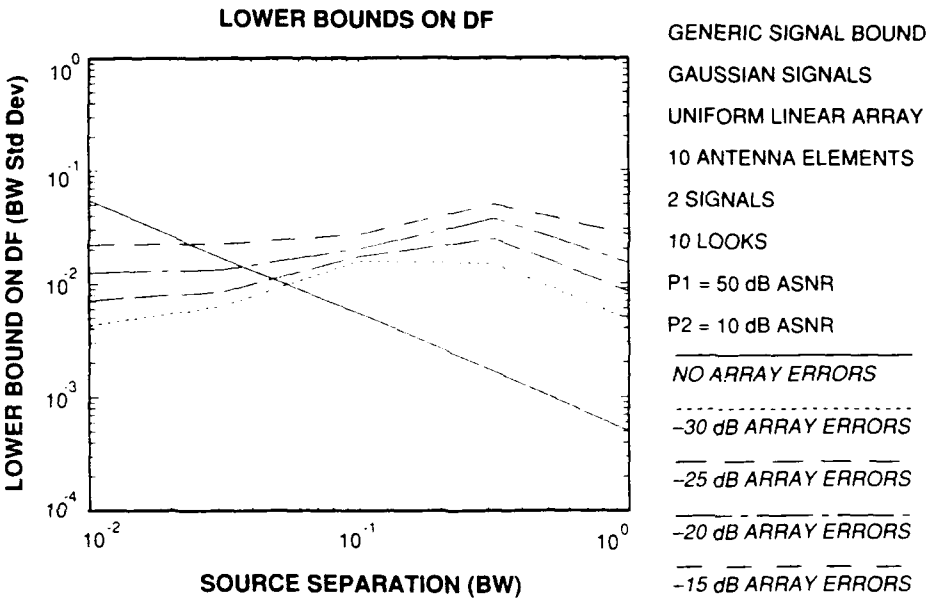

Figure E-25. Generic signal bounds - 2 complex Gaussian signals, 10 looks, SOI ASNR = 50 dB, interferer ASNR = 10 dB.

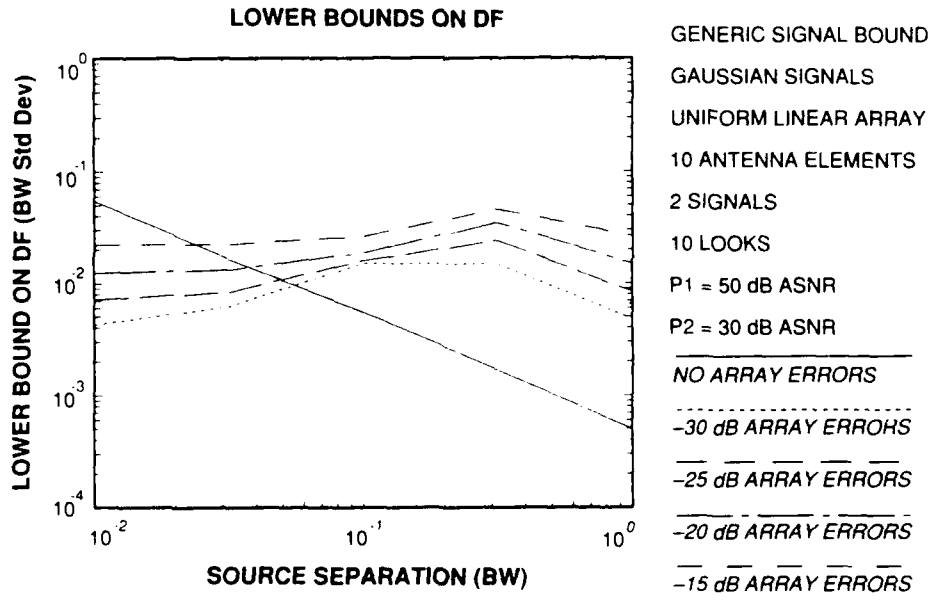

Figure E-26. Generic signal bounds - 2 complex Gaussian signals, 10 looks, SOI ASNR = 50 dB, interferer ASNR = 30 dB.

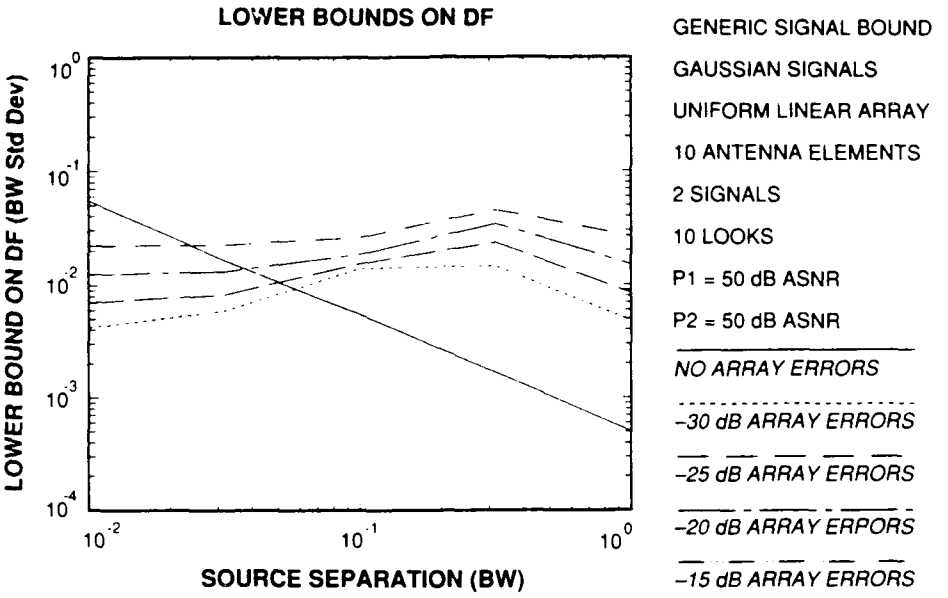

116880-30

Figure E-27. Generic signal bounds - 2 complex Gaussian signals, 10 looks, SOI ASNR = 50 dB, interferer ASNR = 50 dB.

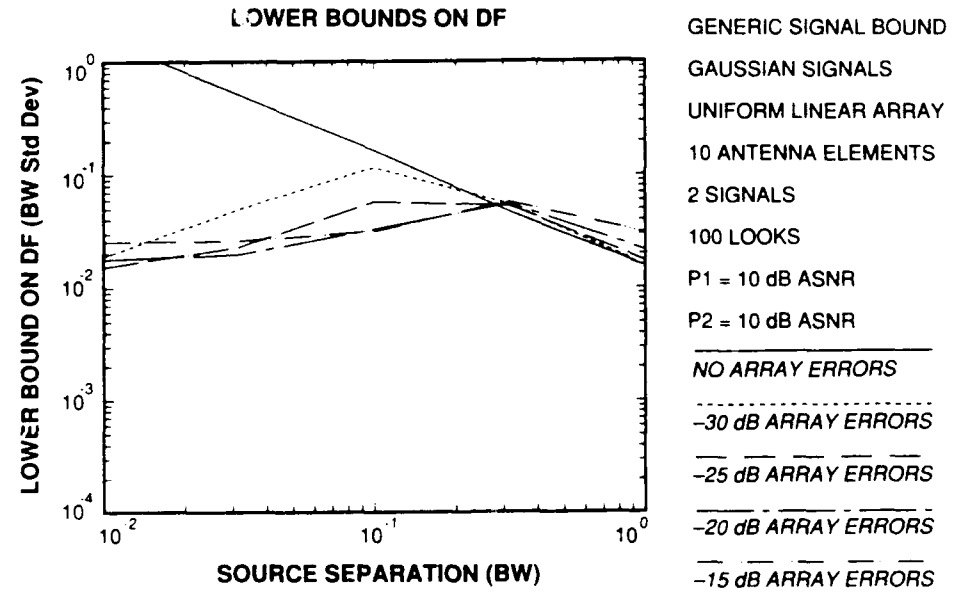

116880-31

Figure E-28. Generic signal bounds - 2 complex Gaussian signals, 100 looks, SOI ASNR = 10 dB, interferer ASNR = 10 dB.

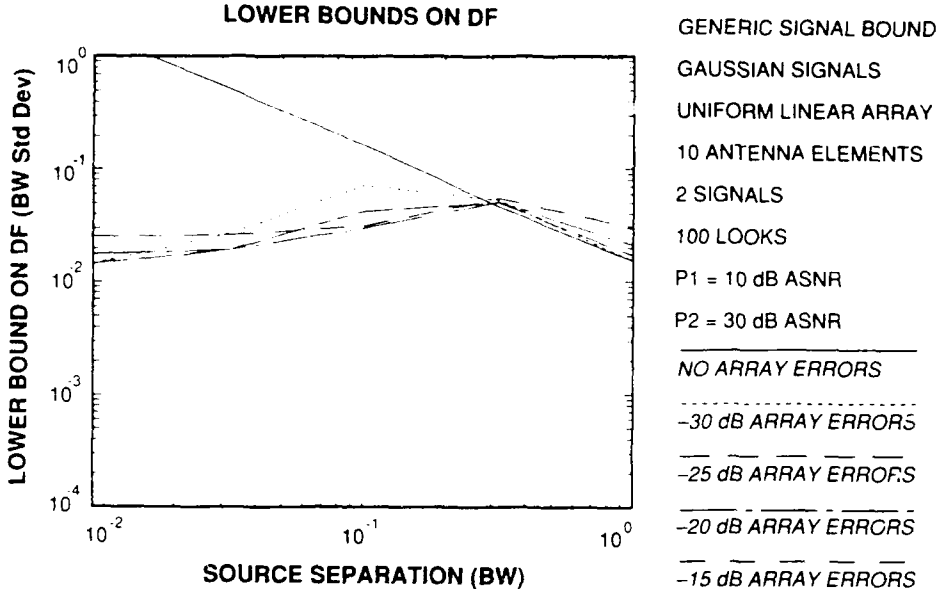

Figure E-29. Generic signal bounds - 2 complex Gaussian signals, 100 looks, SOI ASNR = 10 dB, interferer ASNR = 30 dB.

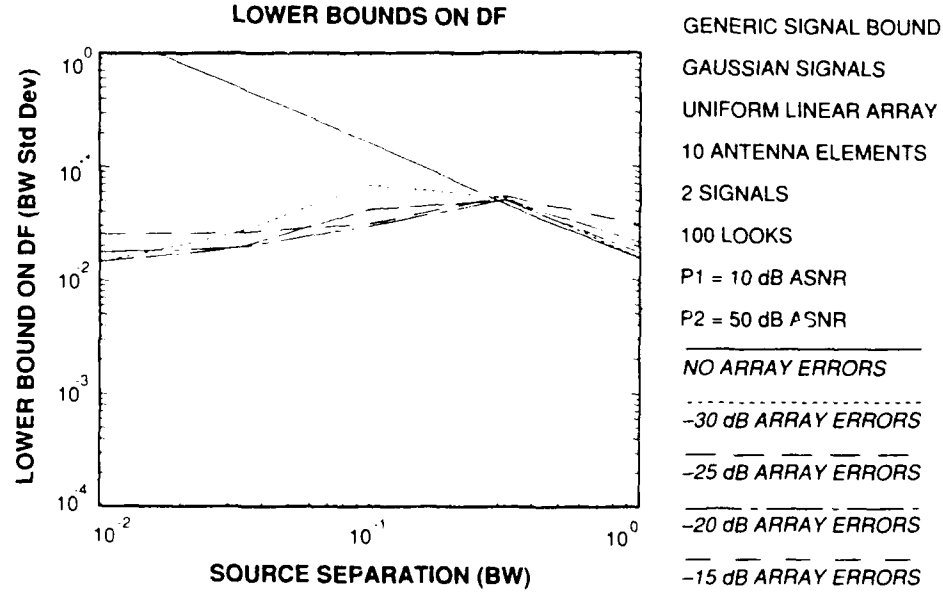

Figure E-30. Generic signal bounds - 2 complex Gaussian signals, 100 looks, SOI ASNR = 10 dB, interferer ASNR = 50 dB.

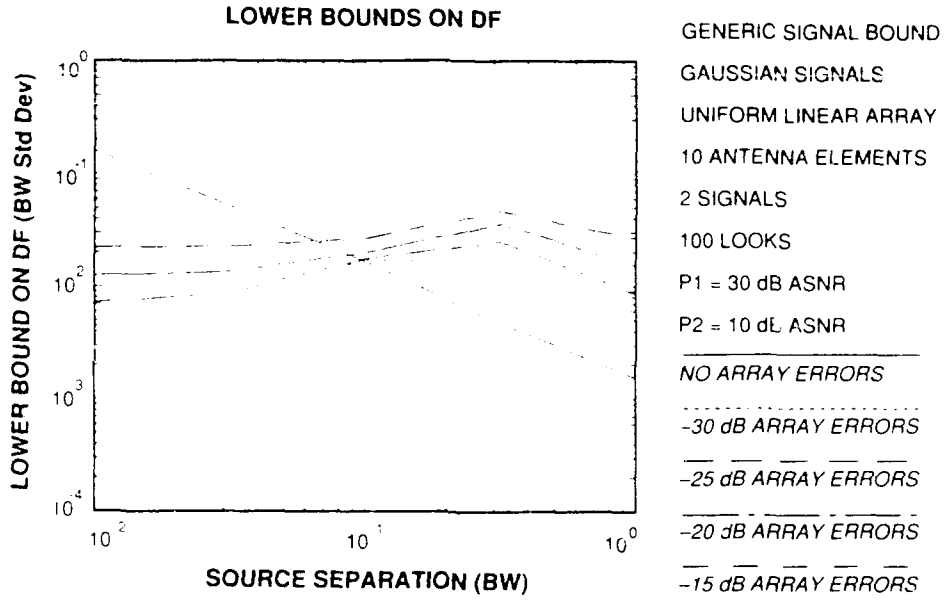

116880-34

Figure E-31. Generic signal bounds - 2 complex Gaussian signals, 100 looks, SOI ASNR = 30 dB, interferer ASNR = 10 dB.

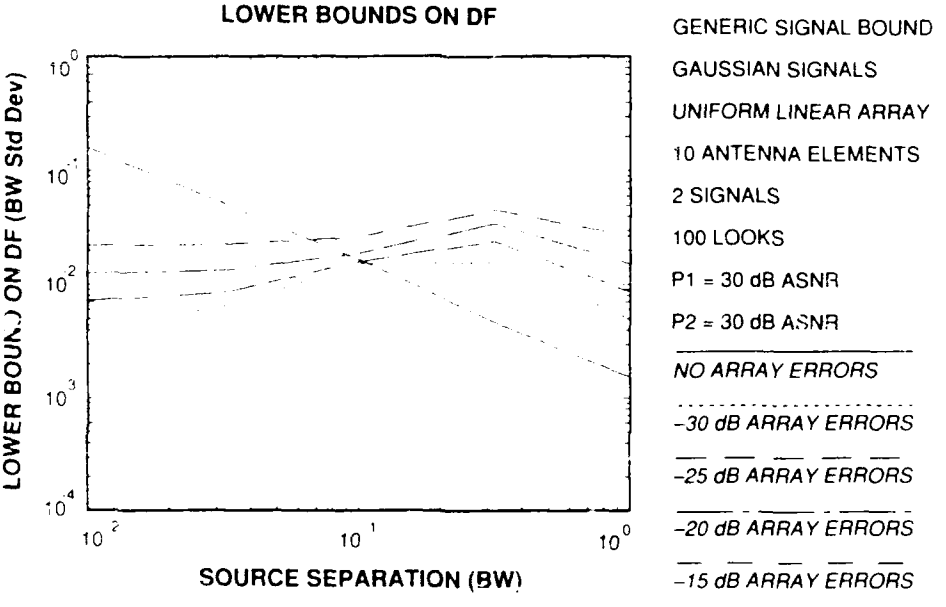

116880-35

Figure E-32. Generic signal bounds - 2 complex Gaussian signals, 100 looks, SOI ASNR = 30 dB, interferer ASNR = 30 dB.

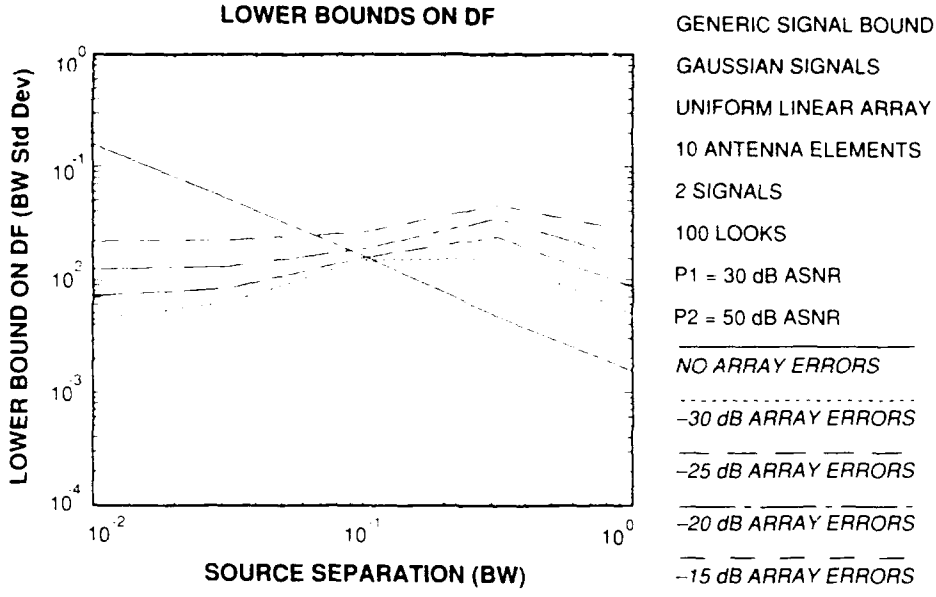

Figure E-33. Generic signal bounds - 2 complex Gaussian signals, 100 looks, SOI ASNR = 30 dB, interferer ASNR = 50 dB.

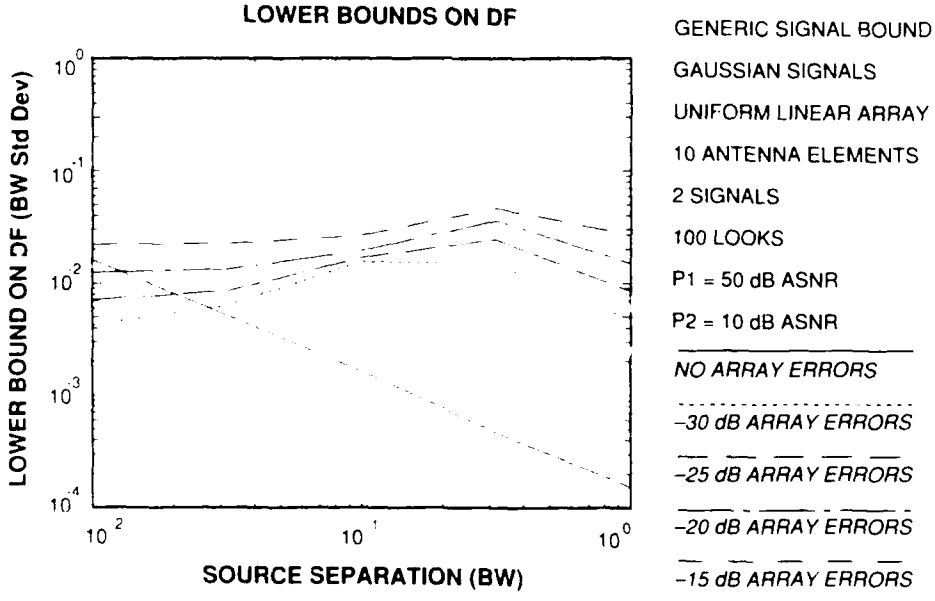

Figure E-34. Generic signal bounds - 2 complex Gaussian signals, 100 looks, SOI ASNR = 50 dB, interferer ASNR = 10 dB.

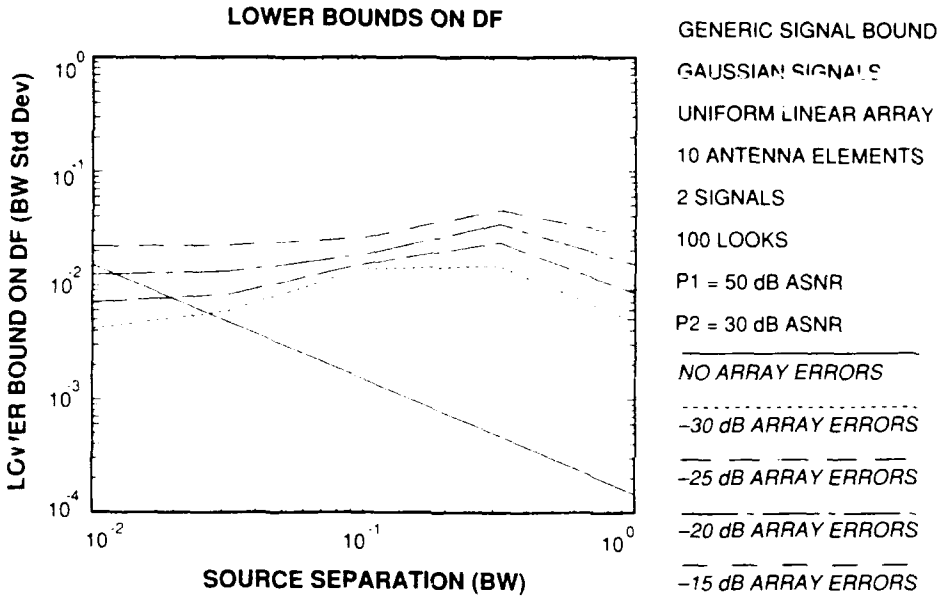

116880-38

Figure E-35. Generic signal bounds - 2 complex Gaussian signals, 100 looks, SOI ASNR = 50 dB, interferer ASNR = 30 dB.

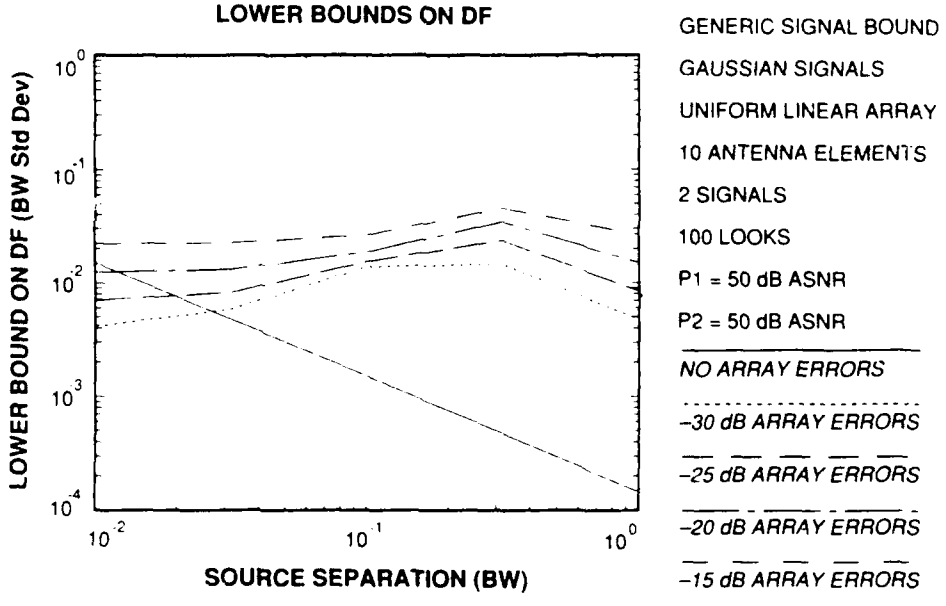

116880-39

Figure E-36. Generic signal bounds - 2 complex Gaussian signals, 100 looks, SOI ASNR = 50 dB, interferer ASNR = 50 dB.

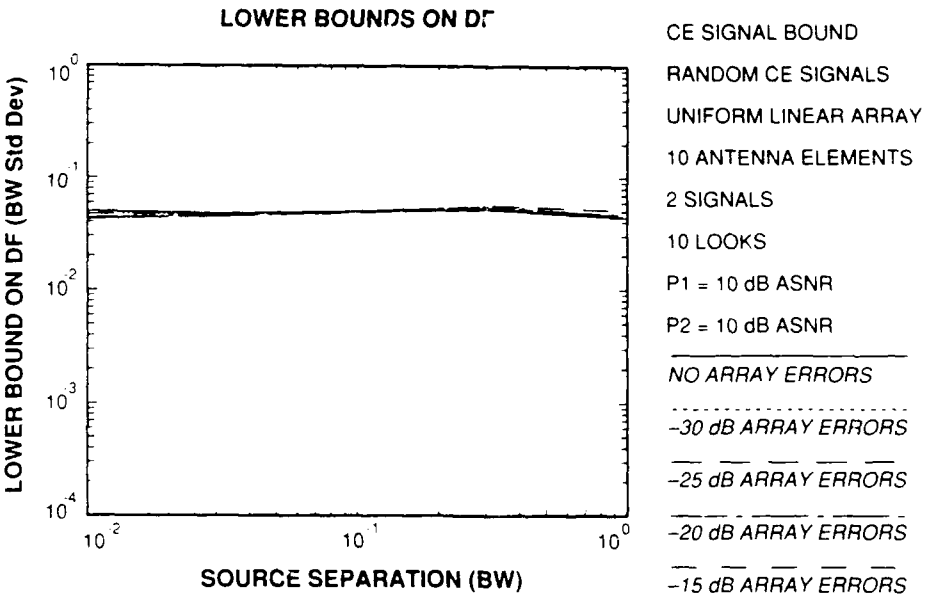

Figure E-37. Constant-envelope signal bounds - 2 random constant-envelope signals, 10 looks, SOI ASNR = 10 dB, interferer ASNR = 10 dB.

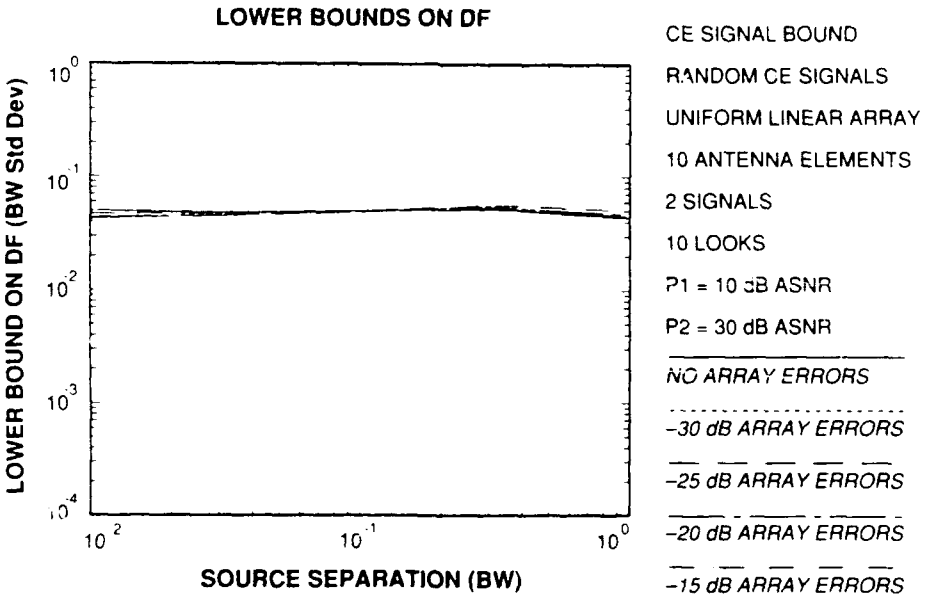

Figure E-38. Constant-envelope signal bounds - 2 random constant-envelope signals, 10 looks, SOI ASNR = 10 dB, interferer ASNR = 30 dB.

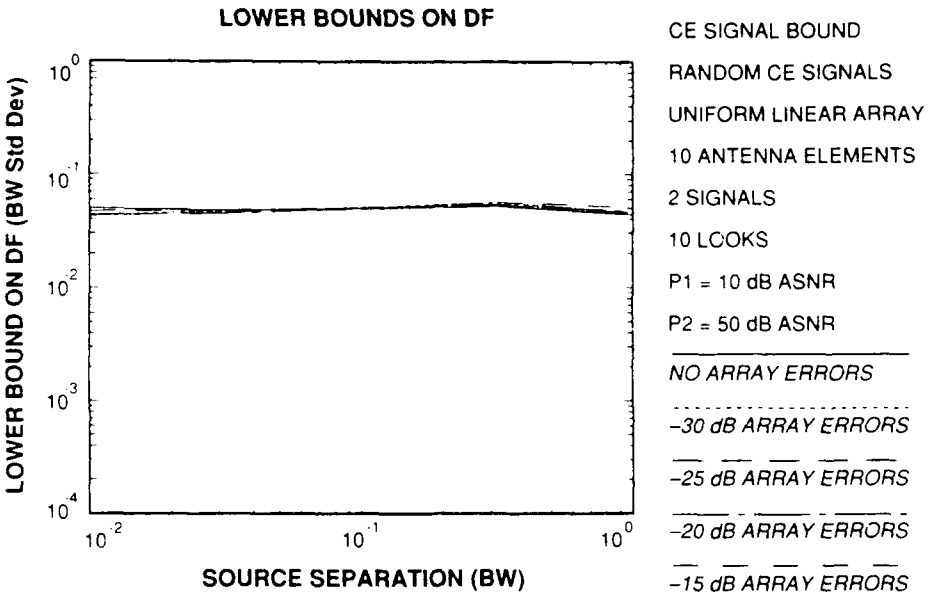

116880-42

Figure E-39. Constant-envelope signal bounds - 2 random constant-envelope signals, 10 looks, SOI ASNR = 10 dB, interferer ASNR = 50 dB.

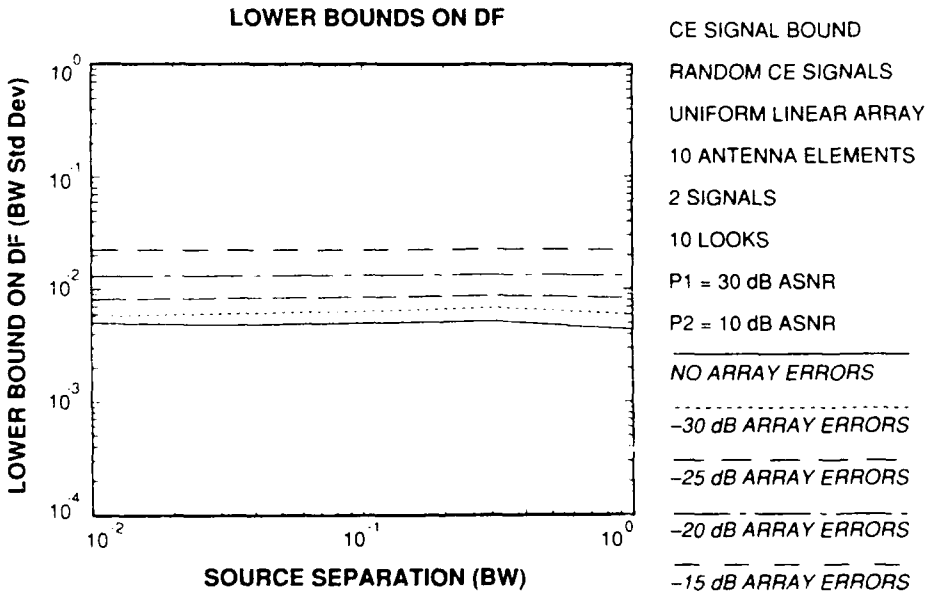

116880-43

Figure E-40. Constant-envelope signal bounds - 2 random constant-envelope signals, 10 looks, SOI ASNR = 30 dB, interferer ASNR = 10 dB.

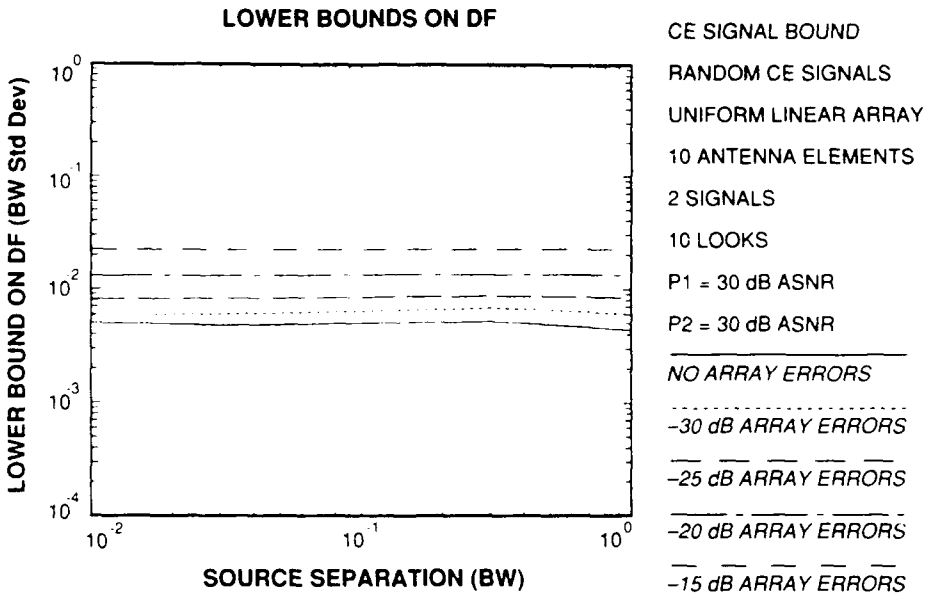

Figure E-41. Constant-envelope signal bounds - 2 random constant-envelope signals, 10 looks, SOI ASNR = 30 dB, interferer ASNR = 30 dB.

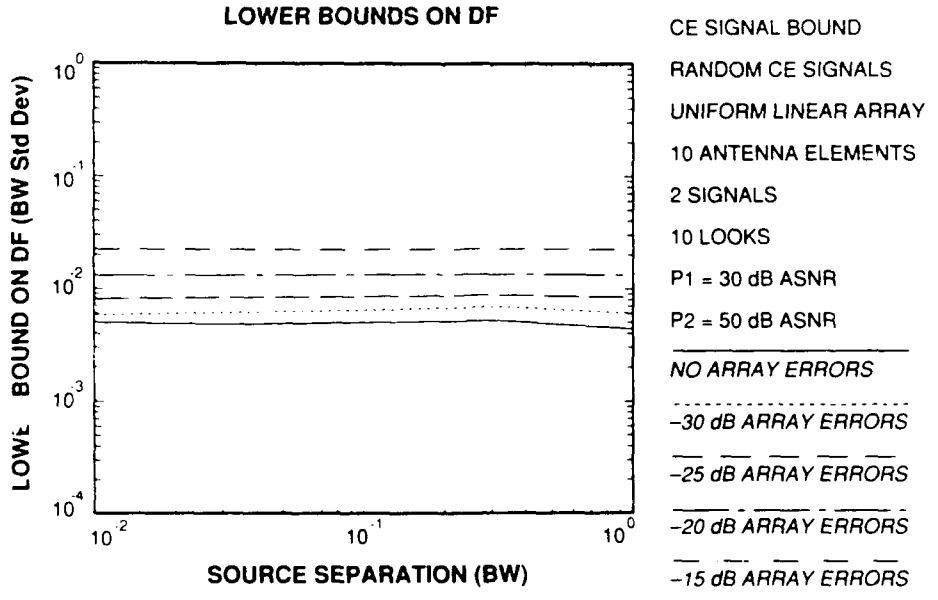

Figure E-42. Constant-envelope signal bounds - 2 random constant-envelope signals, 10 looks, SOI ASNR = 30 dB, interferer ASNR = 50 dB.

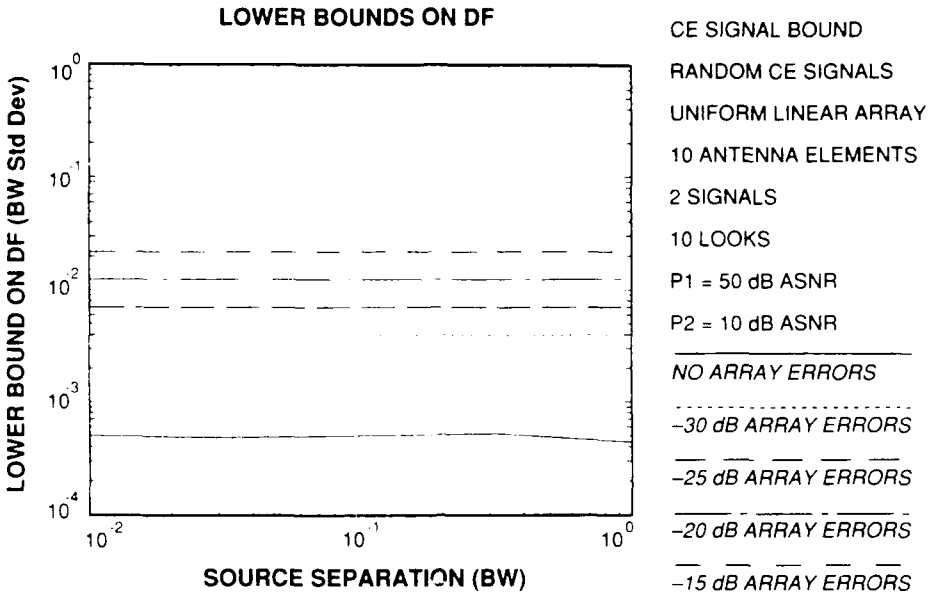

116880-46

Figure E-43. Constant-envelope signal bounds - 2 random constant-envelope signals, 10 looks, SOI ASNR = 50 dB, interferer ASNR = 10 dB.

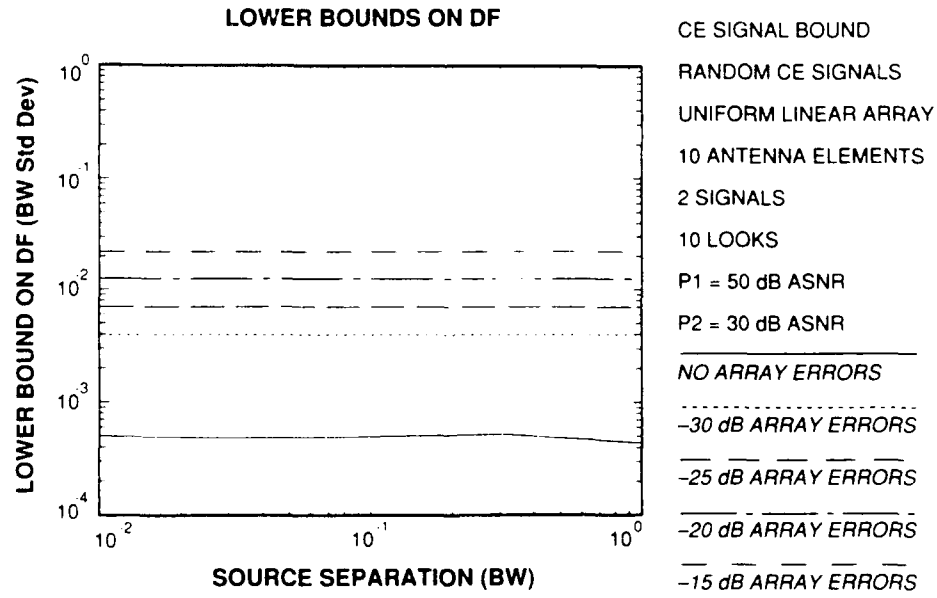

116880-47

Figure E-44. Constant-envelope signal bounds - 2 random constant-envelope signals, 10 looks, SOI ASNR = 50 dB, interferer ASNR = 30 dB.

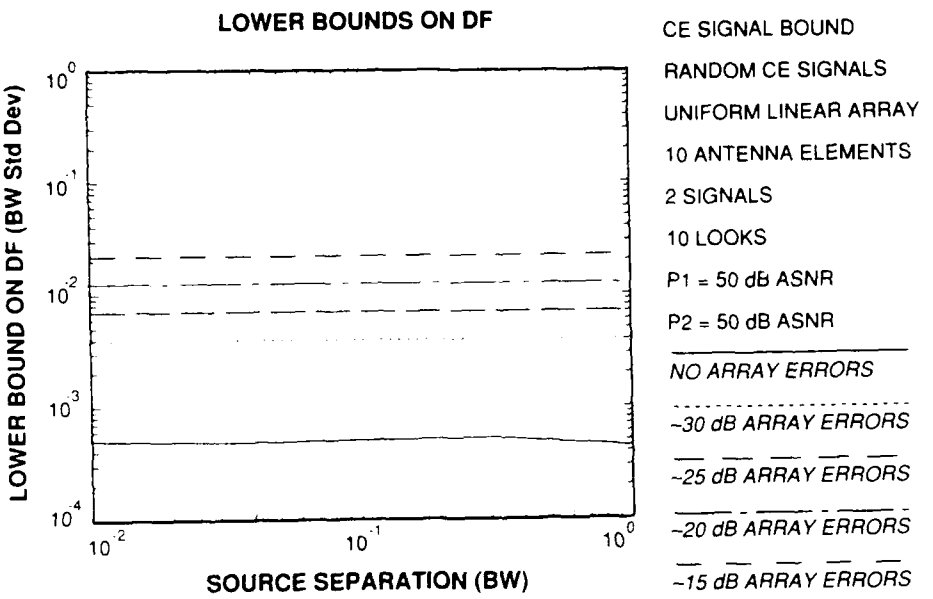

Figure E-45. Constant-envelope signal bounds - 2 random constant-envelope signals, 10 looks, SOI ASNR = 50 dB, interferer ASNR = 50 dB.

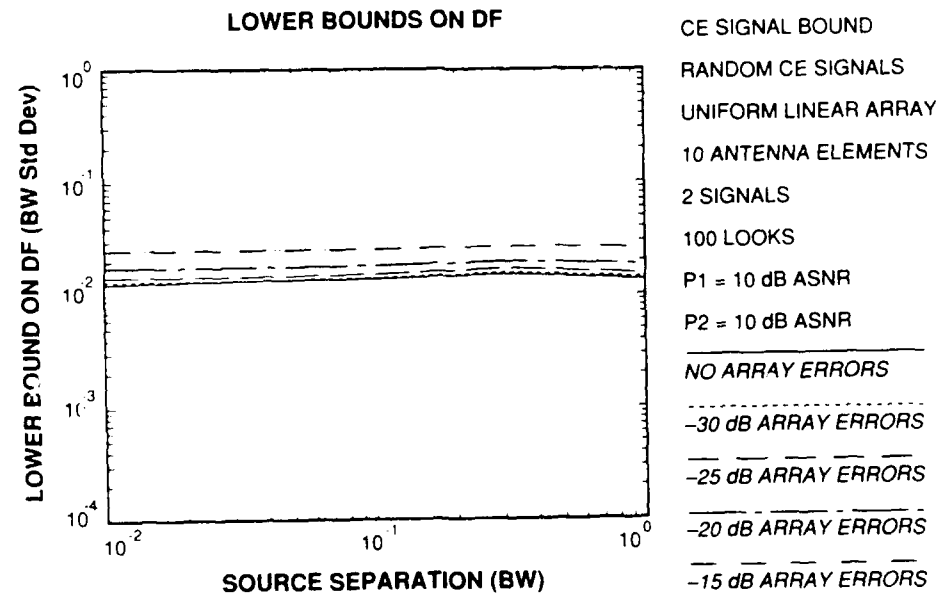

Figure E-46. Constant-envelope signal bounds - 2 random constant-envelope signals, 100 looks, SOI ASNR = 10 dB, interferer ASNR = 10 dB.

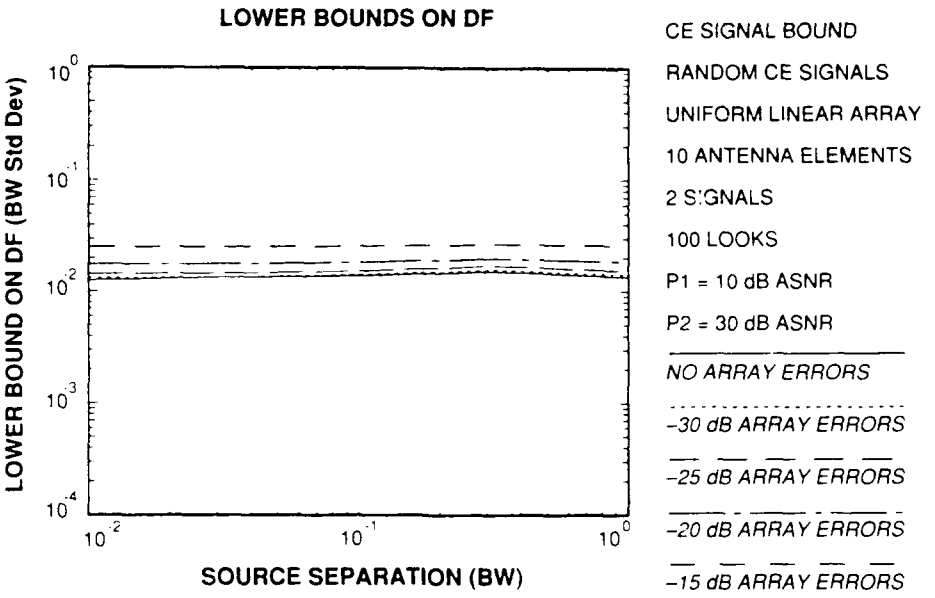

Figure E-47. Constant-envelope signal bounds - 2 random constant-envelope signals. 100 looks. SOI ASNR = 10 dB, interferer ASNR = 30 dB.

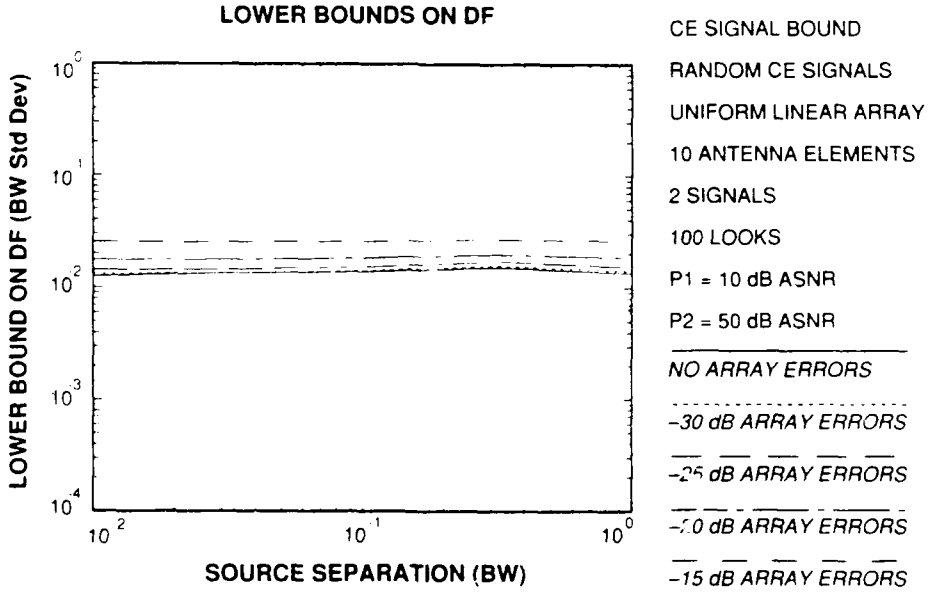

Figure E-48. Constant-envelope signal bounds - 2 random constant-envelope signals. 100 looks. SOI ASNR = 10 dB, interferer ASNR = 50 dB.

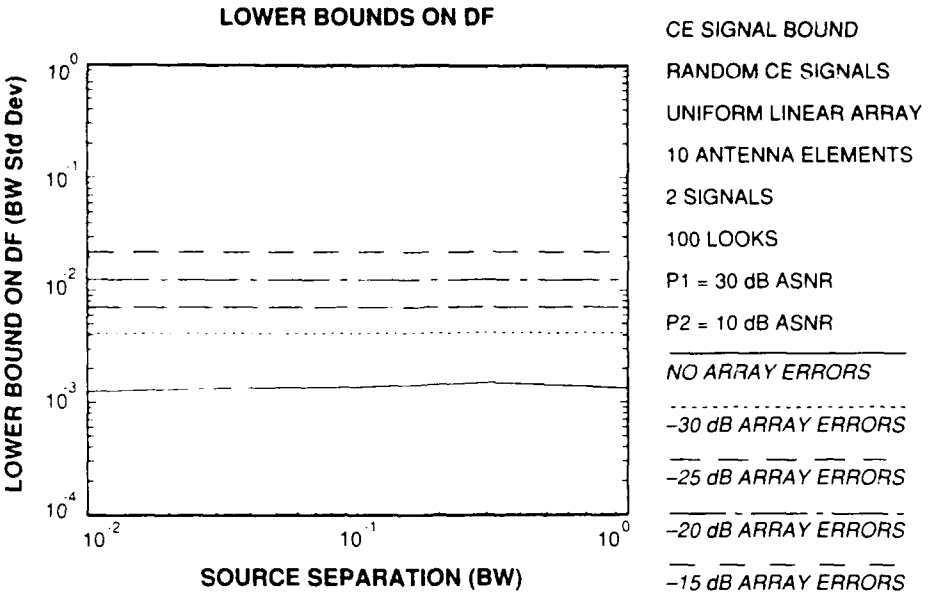

Figure E-49. Constant-envelope signal bounds - 2 random constant-envelope signals, 100 looks, SOI ASNR = 30 dB, interferer ASNR = 10 dB.

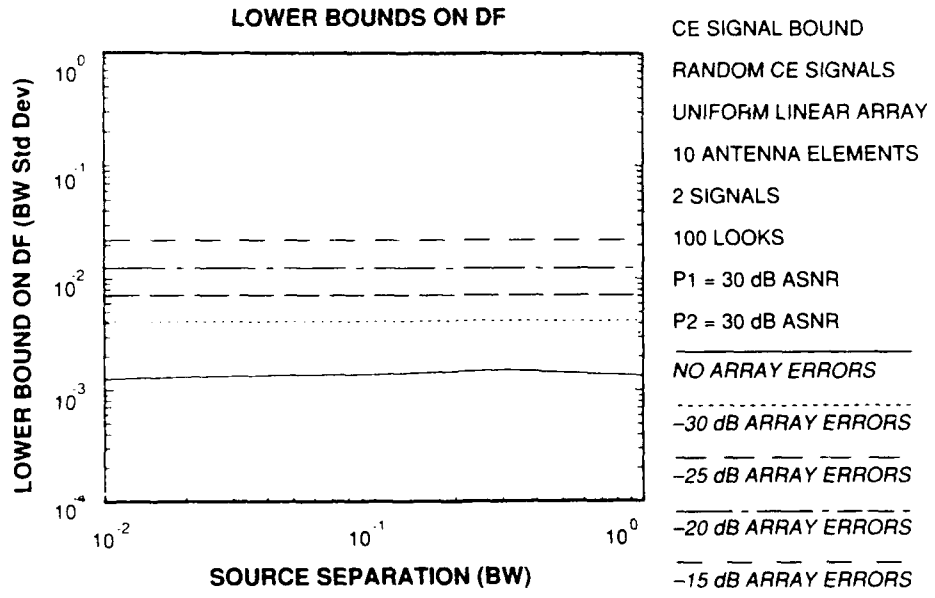

Figure E-50. Constant-envelope signal bounds - 2 random constant-envelope signals, 100 looks, SOI ASNR = 30 dB, interferer ASNR = 30 dB.

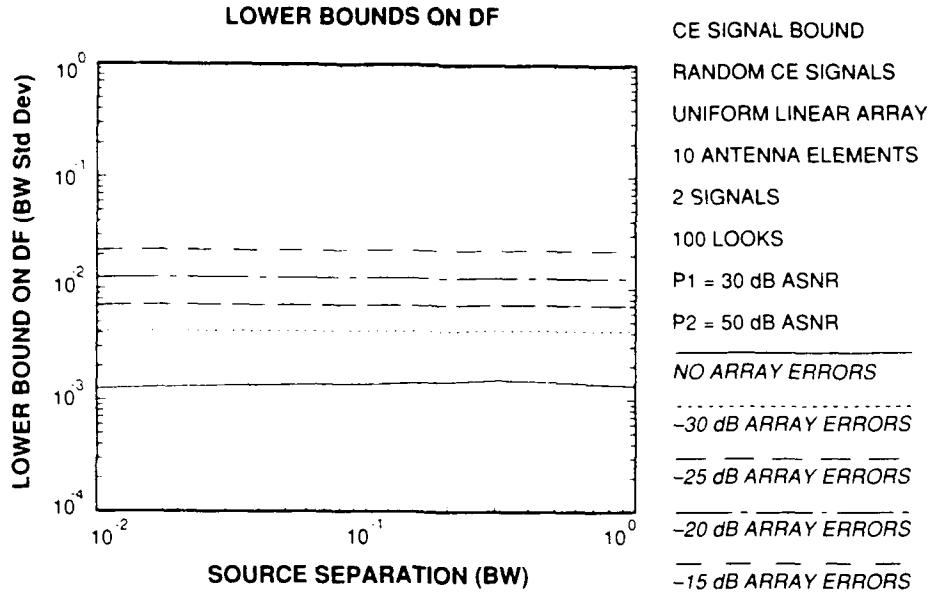

116880-54

Figure E-51. Constant-envelope signal bounds - 2 random constant-envelope signals, 100 looks, SOI ASNR = 30 dB, interferer ASNR = 50 dB.

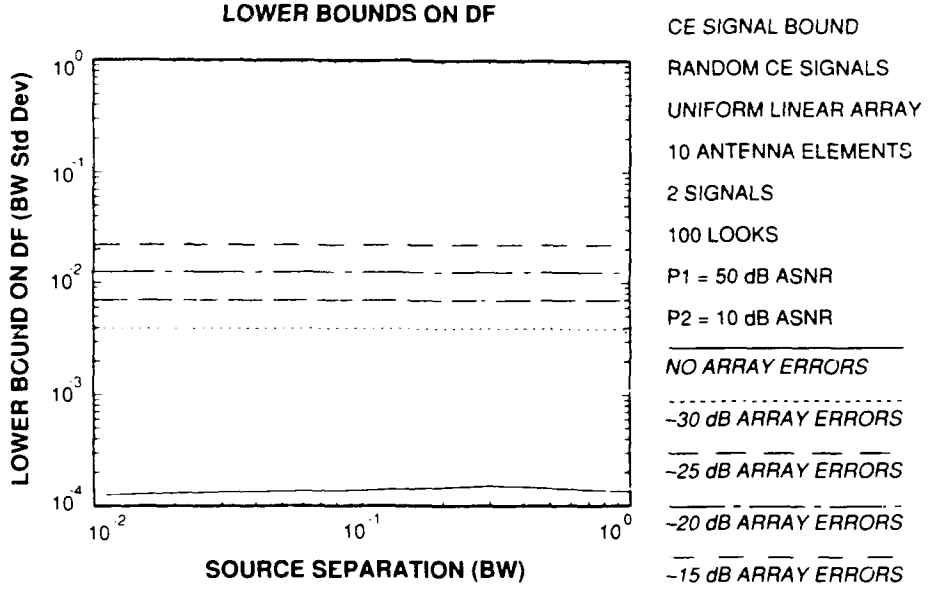

116880-55

Figure E-52. Constant-envelope signal bounds - 2 random constant-envelope signals, 100 looks, SOI ASNR = 50 dB, interferer ASNR = 10 dB.

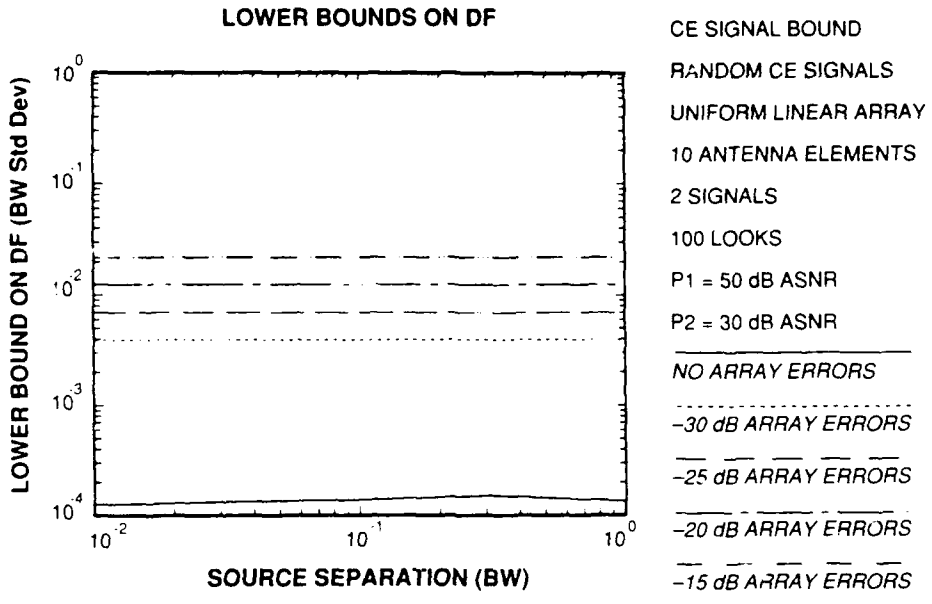

Figure E-53. Constant-envelope signal bounds - 2 random constant-envelope signals, 100 looks, SOI ASNR = 50 dB, interferer ASNR = 30 dB.

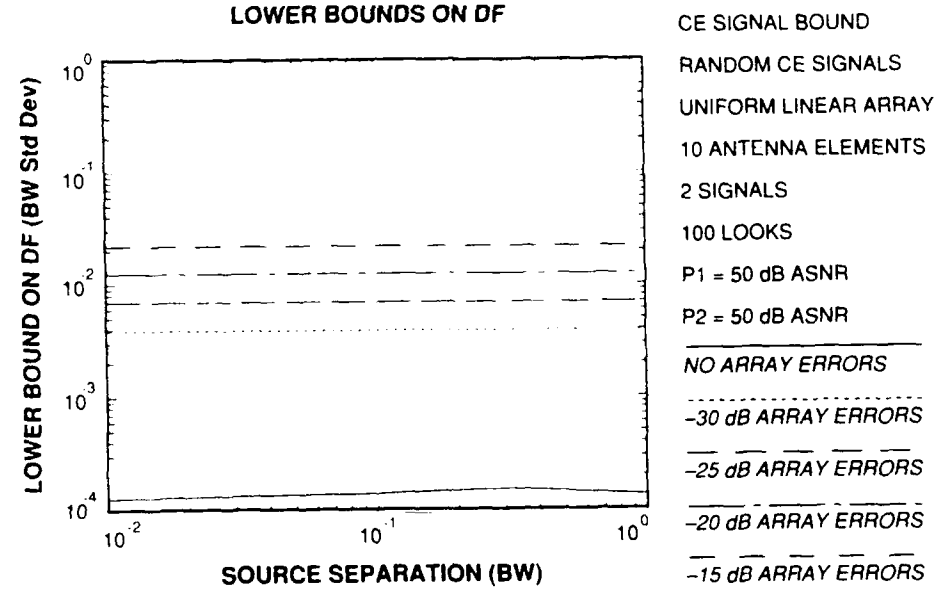

Figure E-54. Constant-envelope signal bounds - 2 random constant-envelope signals, 100 looks, SOI ASNR = 50 dB, interferer ASNR = 50 dB.

REFERENCES

1. D.F. DeLong, "Multiple Signal Direction Finding with Thinned Linear Arrays," Project Report TST-68, Lincoln Laboratory, MIT (13 April 1983). DTIC AD-A128924.

2. A. Graham, *Kronecker Products and Matrix Calculus: With Applications*, (John Wiley and Sons, New York, 1981).

3. E.L. Lehmann, *Theory of Point Estimation*, (John Wiley and Sons, New York, 1983).

4. C.R. Rao and S.K. Mitra, *Generalized Inverse of Matrices and its Applications*, (John Wiley and Sons, New York, 1971).

5. F.C. Schweppe, *Uncertain Dynamic Systems*, (Prentice-Hall, Inc., Englewood Cliffs, NJ, 1973).

6. B. Steinberg, *Principles of Aperture and Array System Design*, (Wiley-Interscience, New York, 1976).

7. H.L. Van Trees, *Detection, Estimation, and Modulation Theory, Part I*, (John Wiley and Sons, New York, 1968).

REPORT DOCUMENTATION PAGE

1a. REPORT SECURITY CLASSIFICATION Unclassified	1b. RESTRICTIVE MARKINGS
2a. SECURITY CLASSIFICATION AUTHORITY	3. DISTRIBUTION/AVAILABILITY OF REPORT Approved for public release; distribution is unlimited.
2b. DECLASSIFICATION/DOWNGRADING SCHEDULE	
4. PERFORMING ORGANIZATION REPORT NUMBER(S) Technical Report 799	5. MONITORING ORGANIZATION REPORT NUMBER(S) ESD-TR-88-321
6a. NAME OF PERFORMING ORGANIZATION Lincoln Laboratory, MIT 6b. OFFICE SYMBOL *(If applicable)*	7a. NAME OF MONITORING ORGANIZATION Electronic Systems Division
6c. ADDRESS *(City, State, and Zip Code)* P.O. Box 73 Lexington, MA 02173-9108	7b. ADDRESS *(City, State, and Zip Code)* Hanscom AFB, MA 01731
8a. NAME OF FUNDING/SPONSORING ORGANIZATION Department of Defense 8b. OFFICE SYMBOL *(If applicable)*	9. PROCUREMENT INSTRUMENT IDENTIFICATION NUMBER F19628-90-C-0002
8c. ADDRESS *(City, State, and Zip Code)* Pentagon Washington, DC 20301	10. SOURCE OF FUNDING NUMBERS PROGRAM ELEMENT NO: 33401G; PROJECT NO: 281; TASK NO:; WORK UNIT ACCESSION NO:

11. TITLE *(Include Security Classification)*
Lower Bounds on Multiple-Source Direction Finding in the Presence of Direction-Dependent Antenna-Array-Calibration Errors

12. PERSONAL AUTHOR(S)
Alvin R. Kuruc

13a. TYPE OF REPORT	13b. TIME COVERED	14. DATE OF REPORT *(Year, Month, Day)*	15. PAGE COUNT
Technical Report	FROM _____ TO _____	24 October 1989	92

16. SUPPLEMENTARY NOTATION
None

17 COSATI CODES			18. SUBJECT TERMS *(Continue on reverse if necessary and identify by block number)*
FIELD	GROUP	SUB-GROUP	direction finding; Cramér-Rao bounds; antenna-calibration errors; linear arrays; array processing

19. ABSTRACT *(Continue on reverse if necessary and identify by block number)*

We consider the problem of direction finding (DF) of multiple, cofrequency narrowband signals with a phased antenna array when direction-dependent array-calibration errors as well as thermal noise are present. Lower bounds on the variance of unbiased estimators for DF are derived under two different types of signal models: completely unknown (i.e., generic) signals and unknown constant-envelope signals. In both models, the complex amplitudes of the signals are modeled as unknown parameters. We derive and evaluate lower bounds on DF of these signals when complex Gaussian array errors and thermal noise are present. In our numerical examples, the bound for generic signals tended to decrease with increasing interference power and, for closely spaced signals, became more optimistic when small array errors were added. With a sufficiently large signal-of-interest (SOI) array signal-to-noise power ratio (ASNR) and number of looks, the bound numerically approached the bound on DF of multiple generic signals with array errors but no thermal noise (i.e., the multiple-*generic-signal, array-errors-only bound*). The latter bound depended on the signal separation and the power of the array errors. It was independent of the signal waveforms and powers and was largest at moderate signal separations (e.g., 0.3 beamwidths). The latter bound approached the single-signal, array-errors-only bound as the signal separation approached zero.

The results for constant-envelope signals showed that the bound with array errors and thermal noise was more optimistic than the analogous generic-signal bound and had little dependence on signal separation and interference power. This was also the case in the absence of direction-dependent errors. The improvements in the bound were more significant at small array errors, low ASNR, small numbers of looks, and moderate signal separations. At all signal separations, with a sufficiently high SOI ASNR and number of looks, the bound numerically approached the single-signal, one-look, array-errors-only bound (the latter bound is the same for generic and constant-envelope signals).

20. DISTRIBUTION/AVAILABILITY OF ABSTRACT	21. ABSTRACT SECURITY CLASSIFICATION
☐ UNCLASSIFIED/UNLIMITED ☒ SAME AS RPT ☐ DTIC USERS	Unclassified
22a. NAME OF RESPONSIBLE INDIVIDUAL Lt. Col. Hugh L. Southall, USAF	22b. TELEPHONE *(Include Area Code)* (617) 981-2330
	22c. OFFICE SYMBOL ESD/TML